555 Eleventh Street, N.W., Suite 1000
Washington, D.C. 20004-1304
Tel: +1.202.637.2200 Fax: +1.202.637.2201
www.lw.com

LATHAM & WATKINS LLP

October 11, 2017

VIA ELECTRONIC FILING

Ms. Marlene H. Dortch
Secretary
Federal Communications Commission
445 12th Street, SW
Washington, DC 20554

Re: ViaSat, Inc., Notice of *Ex Parte* Presentation, GN Docket No. 14-177; IB Docket Nos. 15-256 & 97-95; RM-11664; and WT Docket No. 10-112

Dear Ms. Dortch:

On October 6, 2017, Mark Dankberg and Chris Murphy of ViaSat, Inc. ("ViaSat"), and the undersigned, met with Commission staff listed below, regarding issues presented in the Spectrum Frontiers proceeding. Attachment 1 formed the basis for the discussion.

During the meeting, ViaSat urged in particular that:

- The Commission maintain the longstanding primary designation of the 48.2-50.2 GHz uplink band segment for unfettered satellite gateway and user terminal deployment.
    - Any terrestrial use that may be permitted in this band segment should not impair satellite uses.
- Satellite earth stations also need access to the 47.2-48.2 GHz and 50.4-52.4 GHz uplink band segments.
    - The inherent compatibility of small gateway earth stations allows them to share these band segments without impairing terrestrial uses.
    - Where no terrestrial impairment would occur, there is no need to restrict the deployment of those gateways.

ViaSat explained that (i) sharing in the 47.2-48.2 GHz and 50.4-52.4 GHz segments (as well as the associated downlink spectrum at 37.5-40 and 42-42.5 GHz) is supported by studies and analyses that ViaSat previously submitted into the record of this proceeding, and (ii) these

satellite-terrestrial wireless sharing concepts easily can be extended to accommodate larger earth stations and NGSO constellations.

Attached for convenience are the following previously-submitted ViaSat studies and analyses:

- Attachment 2: Report on earth station testing in Carlsbad, California analyzing the ability of millimeter-wave-band satellite earth stations to co-exist with terrestrial wireless services in typical roof top mounting scenarios.[1]

- Attachment 3: Report prepared by Roberson and Associates, LLC demonstrating the ability of small satellite earth station uplinks in the 47.2-48.2 GHz and 50.4-52.4 GHz band segments to coexist with terrestrial wireless operations.[2]

- Attachment 4: Engineering report illustrating how satellite earth station receivers in the 37.5-40 GHz band segment can coexist with terrestrial wireless operations.[3]

Please contact the undersigned if you have any questions regarding this submission.

Respectfully submitted,

/s/

John P. Janka
Elizabeth R. Park

---

[1] ViaSat, Inc., *Ex Parte* Submission, GN Docket No. 14-177, *et al*. (filed Apr. 12, 2017). ViaSat filed an erratum to this submission that included Annex 2 to the report, which consists of antenna test patterns. *See* ViaSat, Inc., Erratum to *Ex Parte* Submission, GN Docket No. 14-177, *et al*. (filed Apr. 20, 2017). Those antenna test patterns are not included here.

[2] ViaSat, Inc., Notice of *Ex Parte* Presentation, GN Docket No. 14-177, *et al*. (filed Sept. 25, 2017).

[3] ViaSat, Inc., *Ex Parte* Submission, GN Docket No. 14-177, *et al*. (filed Oct. 2, 2017).

Attachments (4)

cc:
Office of Engineering and Technology
Julius Knapp
Ronald Repasi
Jamison Prime
Michael Ha
Bahman Badipour
Nicholas Oros

International Bureau
Thomas Sullivan
Jim Schlichting
Robert Nelson
Jose Albuquerque

Wireless Telecommunications Bureau
Donald Stockdale
Nese Guendelsberger
Dana Shaffer
Joel Taubenblatt
Blaise Scinto
John Schauble

ATTACHMENT 1

Spectrum Frontiers

Satellite Broadband Access and V Band Coexistence

ViaSat History

- Founded 1986
- Uniquely American story
- No outside capital
- Garage start-up

- Today
- NASDAQ listed
- ~4700 employees in 11 states
- $3.8B market cap
- Satellite, wireless, fiber optics, cybersecurity

Satellite Broadband Demand

- ViaSat connects people to fiber through state-of-the-art broadband networks EVERYWHERE
  - Cloud services require continuous & ubiquitous connectivity
- Exponential growth in demand for satellite broadband
  - Rural broadband (especially video streaming and downloads)
  - In-flight connectivity (36M/yr active users today to several 100M/yr in 2021)
  - Mobile vehicles (connected cars, drones, trains, ships)
  - National defense
  - Continuity of government
  - Border protection
- Demand outstrips current supply!

Because no other satellite company would…

ViaSat-1

- 140 Gbps
- 1.5 GHz spectrum
- Launched 2011

ViaSat-2

- 300 Gbps
- 2.1 GHz spectrum
- Launched 2017

ViaSat-3

- Over 1 Tbps
- Under construction

New ViaSat-3 Manufacturing Facility

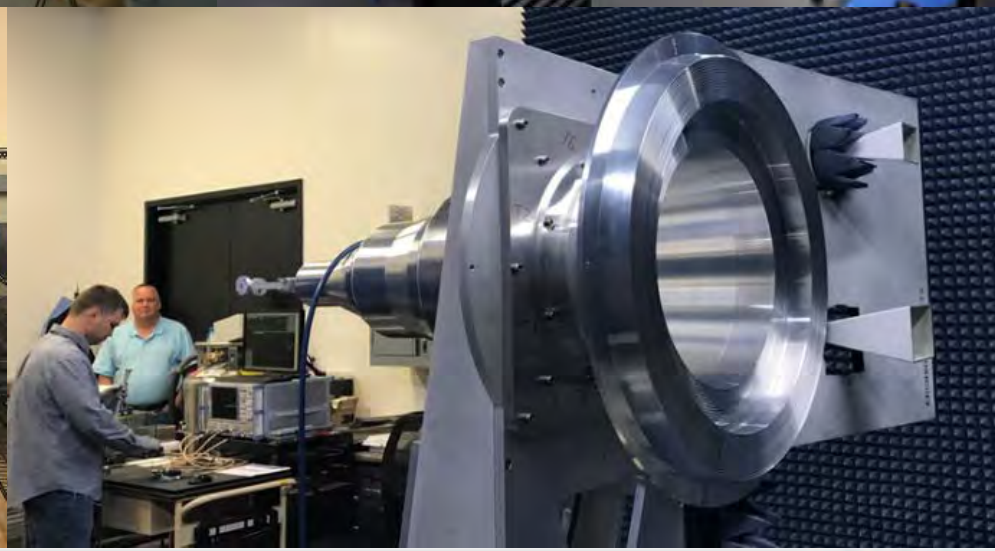

ViaSat-3 State-of-the-Art Infrastructure

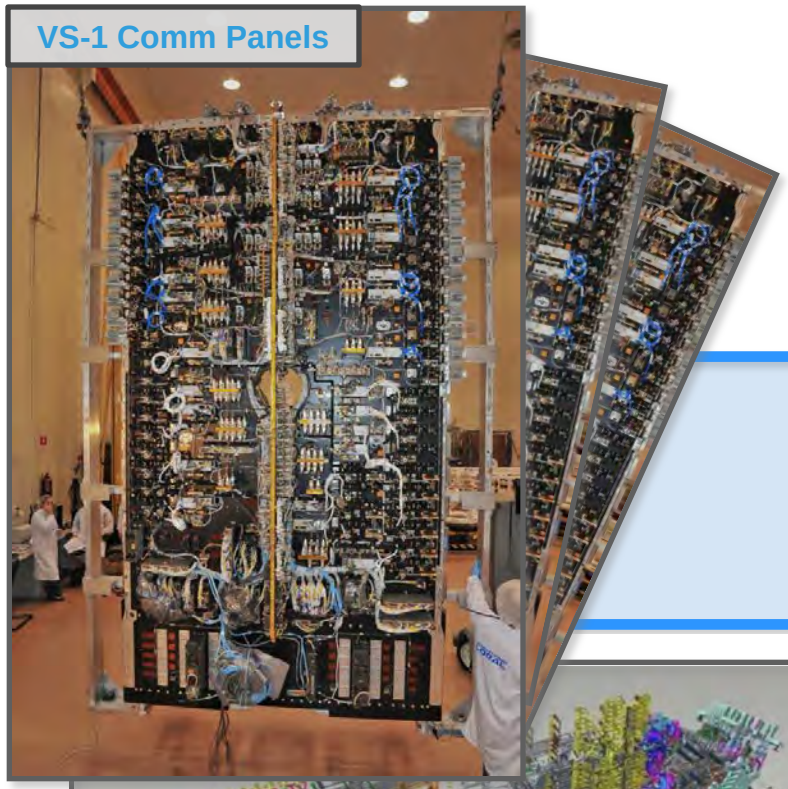

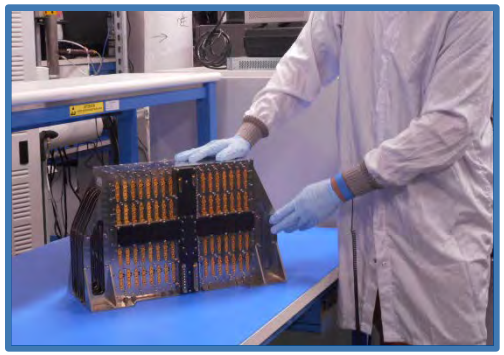

Each ViaSat-3 has nearly ~10x the bandwidth of ViaSat-1

Demand Requires V Band Access for Satellite

- Ka band is essentially filled
  - Modern satellites are very close to theoretical spectral capacity limits
  - ViaSat satellites are the highest capacity commercial satellite networks ever built
- V band access for satellite is critical
  - More bandwidth enables
    - Faster speeds
    - More GigaBytes
    - Lower prices
    - New services
    - Extending coverage to millions of rural Americans
  - To complement terrestrial 5G – in the air, on the ground, at sea, border protection, national defense, in space
- Retaining core 2 x 2 GHz for satellite is essential
- Spectrum sharing in additional spectrum requires new approaches

V-Band: Current Plan and Proposals

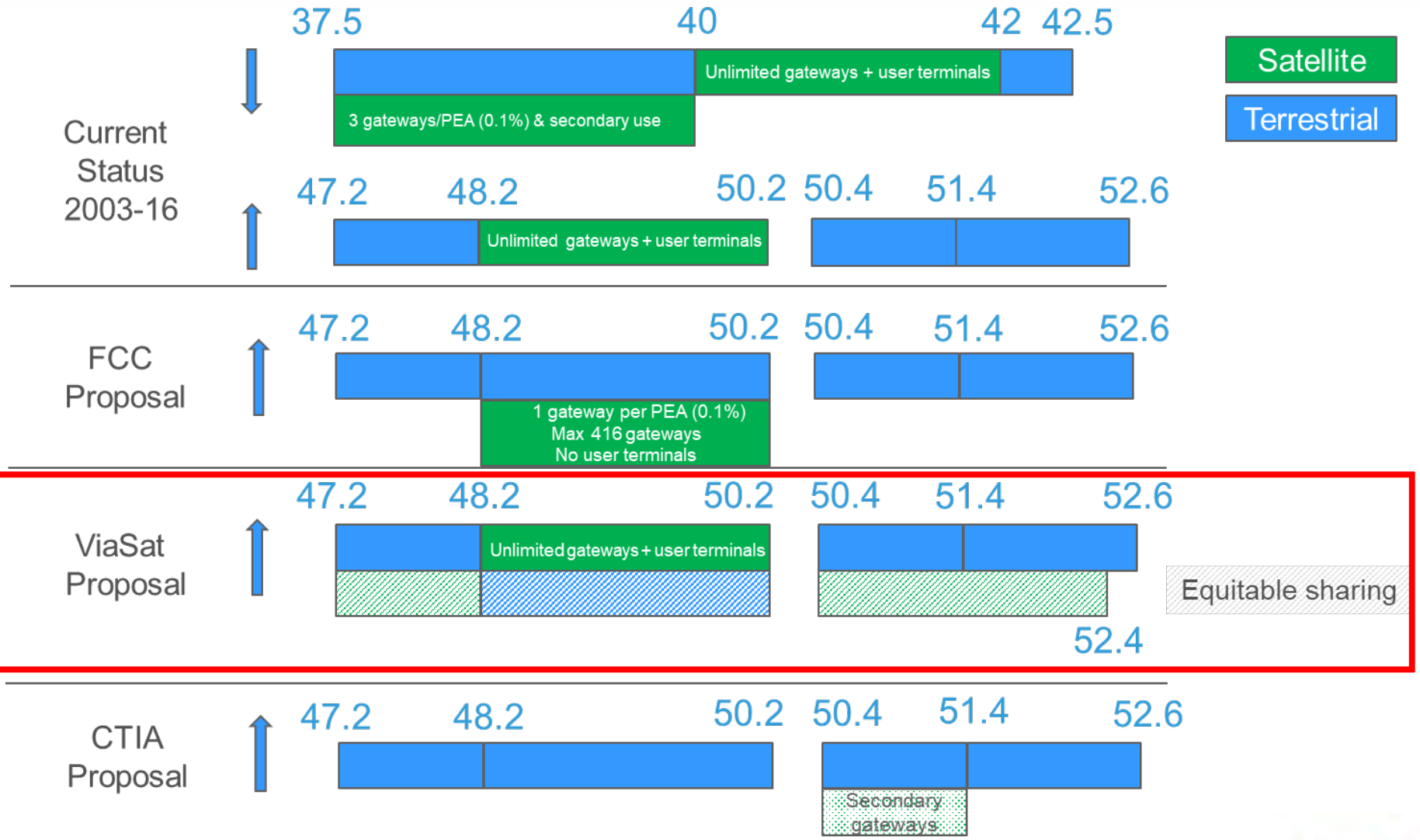

ViaSat 5G Coexistence Studies

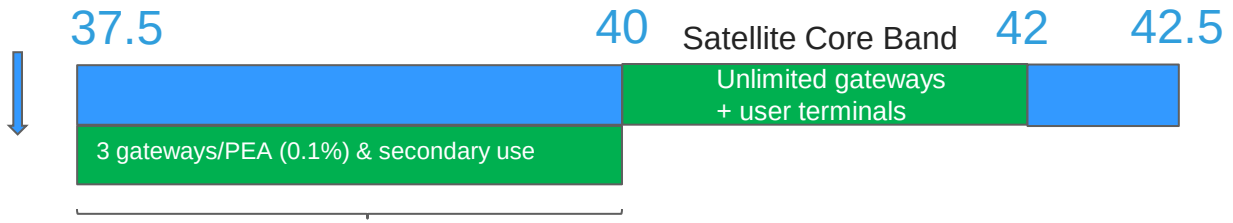

Hunter 5G Coexistence Study

Satellite

Terrestrial

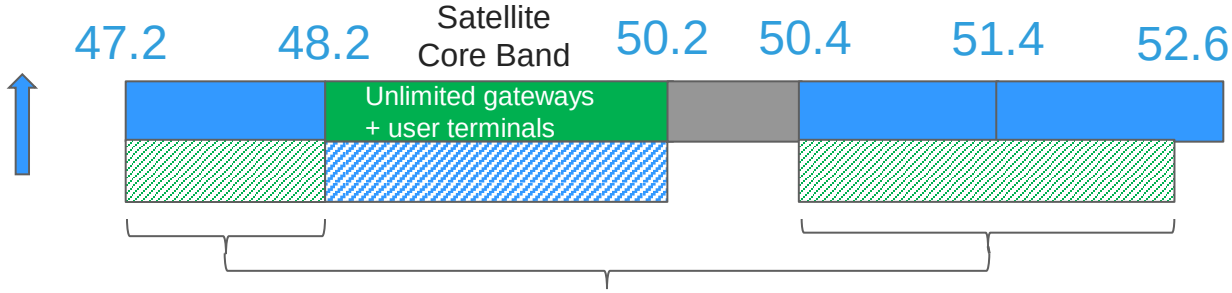

Roberson 5G Coexistence Study

Equitable Sharing
(de minimis effect)

Small Impact of Satellite V-band Sharing

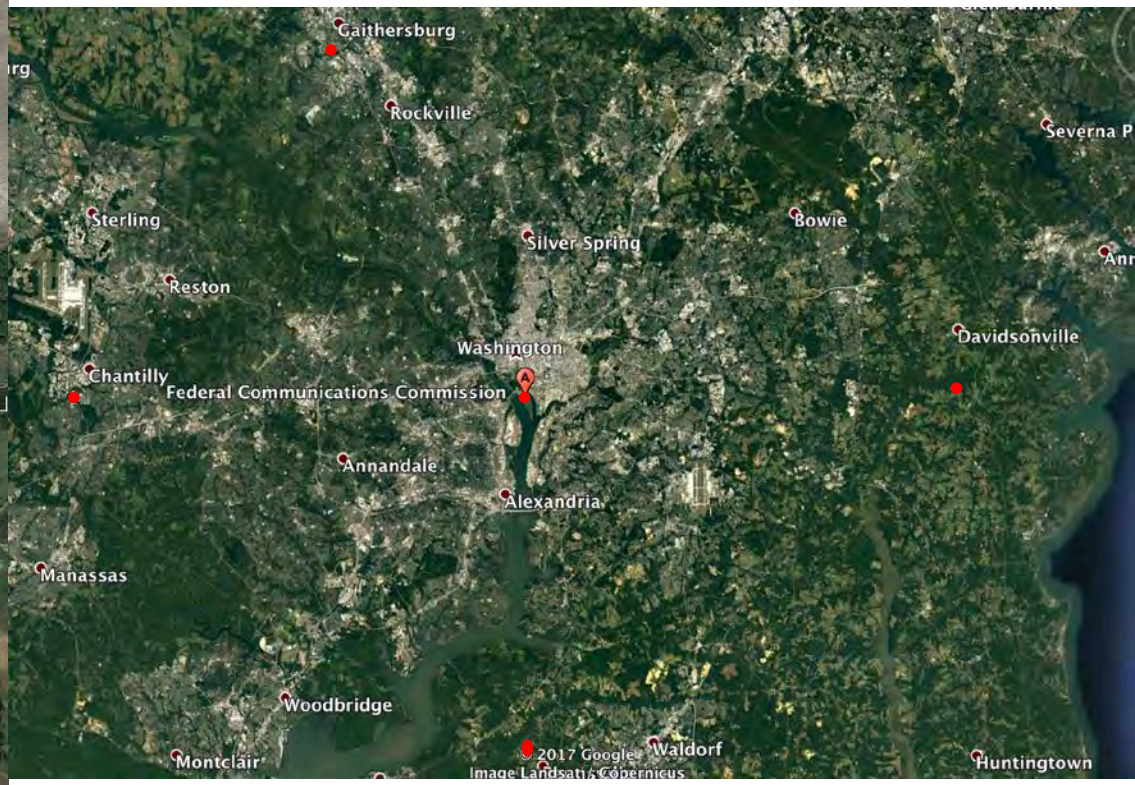

Huge Impact of Enabling Satellite V Band Access

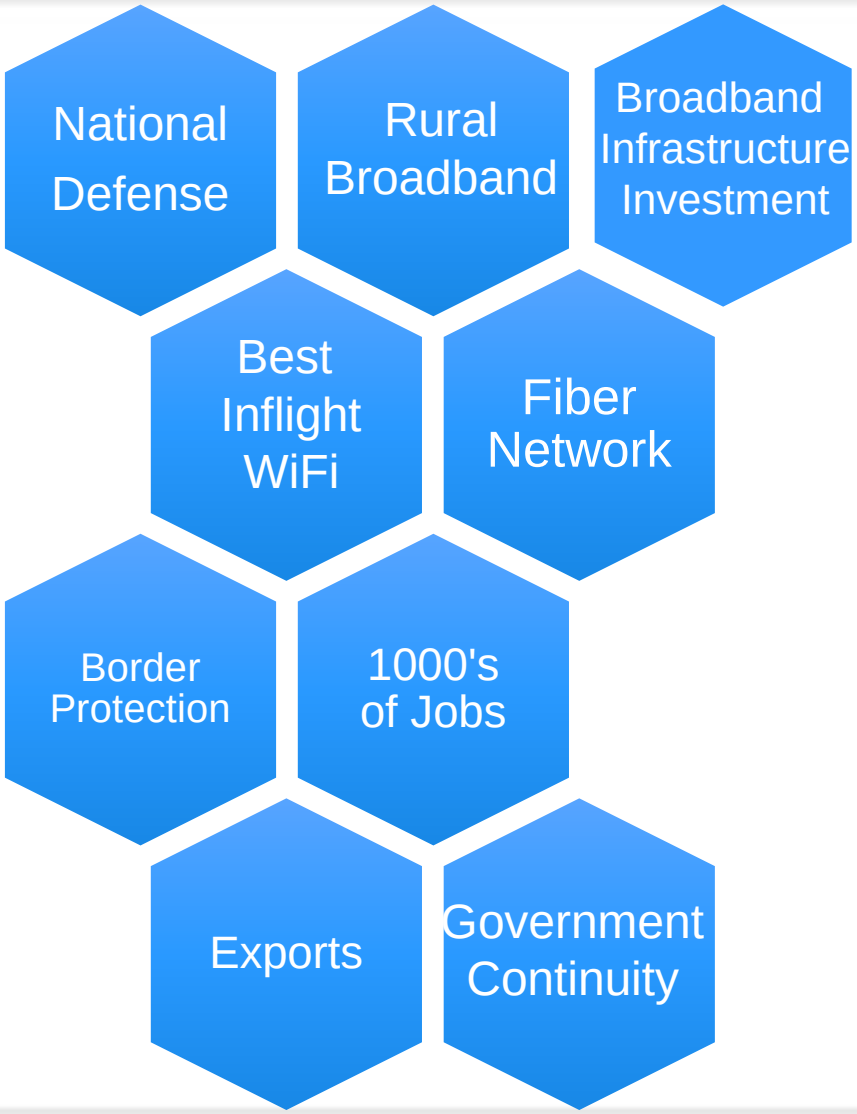

ViaSat Coexistence Proposal (1)

- 48.2-50.2 GHz and 40-42 GHz
  - Maintain longstanding designation for unfettered satellite gateways and user terminals
  - Any terrestrial use should not impair satellite use
- 47.2-48.2/50.4-52.4 GHz (uplinks)
  - Inherent small GSO earth station compatibility --- no 5G impairment
    - Feasible to deploy many small gateways via roof mounts and shielding techniques
      - Avoids population
      - Avoids major roads, rail lines, venues
    - Urban, suburban and rural areas alike
  - Where no impairment occurs, no need to restrict gateway deployment
  - Defining protection criteria enables
    - Development of suitable sharing rules
    - Maximization of spectrum use
    - Reliable operation of both services
  - ITU criteria for 5G enables calculation of suitable criteria today
    - Earth station emissions below that level/away from 5G receivers are not an issue
- 37.5-40 GHz (downlinks)
  - Same types of techniques allow earth station receivers to coexist with 5G
    - Urban, suburban and rural areas alike

ViaSat Coexistence Proposal (2)

- Concepts easily can be extended to accommodate larger earth stations and NGSO constellations

- But no basis to revisit prior rejection of proposals to exclude earth station deployment in urban areas
  - Such restrictions would “provide[] less predictability regarding the locations of future earth stations, and . . . limit[] the ability of FSS to deploy near population centers.” Spectrum Frontiers Order, para 60.

Conclusion

- High impact, low cost sharing solutions are available
- Feasible to accommodate both satellite and terrestrial needs
- Facilitating multiple technologies provides maximum consumer benefit

ATTACHMENT 2

555 Eleventh Street, N.W., Suite 1000
Washington, D.C. 20004-1304
Tel: +1.202.637.2200 Fax: +1.202.637.2201
www.lw.com

LATHAM & WATKINS LLP

April 12, 2017

VIA ELECTRONIC FILING

Marlene H. Dortch
Secretary
Federal Communications Commission
445 12th Street, S.W.
Washington, D.C. 20554

Re: ViaSat, Inc., *Ex Parte* Submission, GN Docket No. 14-177; IB Docket Nos. 15-256 & 97-95; RM-11664; WT Docket No. 10-112

Dear Ms. Dortch:

As part of the ongoing *Spectrum Frontiers* proceeding, ViaSat provides the attached Report Summary and Comsearch Report on earth station testing in Carlsbad, California ("Carlsbad Earth Station Testing Report"). The Report analyzes the ability of 28 GHz satellite earth stations to co-exist with terrestrial fixed and mobile services, including 5G/UMFU, in typical roof top mounting scenarios, including in urban and suburban settings.

Specifically, the Carlsbad Earth Station Testing Report consists of measured data in the vicinity of an existing earth station that was deployed well before the release of the *Spectrum Frontiers Order* last summer, and whose location thus was selected without reference to the terms of that Order. The measurements are based on the actual performance of the earth station and on existing site conditions. Consistent with Section 25.136(a)(4) of the Commission's rules, the measurements were conducted to determine the "area in which the earth station generates a power flux density (PFD), at 10 meters above ground level, of greater than or equal to -77.6 dBm/m^2/MHz."

As explained in the Carlsbad Earth Station Testing Report, even without any attempt to mitigate emitted signal levels toward the horizon from this typical commercial roof top site, the measured levels at all but one location, as expected, were below the -77.6 dBm/m^2/MHz threshold level. The one exception involved an exceedance by less than 1 dB at a location with a significant ground elevation above the base of the building on which the earth station is deployed. ViaSat explains that even in this one case, it would be easy to install shielding that would reduce the generated PFD at this location by about 1 dB to below that threshold level.

In short, this report supports ViaSat's position that the careful design, placement, and installation of 28 GHz earth stations readily would allow their deployment virtually anywhere 5G/UMFU may also deploy, even in urban and suburban environments.

Please contact the undersigned if you have any questions regarding this submission.

Respectfully submitted,

/s/

John P. Janka

Attachment

cc: Jose Albuquerque
Bahman Badipour
Simon Banyai
Brian Butler
Chip Fleming
Michael Ha
Tim Hilfiger
Dante Ibarra
Ira Keltz
Antonio Lavarello
Michael Mullinix
Robert Nelson
Charles Oliver
Nicholas Oros
Barbara Pavon
Matthew Pearl
John Schauble
Catherine Schroeder
Blaise Scinto
Jeff Tignor
Janet Young
Nancy Zaczek

Analysis of 1.8 meter Antenna Measurement Test Results for 27.5 – 28.35 GHz

Introduction

ViaSat has been a consistent proponent of spectrum sharing on reasonable and equitable terms throughout the FCC's Spectrum Frontiers proceeding (*Spectrum Frontiers*).[1] As part of that discussion, ViaSat has provided supporting information about the ability of satellite earth stations to co-exist with future terrestrial fixed and mobile services, including UMFU or 5G. This additional report, combined with independent, third party testing from industry-leading experts using state-of-the-art measurement gear and techniques, further substantiates ViaSat's previous submissions.[2]

Background

ViaSat previously submitted an "Analysis of EIRP density toward the horizon for ViaSat site licensed aggregation and interconnection facilities (AIF)."[3]

That analysis considered three antenna size classes that were representative of the earth stations employed or planned to be employed as AIFs for its three generations of High Capacity Service (HCS) satellites.

Subsequent to submittal of that analysis, ViaSat performed testing around an existing 1.8 m antenna at its Carlsbad, California headquarters and found no detectable signal level above the spectrum analyzer noise floor at each ground level measurement location.[4]

Following release of the *Spectrum Frontiers Order* in July 2016 and the adoption of sharing criteria for protected earth stations of -77.6 dBm/(m^2 * MHz) as measured 10 m above ground level (AGL), ViaSat engaged Comsearch to conduct measurements ("Comsearch Testing") around a 1.8 m antenna at 2 m (ground level) and 10 m AGL (the FCC-specified antenna height for measurement). A report of the Comsearch Testing is attached as Annex 1.

The goal of the testing was twofold. First, to determine whether free space loss conditions alone applied or whether additional losses were present along the azimuths to the various test

---

[1] *See, e.g.*, Comments of ViaSat, Inc., Further Notice, GN Docket No. 14-177, et al., at 4 (Sept. 30, 2016); *Use of Spectrum Bands Above 24 GHz for Mobile Radio Services*, Report and Order, 31 FCC Rcd 8014 (2016) ("*Spectrum Frontier Order*").

[2] ViaSat commissioned Comsearch, a national radio frequency expert consultancy. Comsearch engineers average over 15 years of field engineering experience, using state-of-the-art measurement equipment and techniques, with extensive propagation experience. URL: http://comsearch.com/services/site-services/rf-test-measurements/.

[3] ViaSat, Inc., Notice of *Ex Parte* Presentation, GN Docket No. 14-177, *et al*., at Attachment 2 (Apr. 21, 2016) ("ViaSat April 21 *Ex Parte*").

[4] ViaSat, Inc., *Ex Parte* Letter, GN Docket No. 14-177, *et al*., at 8 (July 7, 2016) ("ViaSat July 7 *Ex Parte*").

measurement locations. Second, to determine if the antenna transmitting at the nominal power density of a third generation AIF would meet the expected power flux density (pfd) value at the distance filed in the ViaSat April 21 *Ex Parte*.

Transmitting Antenna Characteristics

While minor performance differences due to different feed configurations can be expected, the 1.8 m antenna in question is representative of the type of 1.8 m antenna to be used for future AIFs for the ViaSat third generation HCS satellites. The antenna is roof mounted on a three-story building with parapet wall of varying height around the roof top. The parapet wall is part of the architectural design of the building and provides visual screening of roof top equipment such as HVAC units and other antennas. The height of the parapet wall varies between one and a half and three feet. In addition to the parapet wall, the roof of the building also includes a recessed area approximately two and half feet deep to further aid in screening roof-top equipment from view.

The 1.8 m antenna is mounted in the roof-top recessed area and aligned to point at the WildBlue-1 satellite at 111.1° W.L. The nominal pointing angles for this spacecraft are 168.8° azimuth and 50.1° elevation.

Because no measureable signal had been detected at ground level during prior testing, the testing with Comsearch was configured to use a CW carrier rather than a modulated carrier to provide a better C/N and increase the likelihood of signal detection at the various measurement locations. To operate the antenna, the testing used a standard ViaSat integrated assembly which incorporates a combined modem and radio frequency transceiver all in one module.

The power into the antenna feed was configured to be 0 dBW (1 W) and verified at the antenna feed port to be -0.4 dBW using calibrated test equipment prior to the start of testing. Comsearch verified that the bursting CW signal being transmitted at the frequency of 28212.5 MHz was readily observable at the roof-top location, inside of the parapet wall, with the spectrum analyzer configured to maximum hold.

Following confirmation of source signal calibration, Comsearch proceeded to make measurements at various locations in the area around the building at both ground level (2 m AGL) and at the FCC reference *Spectrum Frontiers Order* UMFU operational antenna height of 10 m AGL. Photos of the test locations and screen shots of the spectrum analyzer plots can be found in Section 3 of the Comsearch report, and a summary of the resultant signal level measurements are provided in Tables 4.1 and 4.2 in Section 4 of the Comsearch report.

Analysis

There are two parts to the analysis. The first part examines whether a signal was present at a location when Comsearch made their measurement, and if so how the signal compared to the

predicted value assuming free space losses alone and whether there were additional losses in the path. The second part uses the measured signal values and other information about the ViaSat AIF to calculate the power flux density associated with each measurement. Both of these analyses are described below.

Signal Presence Measurement and Additional Losses Analysis

Comsearch performed measurements with calibrated test equipment using the industry standard signal substitution method, as recommended by the National Spectrum Management Association (NSMA).[5] The signal value results recorded in Tables 4.1 and 4.2 of the Comsearch report and represent the measured level of the CW carrier transmitted from the 1.8 m antenna system being tested, as reduced by path loss and additional losses between the antenna and measurement location. It should be noted that the recorded values suffixed with NF indicate that no signal was observed above the measurement system's noise floor (i.e., the recorded value was that of the noise floor in that instance). Because a spectrum analyzer functions like any other receiver, its noise floor is affected in the same way by signals (or interference) being received. The increase in the displayed response above the noise floor in dB is calculated as:

$10\ \log_{10}\left(1+10^{\frac{I/N}{10}}\right)$, where I and N are the actual interference and noise levels (1)

For example, if the received signal is equal to the noise floor, the two add in amplitude and the displayed response is twice that of the noise alone and a 3 dB rise above the noise floor is observed. A signal -12.2 dB lower than the noise floor results in a 0.25 dB increase in the displayed value. Given that no visible response was seen on the analyzer, the actual signal value then was likely more than 10 dB below the noise floor[6].

To determine the additional loss, if any, over and above free space path loss in the direction of the measurement location, the EIRP in the direction of the measurement location must first be determined.

To do this, antenna gain in the direction of the measurement location is added to the transmitter power being applied the antenna feed. Tables 4.1 and 4.2 of the Comsearch report contain the azimuths to and from the transmitting antenna, as well as the distance in meters. The Comsearch tables do not, however, reference the bearing along which the antenna is transmitting, nor is the elevation angle of the transmitting antenna included.

[5] The National Spectrum Management Association (see URL: http://nsma.org/), Recommendation WG 4.88.013 Rev.1

[6] Spectrum Analyzer Noise Measurements, HP Application Note 150-4, 1974; and Spectrum Analyzer Measurements and Noise, Agilent Application Note 1303.

The transmit antenna's bearing and the elevation angle information are needed in order to determine the off-axis angle in azimuth and in elevation in order to determine the estimated off-axis gain discrimination in the direction of the signal measurement site. This information is provided in the Transmitting Antenna Characteristics section above. The operating azimuth angle of the 1.8 m antenna is 168.82° (as referenced to True North at 0°) and the elevation angle is 50.1°.

With this information and the antenna gain patterns, the EIRP density in the direction of the measurement site can be calculated. For example, for measurement Site 1, the azimuth angle from the transmitting antenna toward the measurement site is given as 170.29° in Table 4.1 of the Comsearch report. Subtracting the transmitting antenna's bearing toward WildBlue-1 of 168.82° from 170.29° yields an off-axis angle of 1.47°. By examining the manufacturer's antenna gain patterns, attached as Annex 2,[7] it can be seen that the off-axis gain discrimination in azimuth is 35 dB and the gain discrimination in elevation is 70 dB, so the larger of the two values is used. In reviewing the off-axis angles for each site, it can be seen that for all measurement locations, the larger 70 dB elevation off-axis gain discrimination value applies.

The nominal gain at 28.212.5 GHz is 52.59 dBi and the input power to the antenna is -0.4 dBW, so the EIRP toward the horizon is -0.4 dBW + (52.59 dBi – 70 dB) = -17.81 dBW.

Using the free space path loss (FSL) formula (2), the expected FSL for the 66.14 m distance is calculated in dB as 97.86 dB.

$$10\ log\left(\left[\frac{4\pi d}{\lambda}\right]^2\right) \qquad (2)$$

The expected measurement value is then the EIRP – FSL = -115.67 dBW. The actual measured value recorded for Site 1 in Table 4.1 was -137.51 dBW. The additional loss is then -115.67 dBW minus -137.51 dBW = 21.84 dBW.

The process was repeated for each of the measurement sites and measurement heights (2 m and 10 m) and the results are recorded in Table 1.

[7] Annex 2, General Dynamics Antenna Test Report.

Measurement Location	Measurement Height (m)	Free Space Loss (dB)	Recorded Signal (dBW)			Expected Signal (dBW)			Additional Losses (dB)
Site 1	10	97.86	-137.51			-115.67			21.84
Site 1	2	97.86	-158.19	NF		-115.67		≫	42.52
Site 2	10	98.30	-149.10			-116.11			32.99
Site 2	2	98.30	-155.56	NF		-116.11		≫	39.45
Site 3	10	103.43	-141.30			-123.24			18.06
Site 3	2	103.43	-159.65	NF		-123.24		≫	36.41
Site 4	10	107.46	-133.25			-125.27			7.98
Site 4	2	107.46	-160.00	NF		-125.27		≫	34.73
Site 5	10	111.46	-140.68			-129.27			11.41
Site 5	2	111.46	-147.78			-129.27			18.51
Site 6	10	112.33	-144.95			-130.14			14.81
Site 6	2	112.33	-154.82			-130.14			24.68
Site 7	10	110.59	-155.96	NF		-128.40		≫	27.56
Site 7	2	110.59	-158.19	NF		-128.40		≫	29.79
Site 8	10	109.03	-158.63	NF		-126.84		≫	31.79
Site 8	2	109.03	-158.63	NF		-126.84		≫	31.79
Site 9	10	111.04	-158.10	NF		-128.85		≫	29.25
Site 9	2	111.04	-159.44	NF		-128.85		≫	30.59
Site 10	10	112.47	-158.60	NF		-130.28		≫	28.32
Site 10	2	112.47	-158.77	NF		-130.28		≫	28.49
Site 11	10	98.87	-157.48	NF		-116.68		≫	40.80
Site 11	2	98.87	-158.78	NF		-116.68		≫	42.10

Table 1 Recorded vs Expected Signals and Additional Losses for Measurement Locations

Examining the results in Table 1 shows that in many cases for the 10 m reference height and for the majority of the 2 m height measurement locations, no signal was observed above the test equipment noise floor. The largest observed signal was at the Site 4 location. The measurement location also had the lowest additional losses above the expected free space loss of 8 dB. This result was anticipated because the terrain at that signal test location is approximately 20 feet above the terrain at the base of the building on which the transmitting antenna is located. Also, from the Comsearch photos it can be seen that the parapet wall on that area of the building where the transmitting antenna is located was at the lowest height and the measuring antenna had a line of sight view to the transmitting antenna. Raising the parapet wall in the direction of the higher terrain would provide additional blockage and increase the losses above the FSL.

Power Flux Density Measurement

The second part of the analysis is to determine the power flux density at each of the measurement locations. To use the Comsearch results meaningfully, the recorded signal level

values must first be scaled to a reference bandwidth and converted to a flux density. That is, converted from dBW to dBW/(m^2 * MHz).

While the transmitted power of the unmodulated CW carrier from the 1.8 m antenna is known, to convert the power to a power density that represents the third generation AIF, the modulated bandwidth associated with that power level in normal operation must be known or calculated for use in the density conversion.

In the ViaSat April 16 *Ex Parte*, the antenna input density for the third generation AIF was projected to be -19.0 dBW/MHz. However, since that *ex parte* was filed, ViaSat has further reduced the expected nominal antenna input power density for this class AIF to -24.3 dBW/MHz.

The equivalent bandwidth over which the -0.4 dBW input power to the 1.8 m antenna would be spread in normal operation of a third generation AIF is then 10^(-0.4/10)/10^(-24.3/10) = 245.5 MHz.

To calculate the power density in dBW/MHz, the bandwidth adjustment in dB is calculated as 10 log (245.5 MHz/1 MHz) = 23.9 dB(MHz). This result is subtracted from the measured value to calculate the power density. For Site 1, this is -137.51 dBW – 23.9 dB(MHz) = -161.41 dBW/MHz.

To complete the conversion from power density to power flux density (pfd), the meter squared area gain is added to the power density.

Meter squared area gain = $10 \log \frac{4\pi}{\lambda^2}$ = 50.46 dB/m^2 (3)

The measured pfd is then -161.41 dBW/MHz + 50.46 dB/m^2 = -111 dBW/(m^2 * MHz), or -81 dBm/(m^2 * MHz).

The conversion process was repeated for each of the measurement sites and measurement heights (2 m and 10 m) and the results were recorded in Table 2.

Measurement Location	Measurement Height (m)	Recorded Signal (dBW)		Power Density (dBW/MHz)	Power Flux Density (dBW/(m^2*MHz)		
Site 1	10	-137.51		-161.44			-110.98
Site 1	2	-158.19	NF	-182.12		≪	-131.66
Site 2	10	-149.10		-173.03			-122.57
Site 2	2	-155.56	NF	-179.49		≪	-129.03
Site 3	10	-141.30		-165.23			-114.77
Site 3	2	-159.65	NF	-183.58		≪	-133.12
Site 4	10	-133.25		-157.18			-106.72
Site 4	2	-160.00	NF	-183.93		≪	-133.47
Site 5	10	-140.68		-164.61			-114.15
Site 5	2	-147.78		-171.71			-121.25
Site 6	10	-144.95		-168.88			-118.42
Site 6	2	-154.82		-178.75			-128.29
Site 7	10	-155.96	NF	-179.89		≪	-129.43
Site 7	2	-158.19	NF	-182.12		≪	-131.66
Site 8	10	-158.63	NF	-182.56		≪	-132.10
Site 8	2	-158.63	NF	-182.56		≪	-132.10
Site 9	10	-158.10	NF	-182.03		≪	-131.57
Site 9	2	-159.44	NF	-183.37		≪	-132.91
Site 10	10	-158.60	NF	-182.53		≪	-132.07
Site 10	2	-158.77	NF	-182.70		≪	-132.24
Site 11	10	-157.48	NF	-181.41		≪	-130.95
Site 11	2	-158.78	NF	-182.71		≪	-132.25

Table 2 Calculated Power Flux Density for Measurement Locations

Examining the results in Table 2 it can be seen that all but one measured value was below the *Spectrum Frontiers Order* sharing criteria limit of -77.6 dBm/(m^2 * MHz). The measured value for Site 4 which had the highest terrain and lowest additional losses, was the only value which exceeded the FCC limit. The exceedance of the limit by 0.9 dB, would easily be mitigated by a modest increase in the parapet wall on that side of the building where terrain is higher.

Conclusion

While the transmitting antenna tested here normally operates in the conventional Ka band, and accordingly was not sited with 5G/UMFU sharing constraints in mind, this type of roof top mounting scenario is quite common for modest sized earth stations in urban or suburban commercial settings. Even with no special care taken to mitigate signal levels toward the horizon, the measured levels for all but one location were below the FCC's sharing criteria, and in many cases significantly so.

With some care used in new installations, it would be fairly easy to shield the antenna from nearby 5G/UMFU operations and thereby allow siting of earth stations close to fiber even in urban environments where 5G/UMFU will be or has deployed.

DECLARATION

I hereby declare that I am the technically qualified person responsible for preparation of the engineering information contained in this report, that I am familiar with Part 25 of the Commission's rules, that I have either prepared or reviewed the engineering information submitted with this report, and that it is complete and accurate to the best of my knowledge, information and belief.

Daryl T. Hunter, P.E.
Senior Director, Regulatory Affairs
ViaSat, Inc.
6155 El Camino Real
Carlsbad, CA 92009

April 12, 2017

Annex 1 – Comsearch Report

RADIO FREQUENCY SIGNAL MEASUREMENT REPORT

Prepared For

ViaSat

Carlsbad, CA

Transmit Station
28 GHz

February 2017

19700 Janelia Farm Boulevard. - Ashburn, Virginia 20147, USA - 703.726.5500 - Fax 703.726.5597

TABLE OF CONTENTS

SECTION

ONE

SECTION 1

INTRODUCTION AND BACKGROUND

1.1 Introduction

On-site Radio Frequency (RF) transmission measurements were performed on behalf of ViaSat, Inc. on February 14,2017 at their existing site in Carlsbad, CA. The purpose of the measurements was to determine relative RF levels in the 27.5-28.35 GHz band with respect to expected free space loss and to evaluate the effectiveness of using a typical rooftop earth station installation to screen transmissions from nearby terrestrial receivers. The purpose of this report is to document the results of these measurements:

- 1.8 Meter TX Antenna
- Satellite Arc: 111.1 Degrees West Longitude
- Frequency Considered: 28,212.5 MHz
- Transmit Power: 1 Watt / 30 dBm
- Type of Reception: CW
- Measured Rx Antenna Center Line: 10 meters Above Ground Level

1.2 Background

ViaSat, Inc requested that Comsearch perform receive level testing using a calibrated system to measure receive signal levels from a CW carrier being transmitted from a rooftop mounted 1.8-meter antenna in the areas surrounding the antenna. The antenna is located on the roof of a 3 story building, in the center portion of the roof, in a depressed area. The coordinates of the test transmit antenna are: 33° 0 7' 38.31"N and 117° 15' 55.13"W. The roof has a short parapet wall (varying between approximately 1.5 feet and 3 feet) at the edge but no other substantial items which would provide blockage. The antenna is located in a depression in the roof which is approximately 2.5 feet deep.

An unmodulated CW carrier was used because previous testing at ground level using a modulated carrier had resulted in no detectable signals. By using a CW carrier, the power density in the measurement bandwidth was increased considerably. Additionally, testing at both ground level (2 m) and 10 m were requested for the new tests in order to improve the likelihood of detecting a signal above the noise floor of the measuring equipment.

The ground test locations were determined by drawing multiple arcs at 50 meter distances from the building and where those circles intersected with the main beam, 45 and 90 degree off main

beam locations. Tests were conducted as close as possible to those crossings where possible. Because of the lack of signals above the noise floor during previous tests and the difficulty of crossing the busy roadway to the West of the antenna with the boom lift, testing on that side of the street was planned only if testing there was deemed warranted.

The measurement sites are identified on a portion of a topographic map shown in Figure 1.2-1. An aerial photo of the site locations are shown in Figure 1.2-2.

1.3 Assumptions &Constraints

The analysis in this report is based upon the following assumptions and constraints.

- It was verified that during the measurement period the transmit antenna was active and operating at the specified transmit power ±1 dB.
- The signal identification and frequencies of the test carrier were specified by ViaSat.
- The actual ground elevation of the site is based on the data from the topographic map.

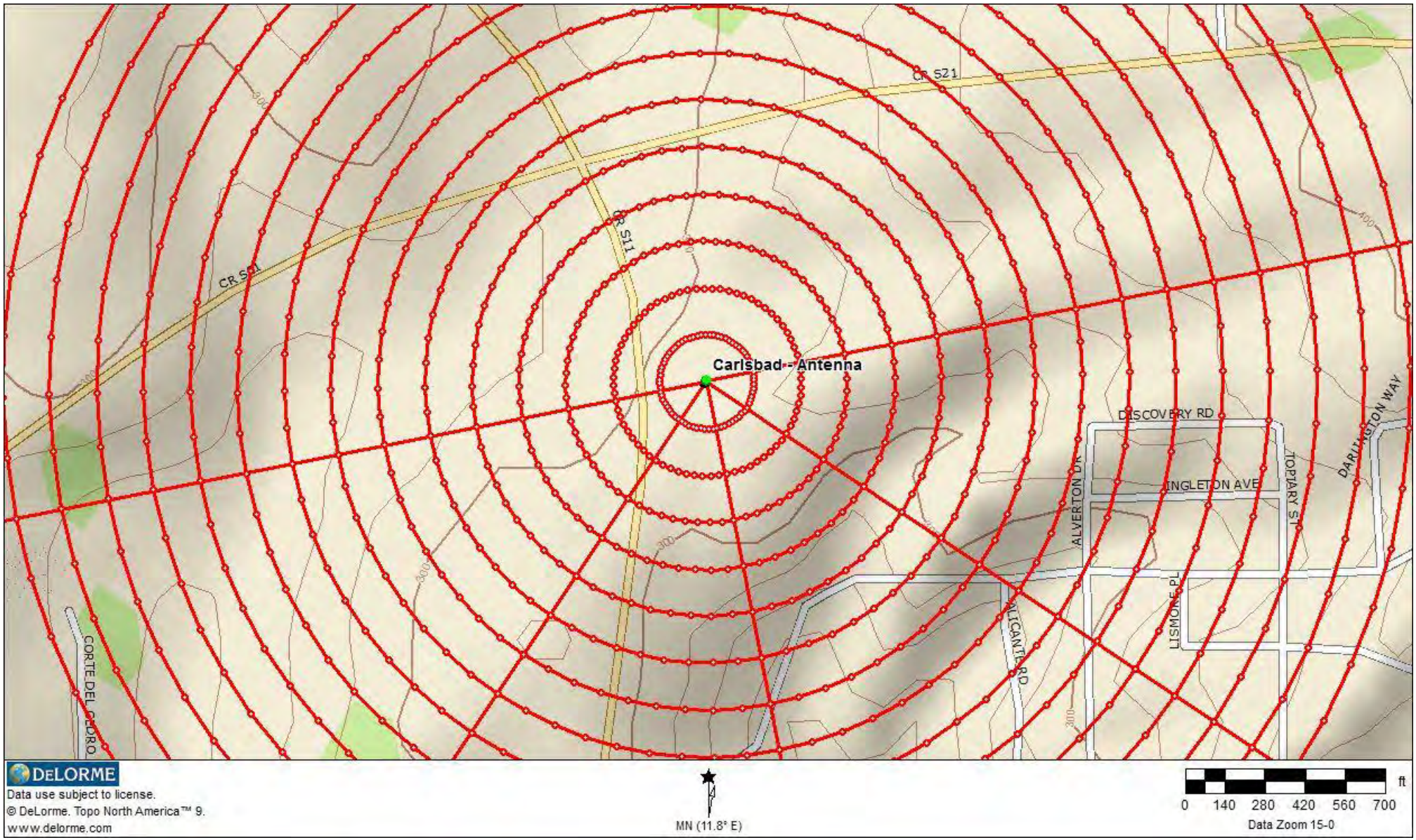

Figure 1.2-1 – Topographic Map

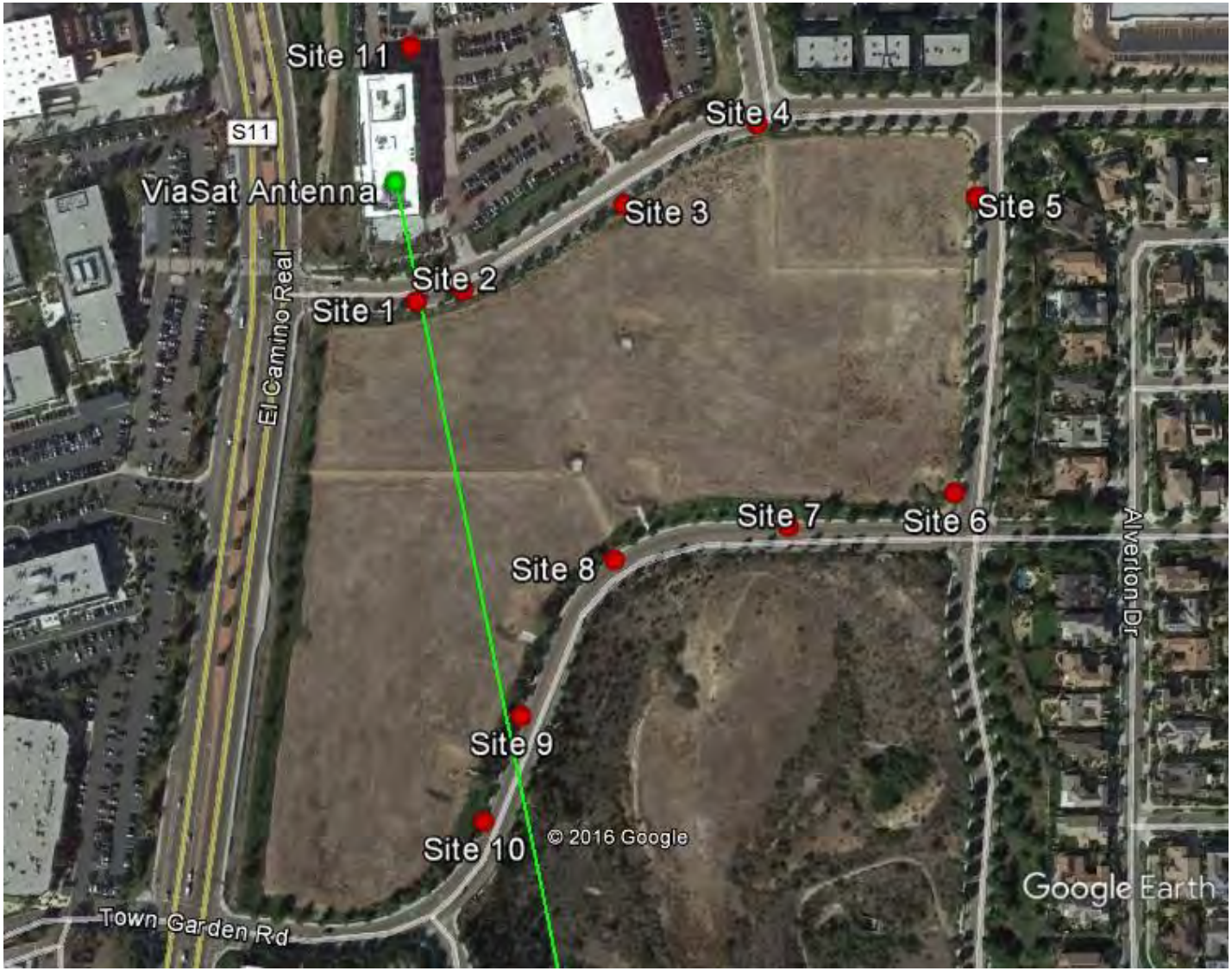

The green line is the main beam azimuth. Red dots show measurement locations,

Figure 1.2-2 – Aerial Photograph

SECTION

TWO

SECTION 2

TEST PROCEDURE

2.1 Calibration

Figures 2.1-1 is the block diagram of the test set for all bands to be tested. All test equipment used was allowed a proper warm-up period prior to calibration. The test set was calibrated by the signal substitution method, as recommended by NSMA, utilizing a synthesized signal generator. The reference signal from the signal generator was adjusted for the center frequency of each band to be tested and measured with a thermal power meter for calibrated reference test level (-60 dBm). This calibrated reference signal from the signal generator was then injected into the end of the coaxial cable of the test set at the point, which normally connects to the test antenna. A spectrum analyzer then measured the reference test signal level after passing through the test set. Upon completion of the calibration process, a known reference level was obtained for the measurements that correspond to a given set of spectrum analyzer display readings.

The following formula is used to transform the measured signal level as read on the spectrum analyzer display (dBm) to an isotropic reference signal level (dBW_I) as seen at the point of test:

$$dBW_I = LI - EG - 30$$

Where: dBW_I = Isotropic level in dBW

LI = Level (dBm) of injected signal

EG = External Gain = Test antenna gain + LNA Gain

at 28 GHz: dBW_I = -60 dBm - 45.9 dB

= -105.9 dBm_I

In this instance, the spectrum analyzer displayed measured signal level of –60 dBm equates to an isotropic signal level of –105.9 dBm_I.

Figure 2.1-2 displays the spectrum photograph of the described calibration procedure employed during these measurements.

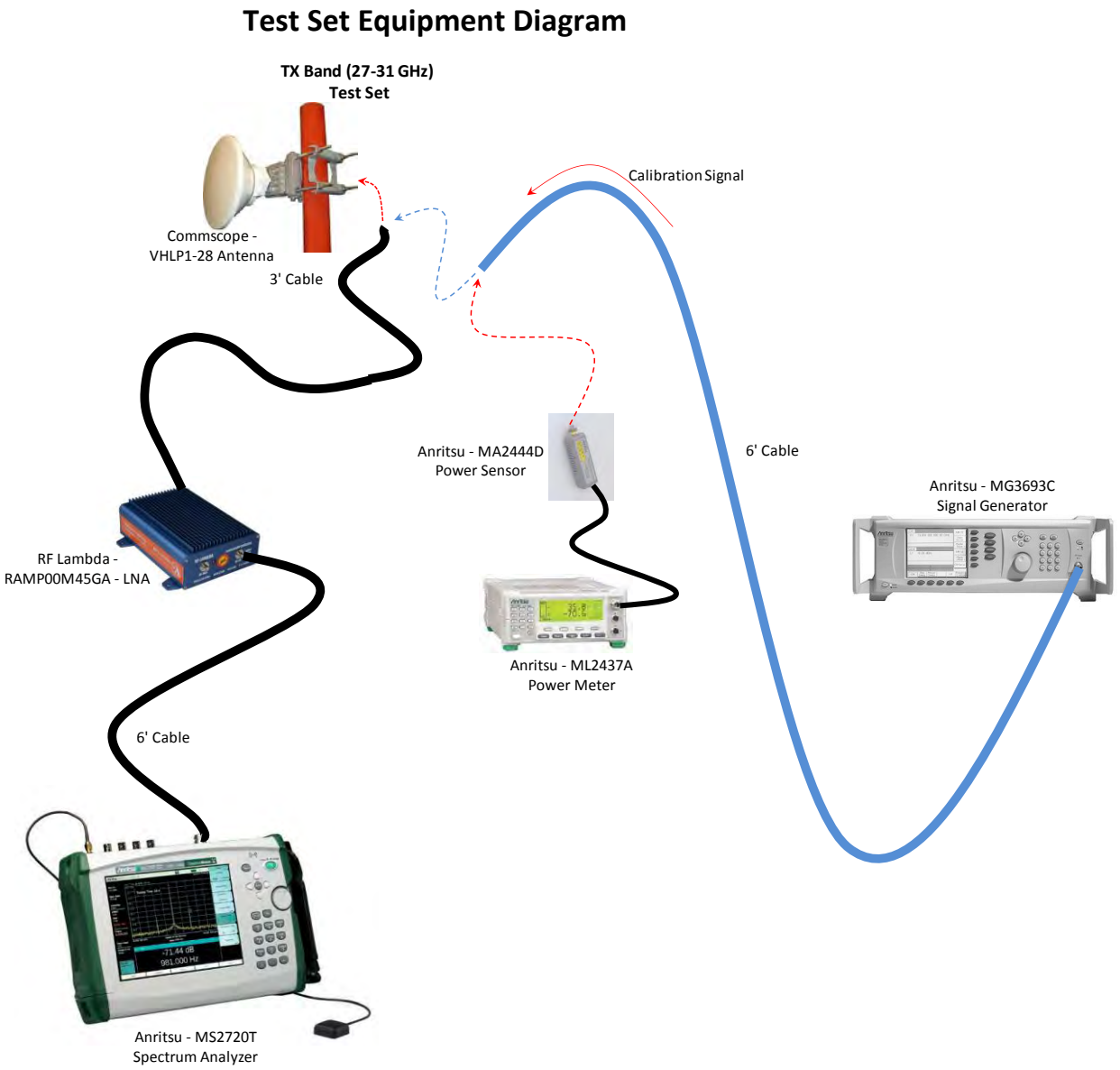

Figure 2.1-1 Receive Test Equipment Block Diagram

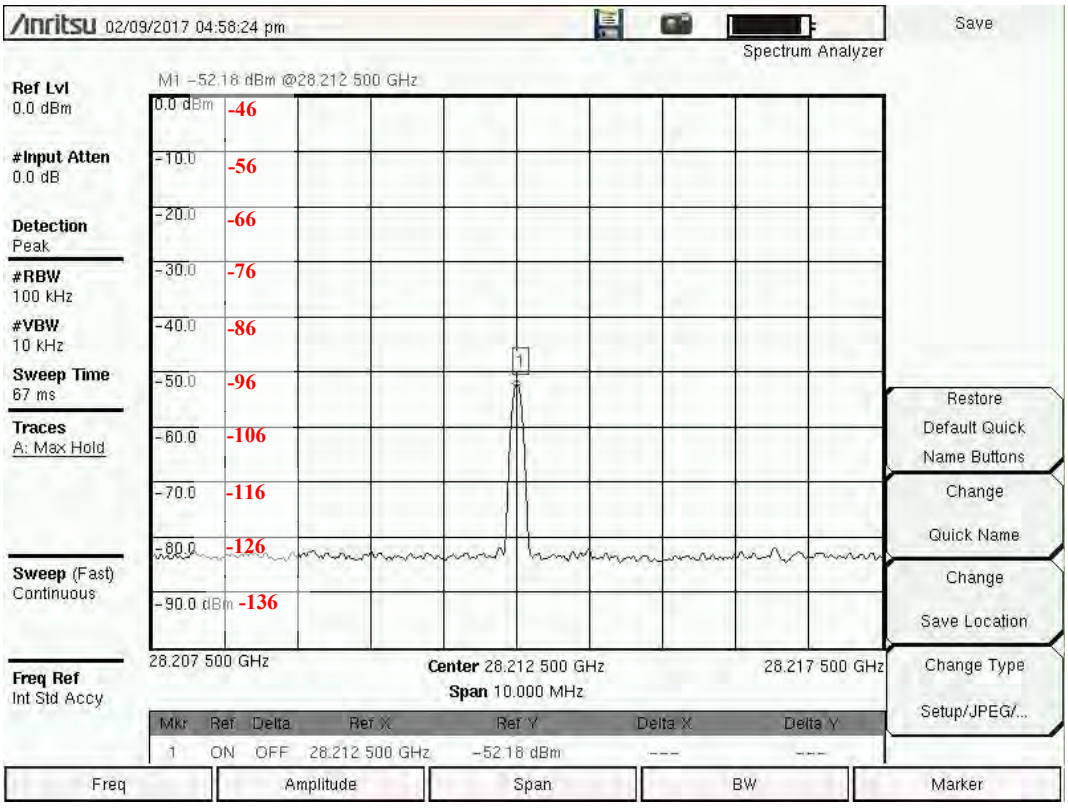

A -52.18 dBm , 28212.5 MHz signal indication on the spectrum photograph represents a -60 dBm signal being injected at the point where the test cable connects to the output of the test antenna.

Displayed reference level is equal:
-60 dBm injected signal
-45.9 dB external gain
-105.9 dBm_I; therefore, a displayed signal level of -70 dBm equals an isotropic level of -116 dBm_I

Adjusted measurement values (dBm_I) shown in red

Figure 2.1-2 Calibration Spectrum Photo 28 GHz

2.2 Methodology

The test equipment was set up and calibrated to measure the RF environment. Measurements were conducted at in such a way that would show if the signal from the transmitter was visible above the test equipment's noise floor for the 27.5-28.35 GHz band. After the equipment calibration was completed, the test antenna was mounted on a motorized boom lift and elevated to a height of 10 meters AGL. The tests were conducted by activating the peak hold function of the spectrum analyzer. This enabled the analyzer to maintain and display the maximum signal level received for the frequency under consideration. The test antenna was peaked while pointed at the transmit antenna to attempt to receive any signal from the transmit antenna. "

Table 3.1-1, item 8. The area on the roof where the TX antenna is located is depressed by approximately 2.5 ft deep.

In tables 4.1 & 4.1, NF = Noise Floor of test measurement system. (So readers won't confuse this with 5G or LMDS equipment NF).

SECTION

THREE

SECTION 3

DATA PRESENTATION

The following section contains the tables and spectrum photos pertaining to the site location measured**.**

3.1 Carlsbad, CA

- Table 3.1-1 presents a site data sheet including all pertinent site information.

- Figures 3.1-1 and 3.1-2 are the photographs depicting the existing earth station site and test locations.

- Figures 3.1-3 (A) through 3.1-3 (V) are the RF spectrum photographs depicting the receive signal measured at the test sites.

TABLE 3.1-1

MEASUREMENT SITE DATA SHEET

1. SYSTEM NAME:	ViaSat, Inc	
2. CITY AND STATE:	Carlsbad, CA	
3. SITE IDENTIFICATION:	Carlsbad	
4. COORDINATES (TX Site): (NAD 1983)	LATITUDE:	33° 07' 38.31" N
	LONGITUDE:	117°15' 55.13" W
5. GROUND ELEVATION:	310 feet AMSL	
6. MEASUREMENT DATE:	February 14, 2017	
7. GEOSTATIONARY ARC RANGE:		
SATELLITE POSITIONS:	111.1° W	
AZIMUTH:	168.8°	
ELEVATION:	50.9°	

8. GEOSTATIONARY ARC VISIBILITY: The TX site is on a 3 story building with a short parapet wall. The TX antenna was also in an area of the roof that is depressed approximately 3 feet.

View of transmit antenna looking north

View of transmit antenna looking south

Figure 3.1-1 (cont.) Earth Station Site Photographs

View of transmit antenna looking south

View of transmit antenna looking west

Figure 3.1-1 (cont.) Earth Station Site Photographs

View from rooftop looking east

View from rooftop looking southeast

Figure 3.1-1(cont.) Earth Station Site Photographs

View from rooftop looking south

View from rooftop looking southwest

Figure 3.1-1 (cont.) Earth Station Site Photographs

View toward TX antenna on rooftop from Site 1 at 10m AGL

View toward TX antenna on rooftop from Site 1 at 10m AGL (zoom)

Figure 3.1-2 Test Locations

View toward TX antenna on rooftop from Site 2 at 10m AGL

View toward TX antenna on rooftop from Site 2 at 10m AGL (zoom)

Figure 3.1-2 (cont.) Test Locations

View toward TX antenna on rooftop from Site 3 at 10m AGL

View toward TX antenna on rooftop from Site 3 at 10m AGL (zoom)

Figure 3.1-2 (cont.) Test Locations

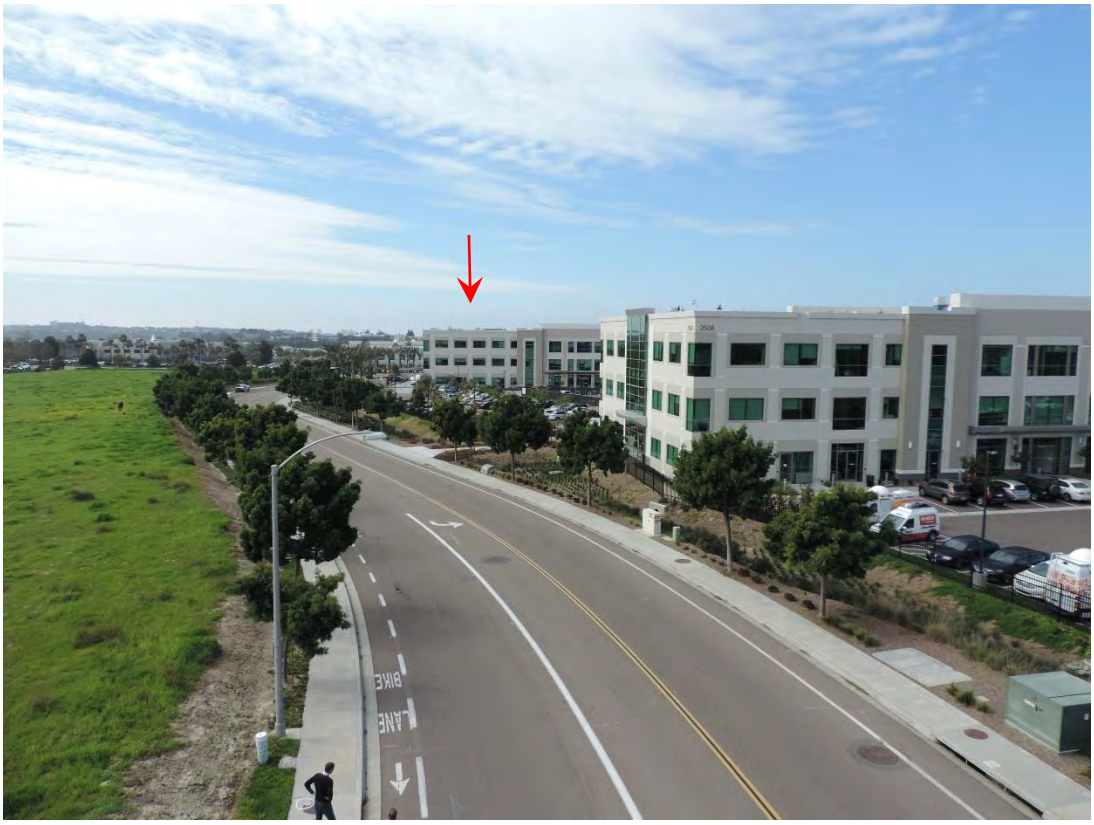

View toward TX antenna on rooftop from Site 4 at 10m AGL

View toward TX antenna on rooftop from Site 4 at 10m AGL (zoom)

Figure 3.1-2 (cont.) Test Locations

View toward TX antenna on rooftop from Site 5 at 10m AGL

View toward TX antenna on rooftop from Site 5 at 10m AGL (zoom)

Figure 3.1-2 (cont.) Test Locations

View toward TX antenna on rooftop from Site 6 at 10m AGL

View toward TX antenna on rooftop from Site 6 at 10m AGL (zoom)

Figure 3.1-2 (cont.) Test Locations

View toward TX antenna on rooftop from Site 7 at 10m AGL

View toward TX antenna on rooftop from Site 7 at 10m AGL (zoom)

Figure 3.1-2 (cont.) Test Locations

View toward TX antenna on rooftop from Site 8 at 10m AGL

View toward TX antenna on rooftop from Site 8 at 10m AGL (zoom)

Figure 3.1-2 (cont.) Test Locations

View toward TX antenna on rooftop from Site 9 at 10m AGL

View toward TX antenna on rooftop from Site 9 at 10m AGL (zoom)

Figure 3.1-2 (cont.) Test Locations

View toward TX antenna on rooftop from Site 10 at 10m AGL

View toward TX antenna on rooftop from Site 10 at 10m AGL (zoom)

Figure 3.1-2 (cont.) Test Locations

View toward TX antenna on rooftop from Site 11 at 2m AGL

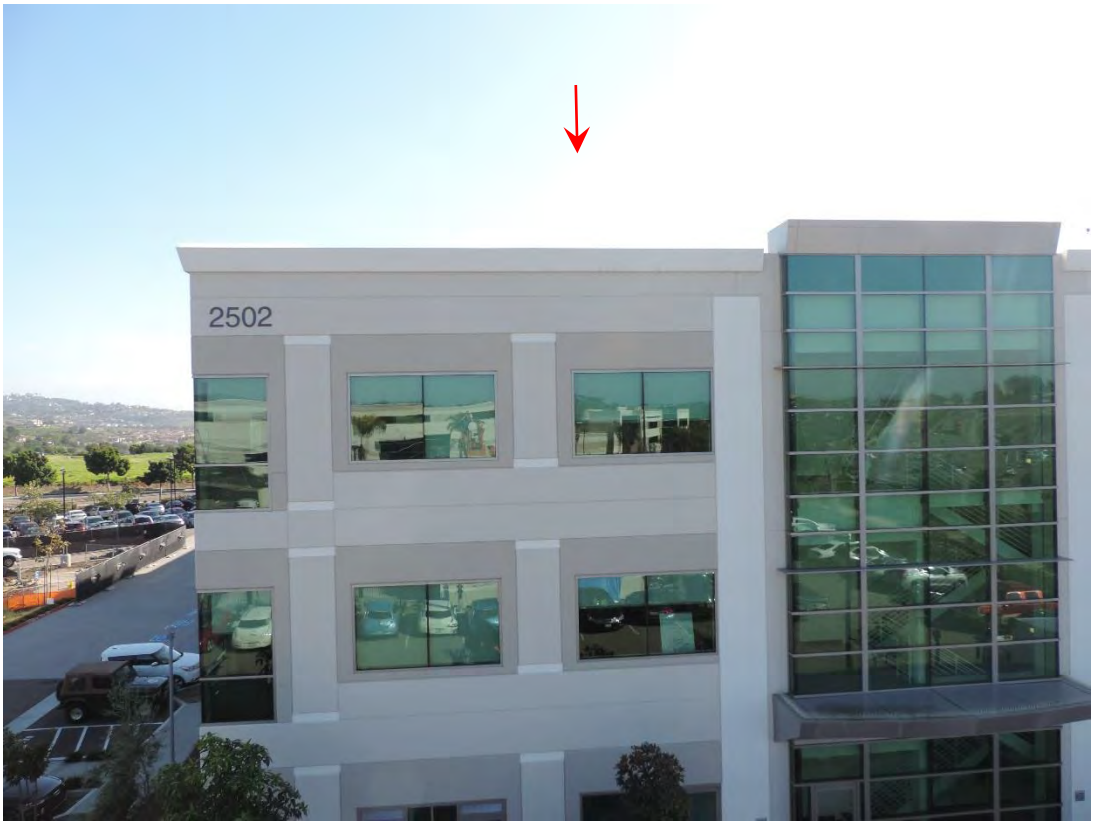

View toward TX antenna on rooftop from Site 11 at 10m AGL (zoom)

Figure 3.1-2 (cont.) Test Locations

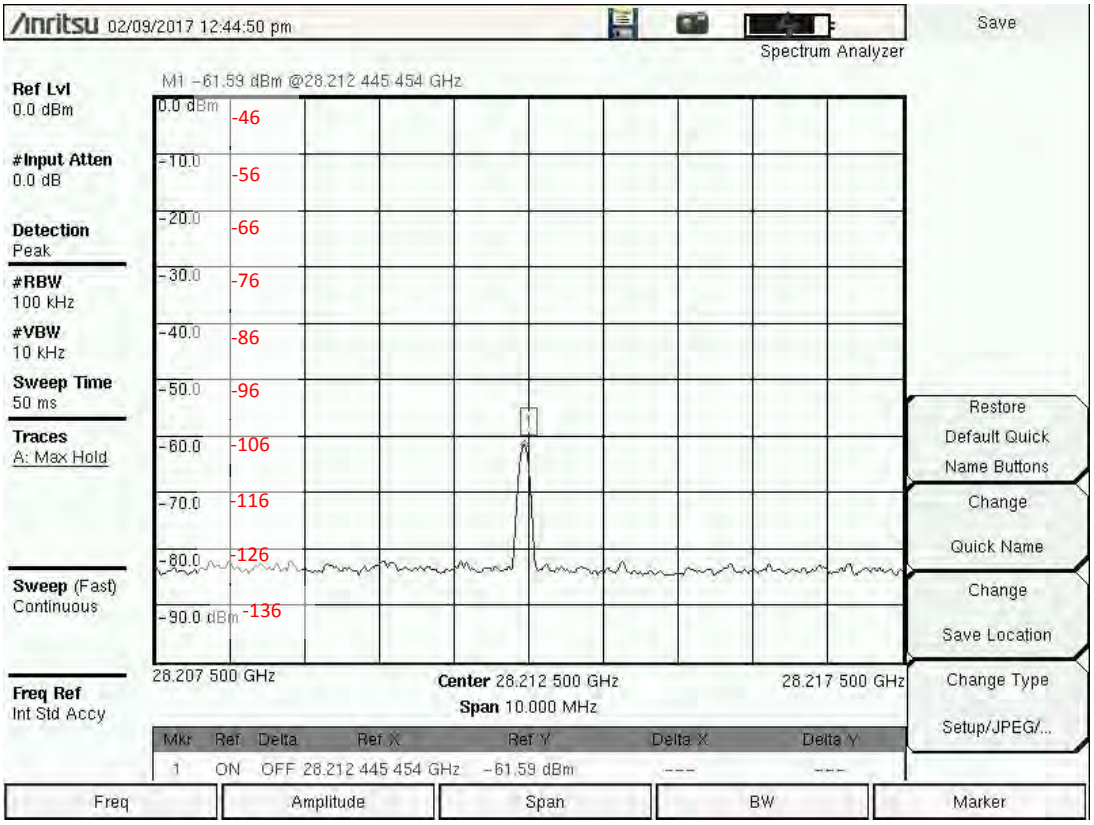

Figure 3.1-3 (A) Spectrum Photos 28 GHz - 100 kHz Res BW Site 1 at 10m AGL

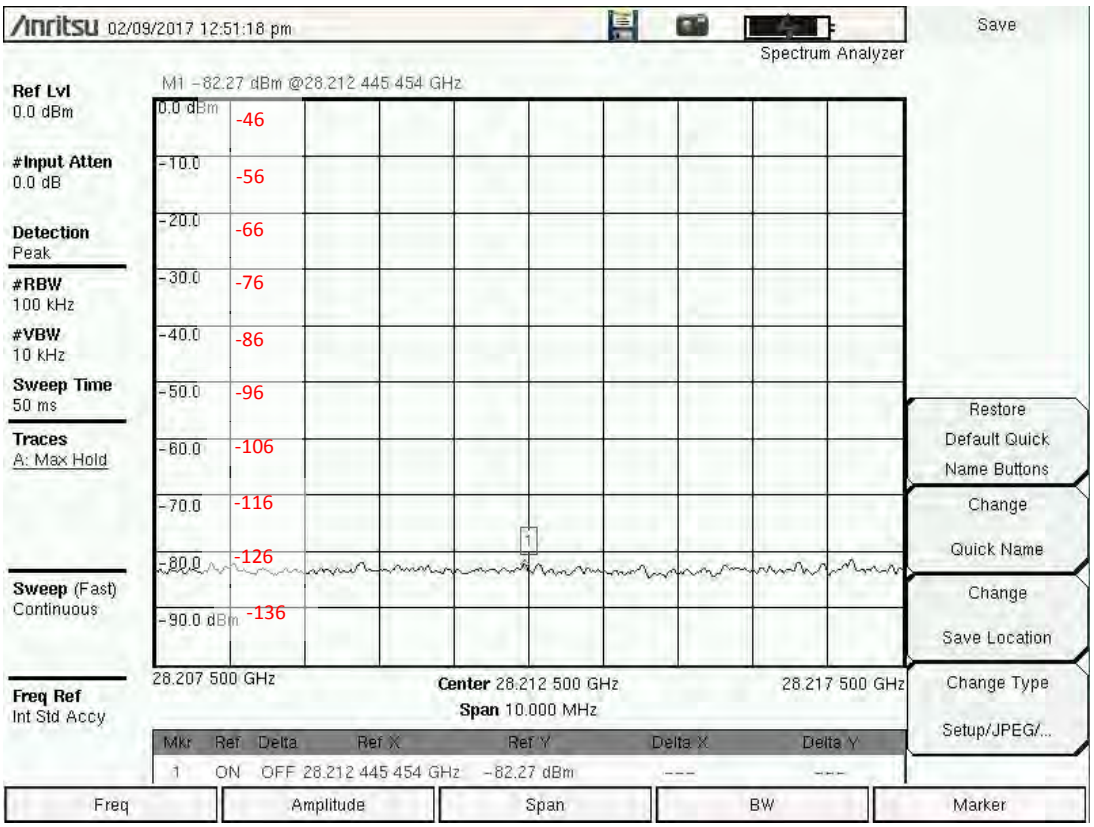

Figure 3.1-3 (B) Spectrum Photos 28 GHz - 100 kHz Res BW Site 1 at 2m AGL

Adjusted measurement values (dBm_I) shown in red

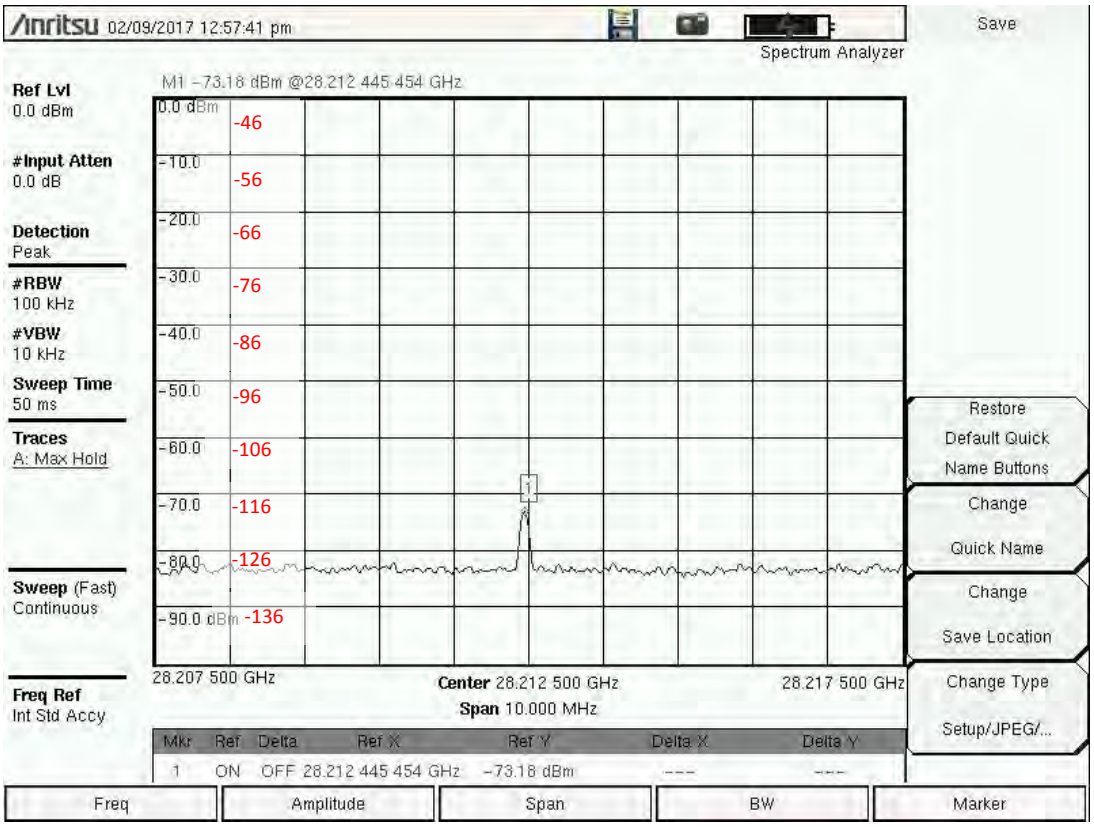

Figure 3.1-3 (C) Spectrum Photos 28 GHz - 100 kHz Res BW Site 2 at 10m AGL

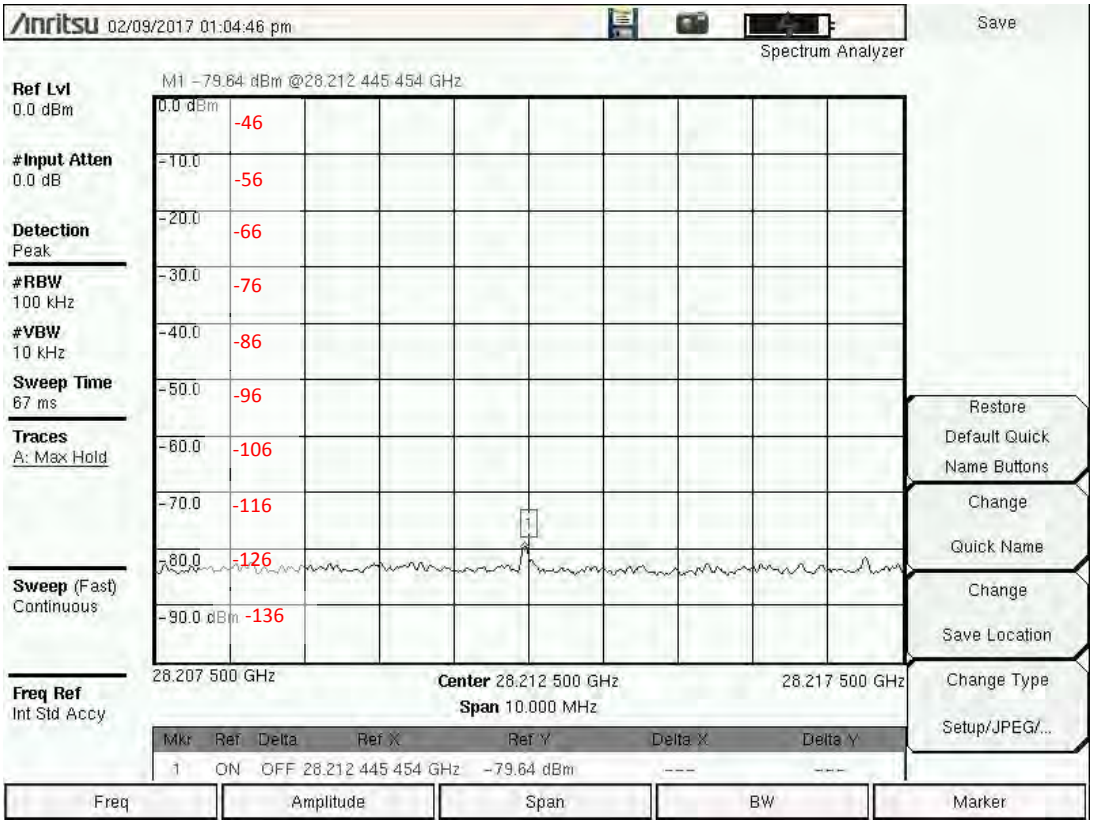

Figure 3.1-3 (D) Spectrum Photos 28 GHz - 100 kHz Res BW Site 2 at 2m AGL

Adjusted measurement values (dBm_I) shown in red

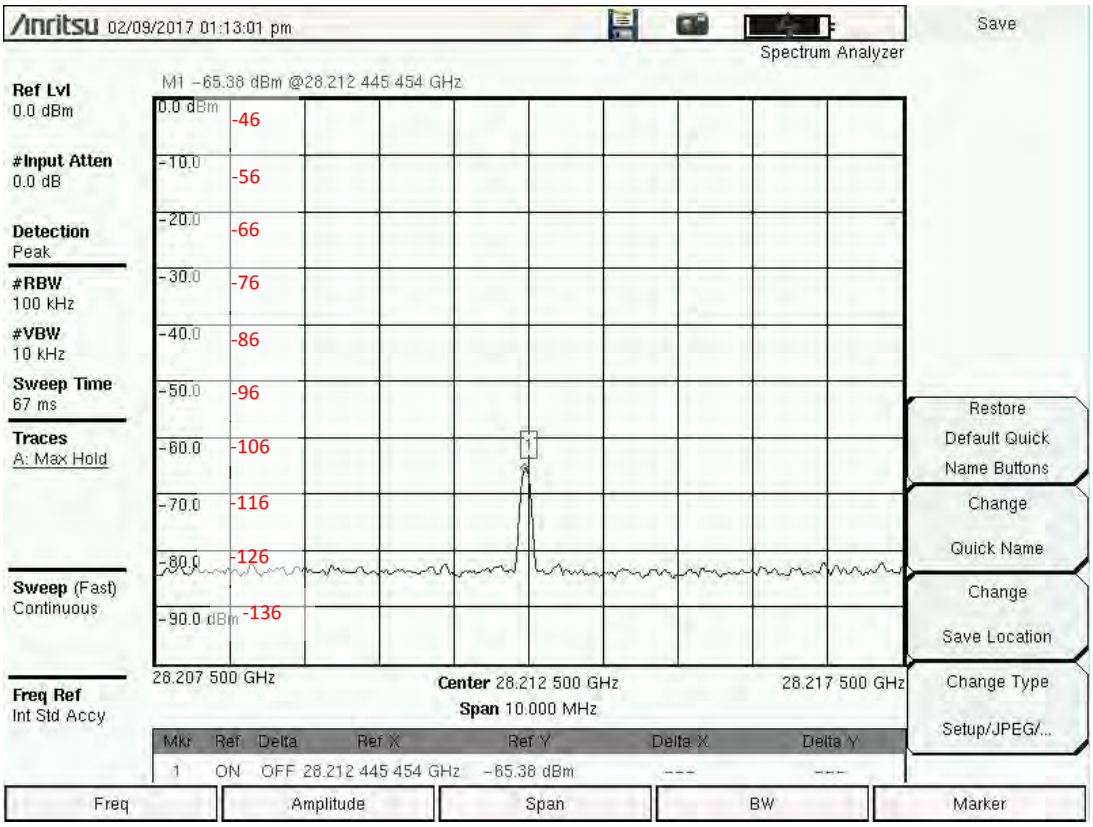

Figure 3.1-3 (E) Spectrum Photos 28 GHz - 100 kHz Res BW Site 3 at 10m AGL

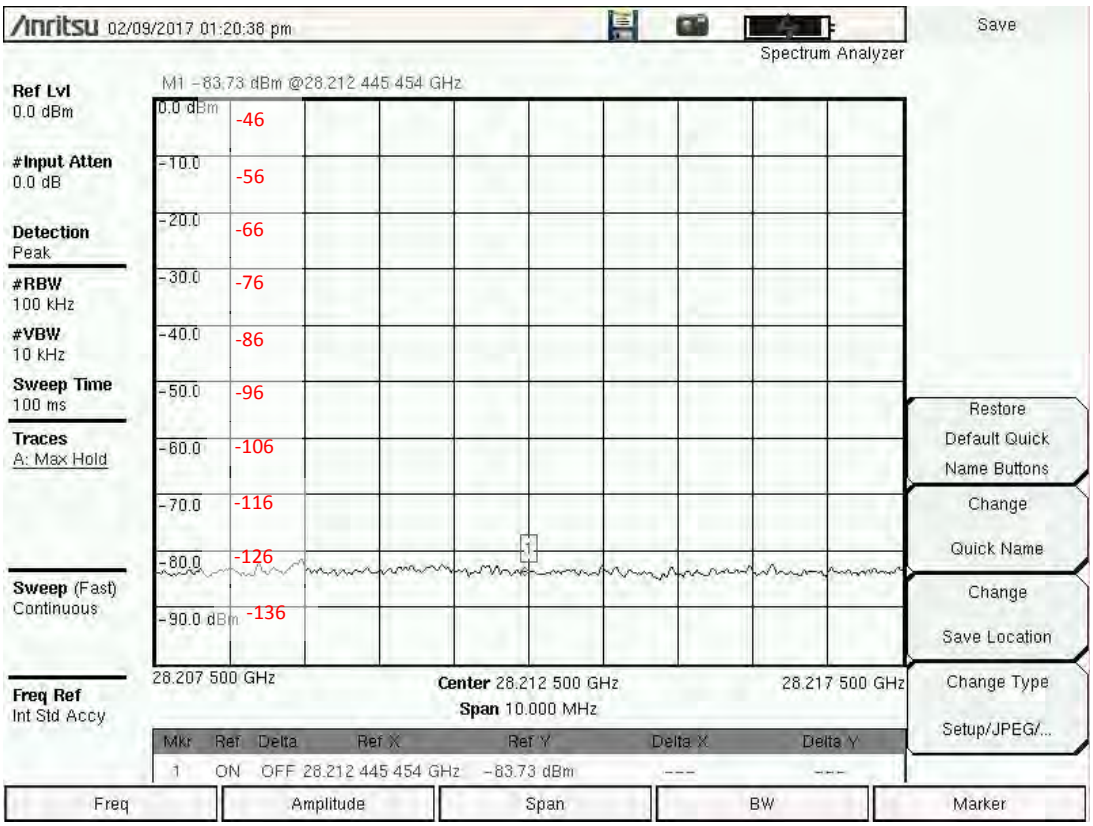

Figure 3.1-3 (F) Spectrum Photos 28 GHz - 100 kHz Res BW Site 3 at 2m AGL

Adjusted measurement values (dBm_I) shown in red

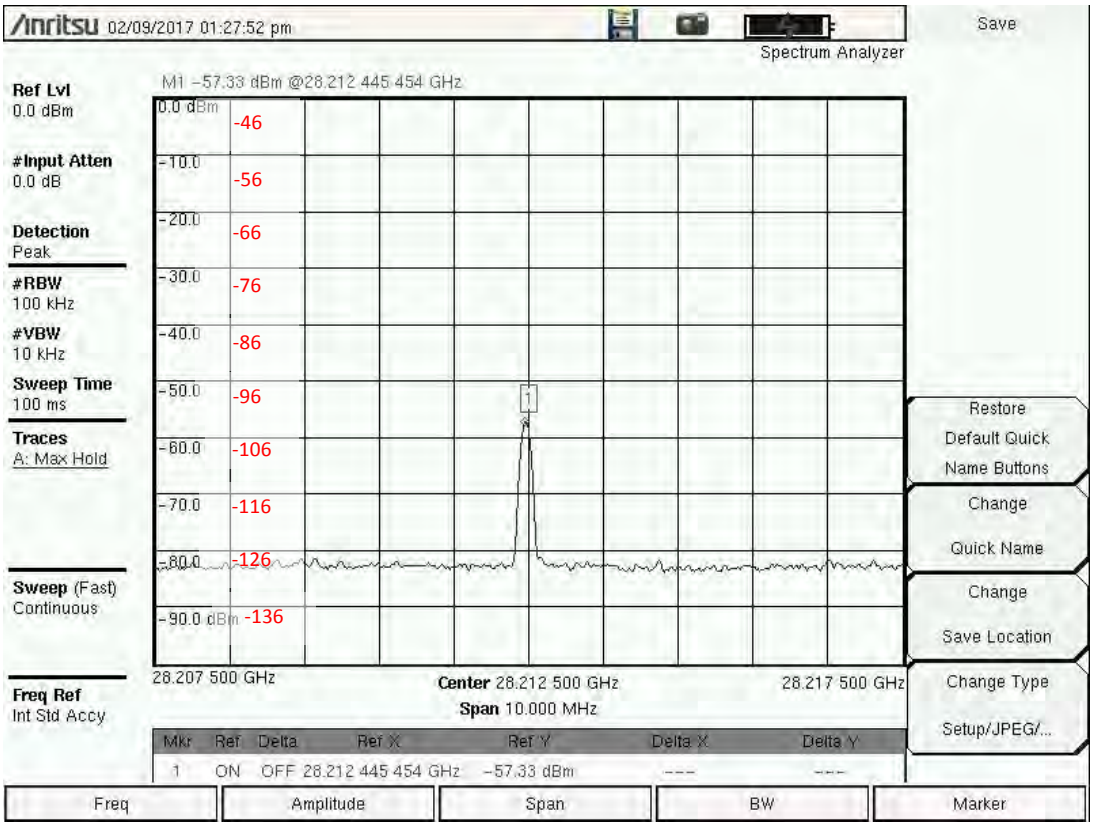

Figure 3.1-3 (G) Spectrum Photos 28 GHz - 100 kHz Res BW Site 4 at 10m AGL

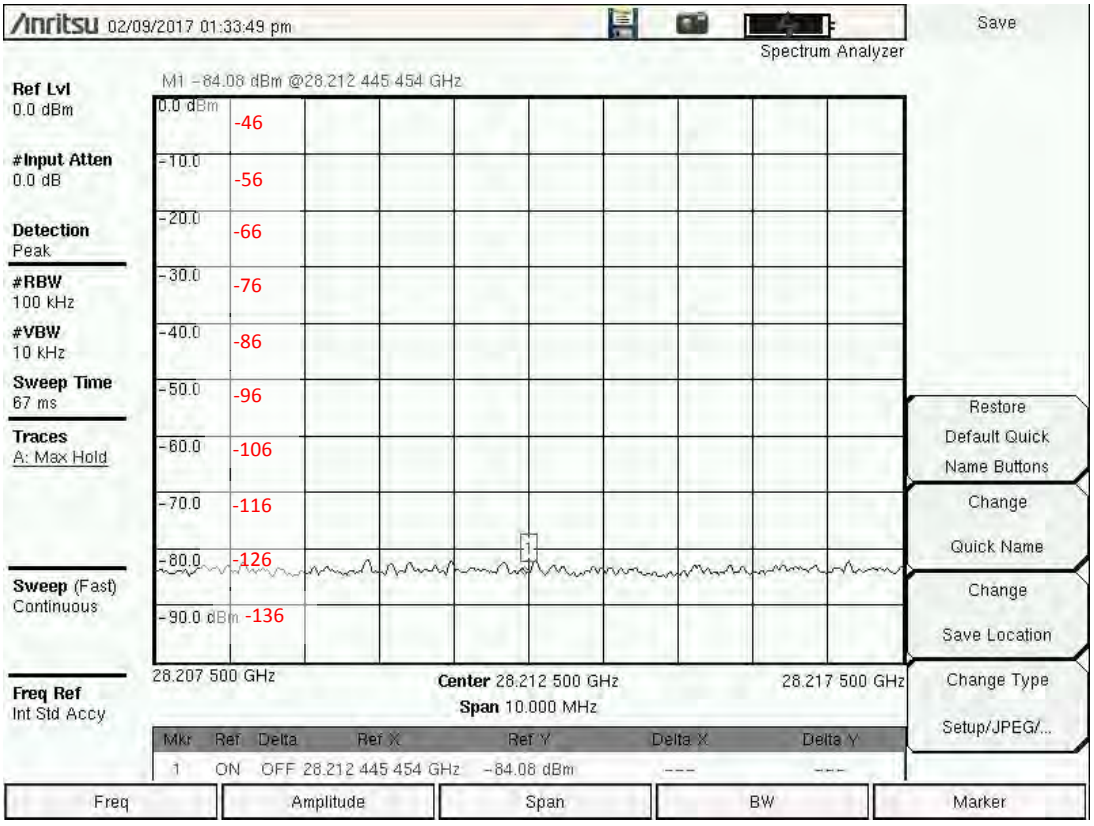

Figure 3.1-3 (H) Spectrum Photos 28 GHz - 100 kHz Res BW Site 4 at 2m AGL

Adjusted measurement values (dBm_I) shown in red

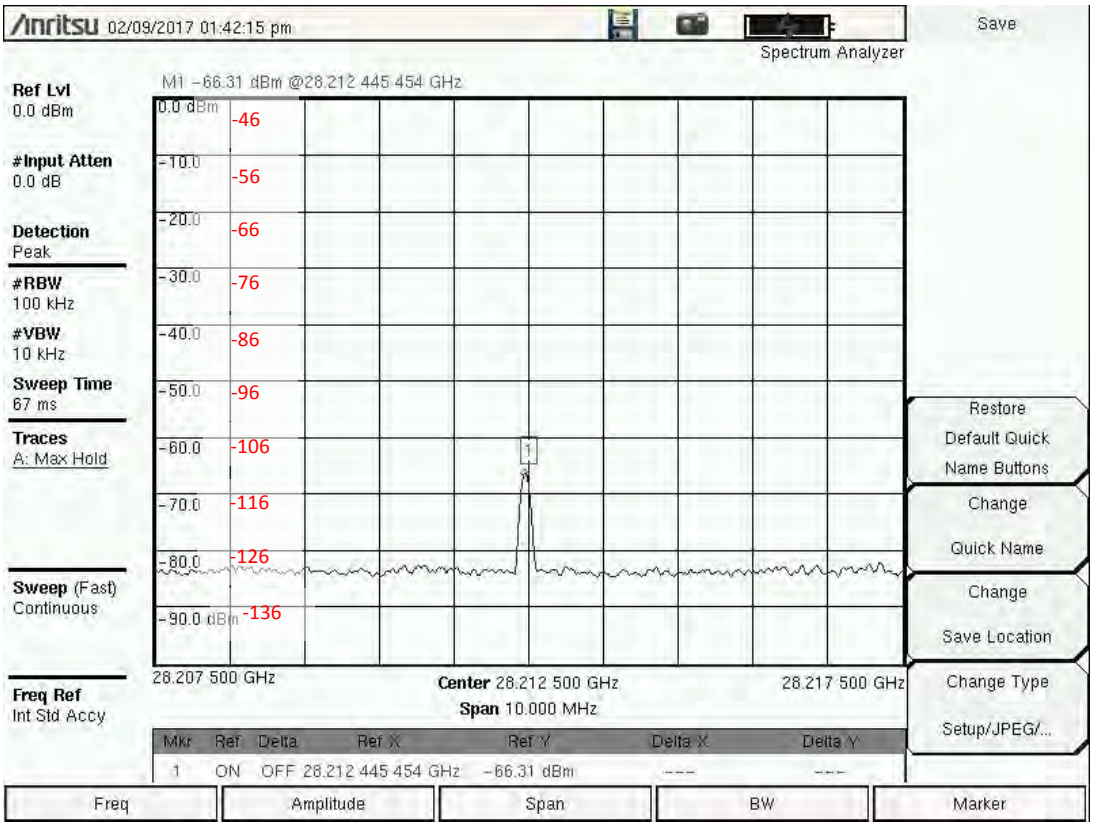

Figure 3.1-3 (I) Spectrum Photos 28 GHz - 100 kHz Res BW Site 5 at 10m AGL

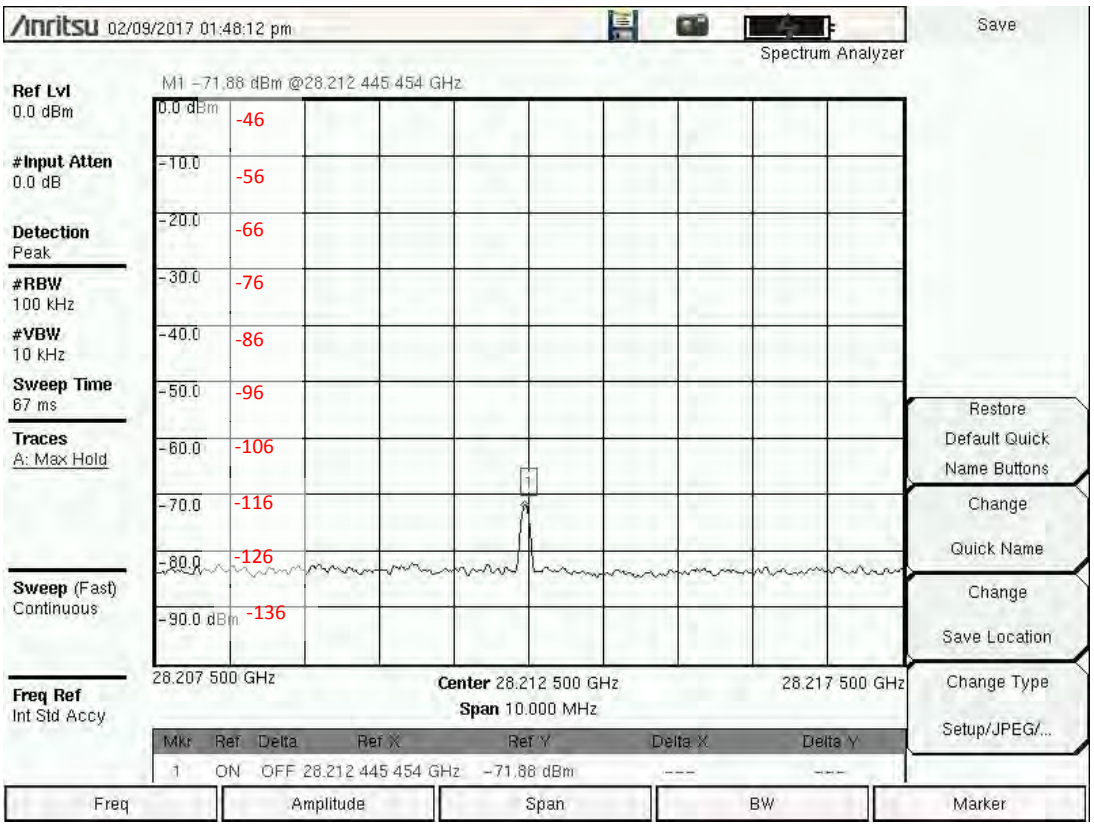

Figure 3.1-3 (J) Spectrum Photos 28 GHz - 100 kHz Res BW Site 5 at 2m AGL

Adjusted measurement values (dBm_I) shown in red

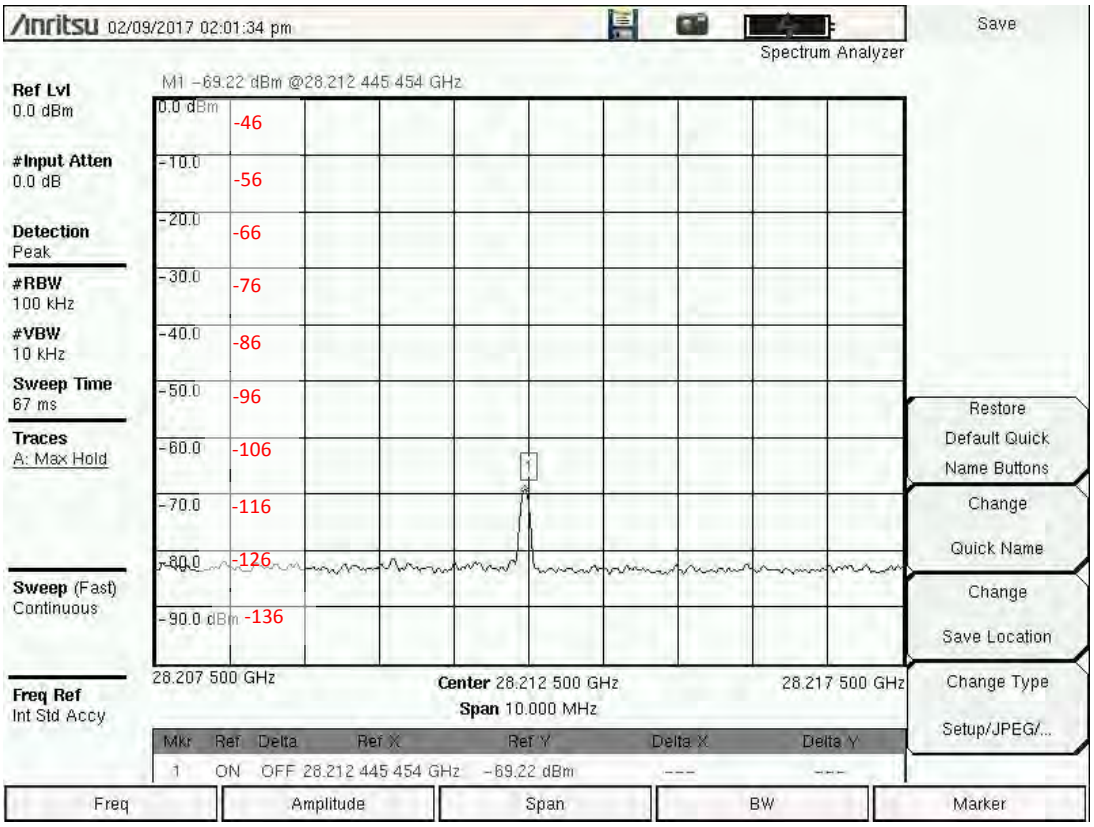

Figure 3.1-3 (K) Spectrum Photos 28 GHz - 100 kHz Res BW Site 6 at 10m AGL

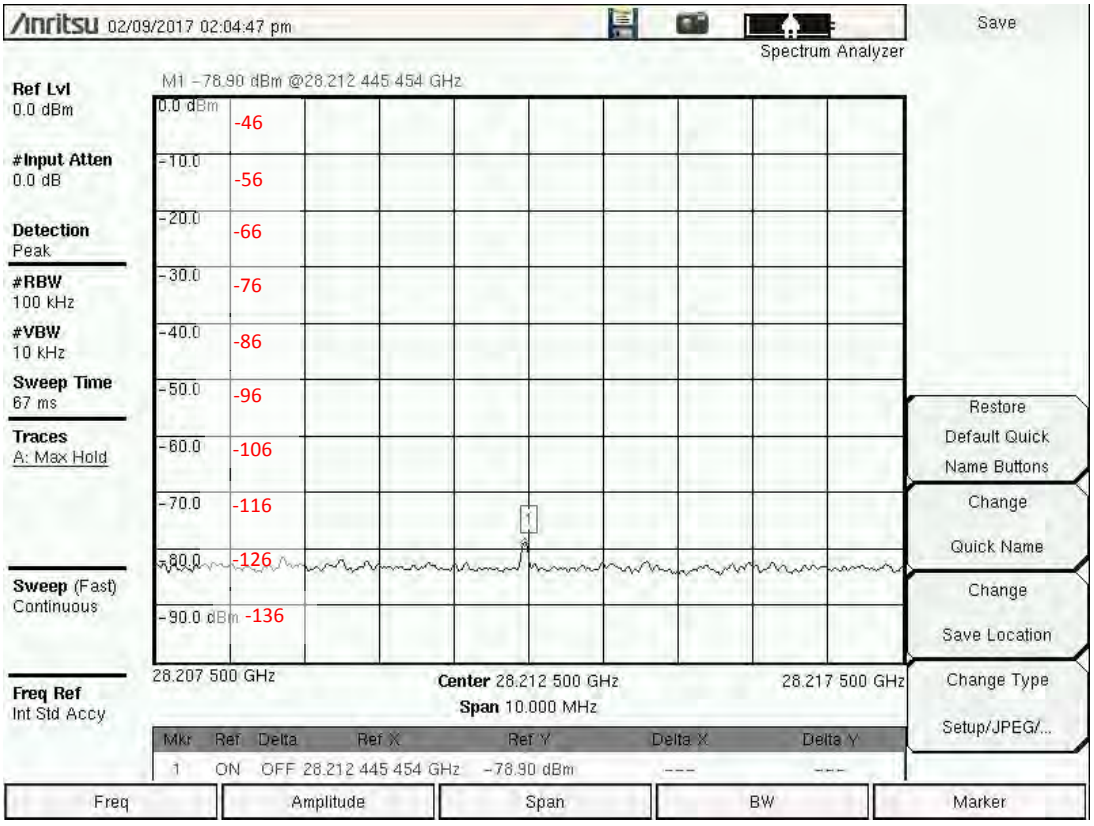

Figure 3.1-3 (L) Spectrum Photos 28 GHz - 100 kHz Res BW Site 6 at 2m AGL

Adjusted measurement values (dBm_I) shown in red

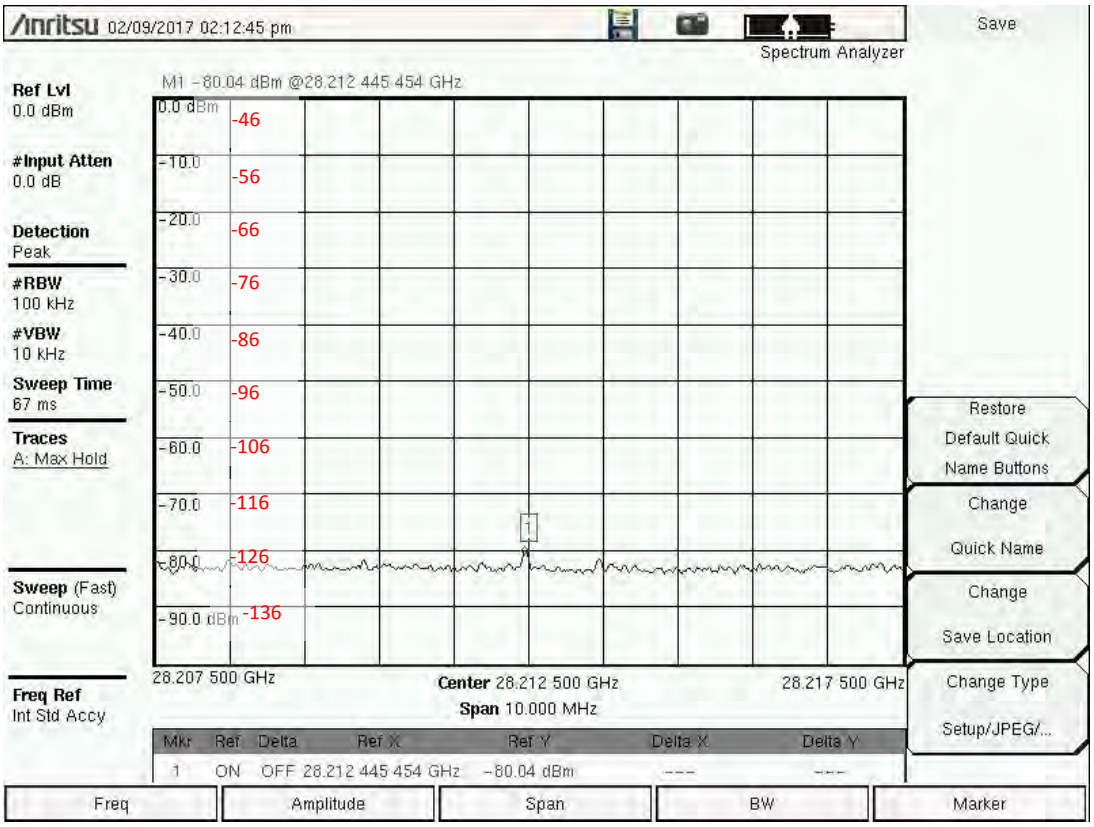

Figure 3.1-3 (M) Spectrum Photos 28 GHz - 100 kHz Res BW Site 7 at 10m AGL

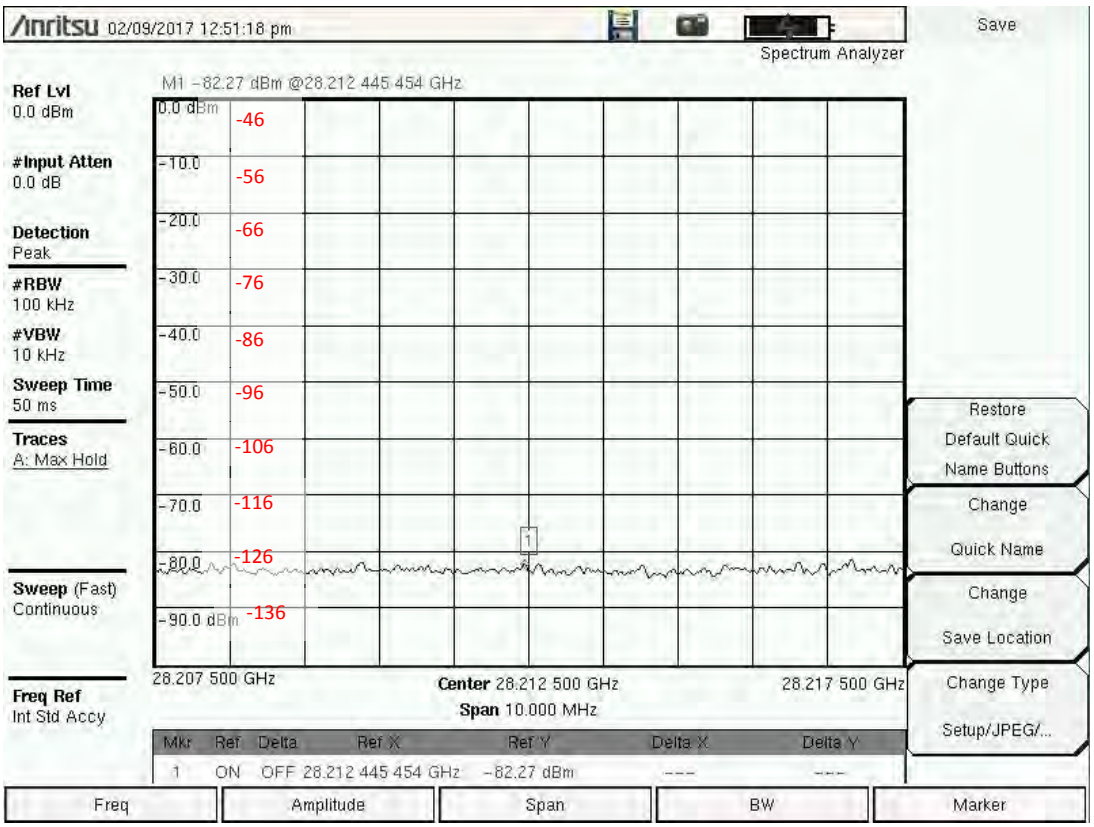

Figure 3.1-3 (N) Spectrum Photos 28 GHz - 100 kHz Res BW Site 7 at 2m AGL

Adjusted measurement values (dBm_I) shown in red

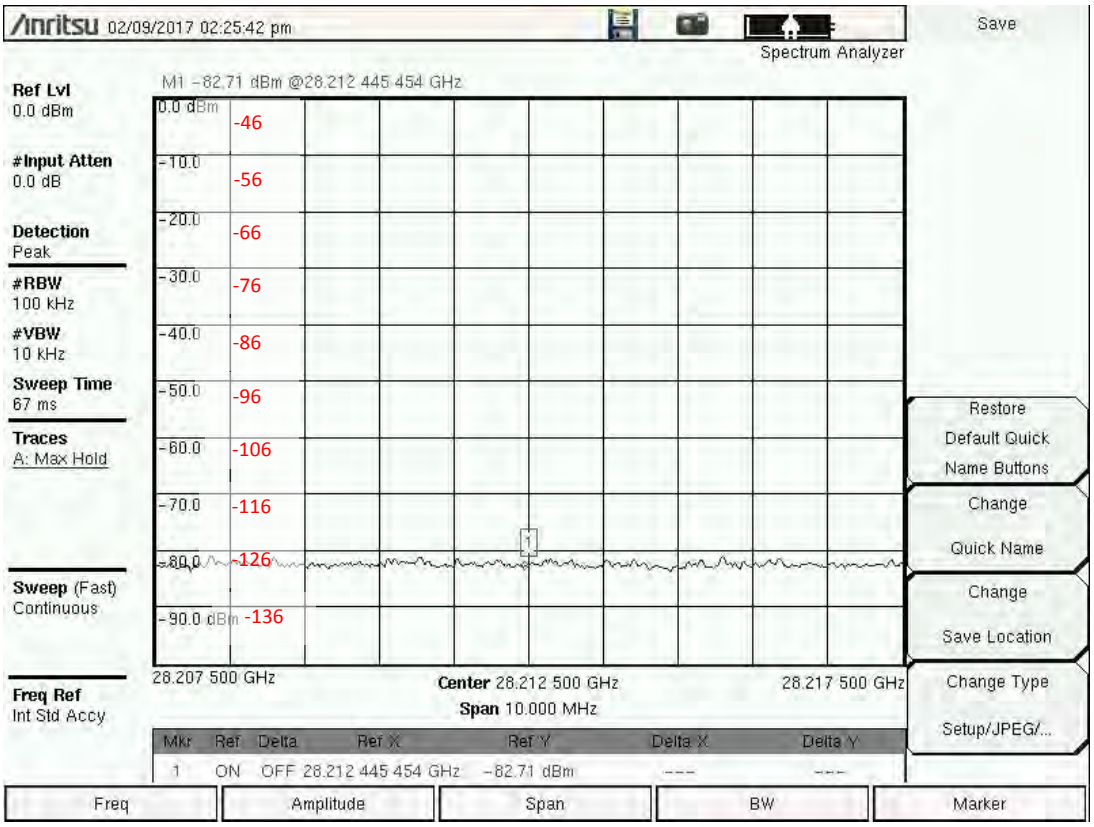

Figure 3.1-3 (O) Spectrum Photos 28 GHz - 100 kHz Res BW Site 8 at 10m AGL

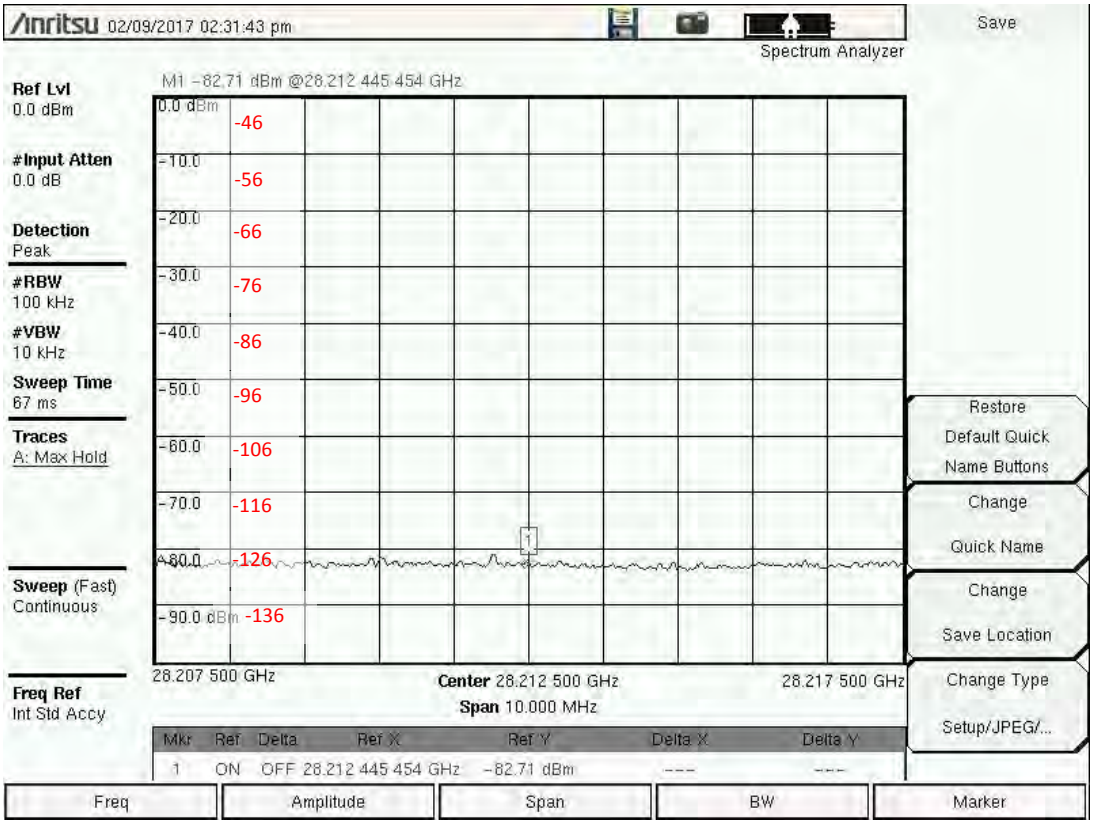

Figure 3.1-3 (P) Spectrum Photos 28 GHz - 100 kHz Res BW Site 8 at 2m AGL

Adjusted measurement values (dBm_I) shown in red

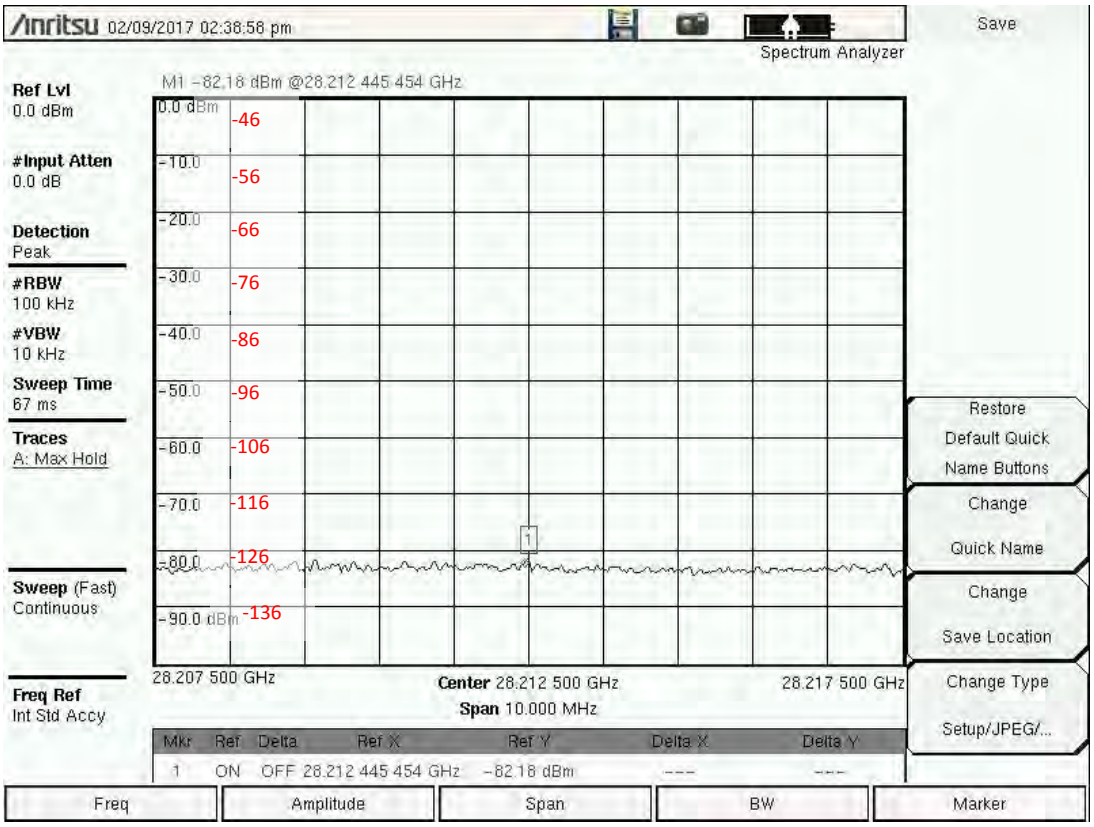

Figure 3.1-3 (Q) Spectrum Photos 28 GHz - 100 kHz Res BW Site 9 at 10m AGL

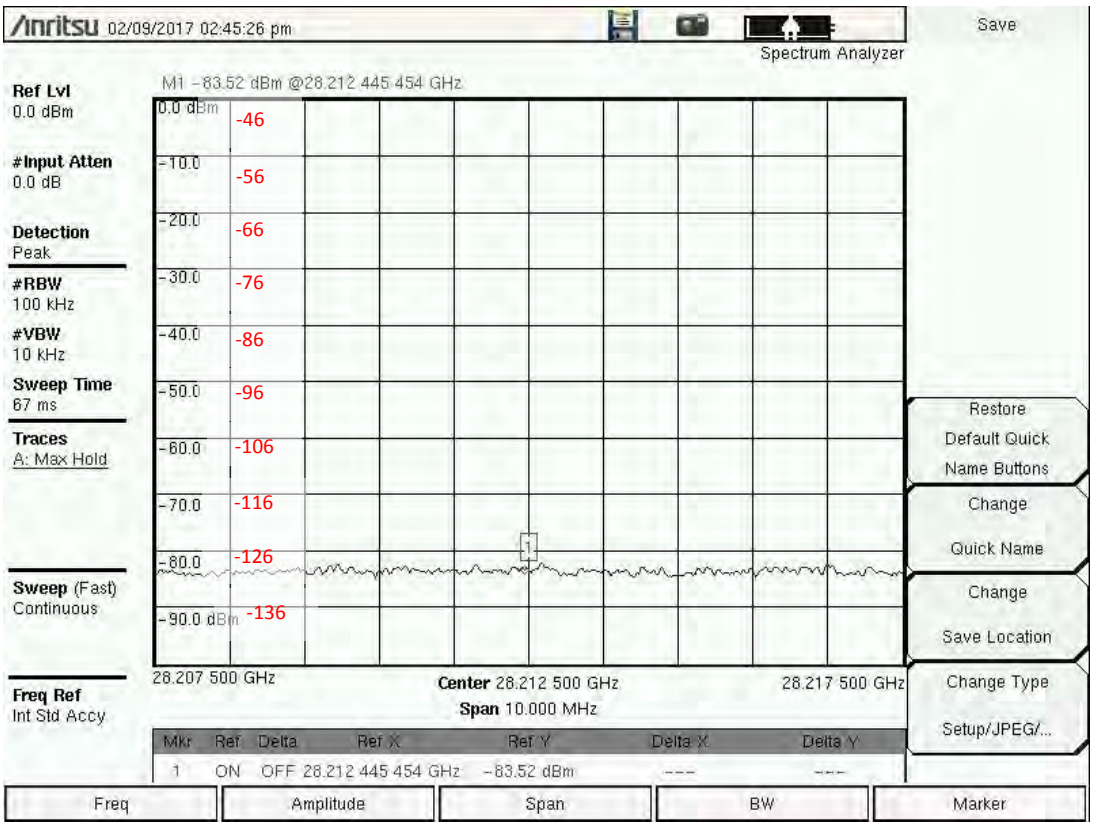

Figure 3.1-3 (R) Spectrum Photos 28 GHz - 100 kHz Res BW Site 9 at 2m AGL

Adjusted measurement values (dBm_I) shown in red

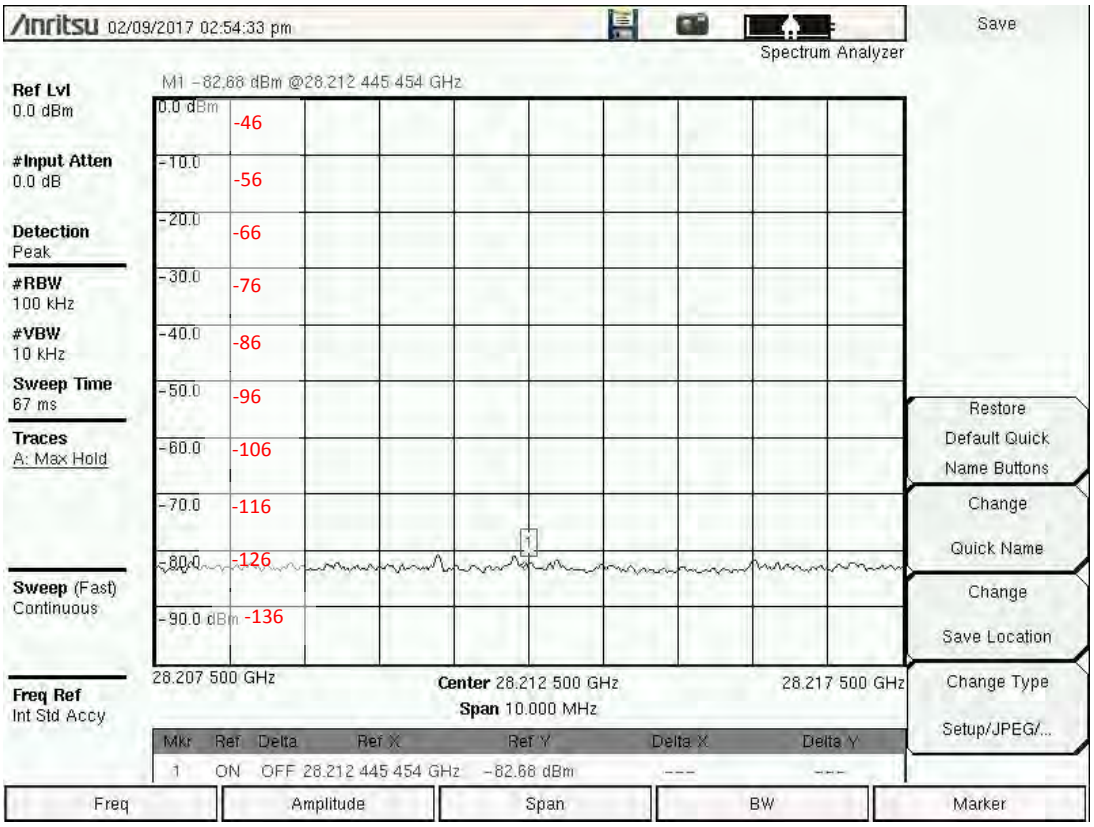

Figure 3.1-3 (S) Spectrum Photos 28 GHz - 100 kHz Res BW Site 10 at 10m AGL

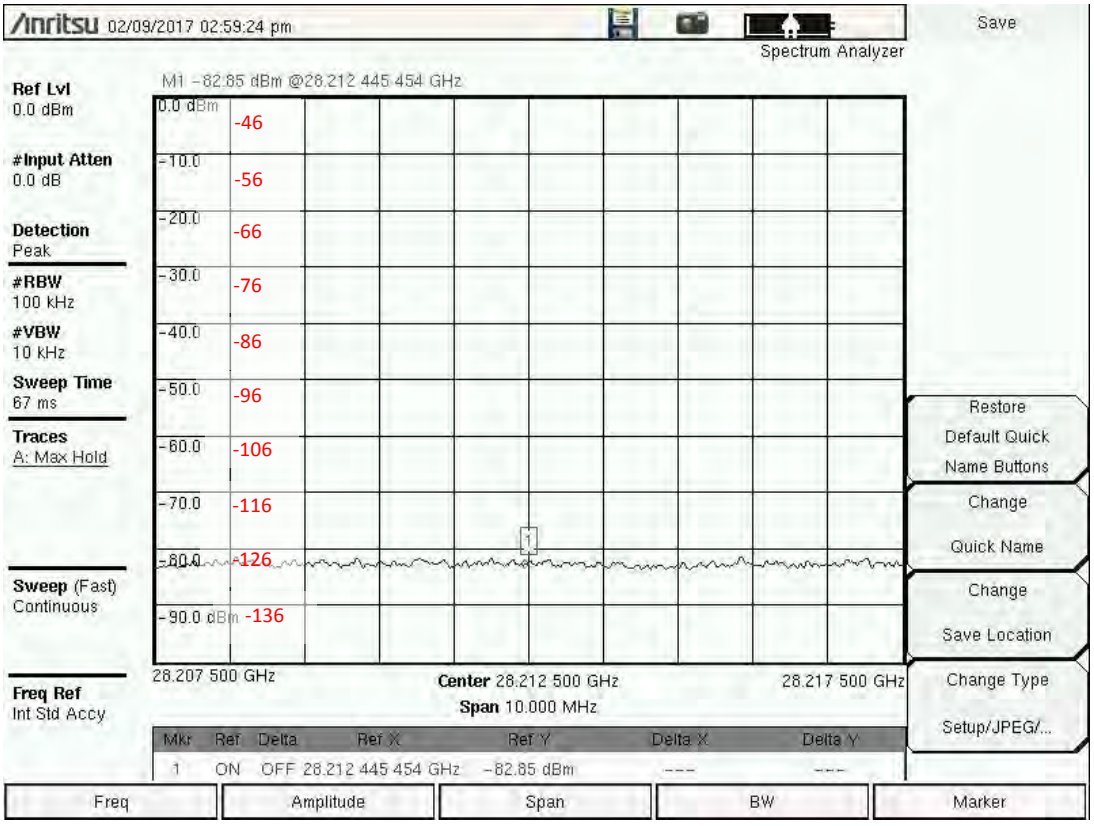

Figure 3.1-3 (T) Spectrum Photos 28 GHz - 100 kHz Res BW Site 10 at 2m AGL

Adjusted measurement values (dBm_I) shown in red

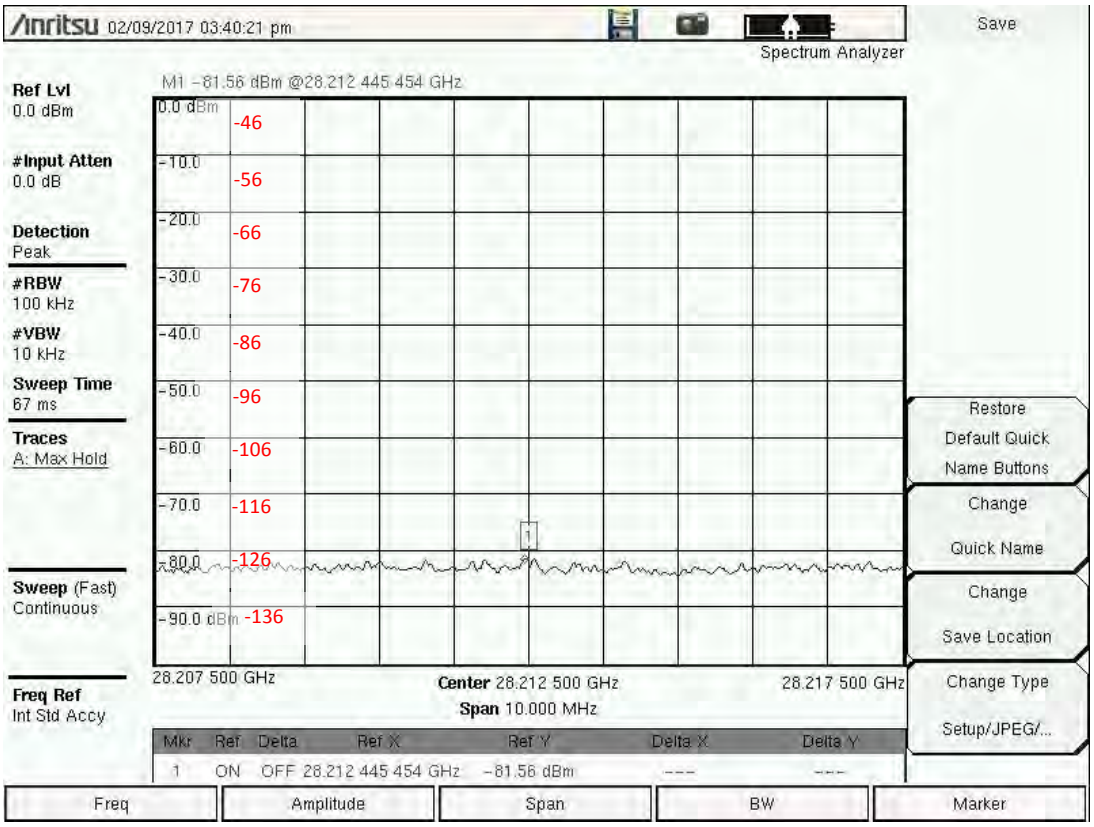

Figure 3.1-3 (U) Spectrum Photos 28 GHz - 100 kHz Res BW Site 11 at 10m AGL-82

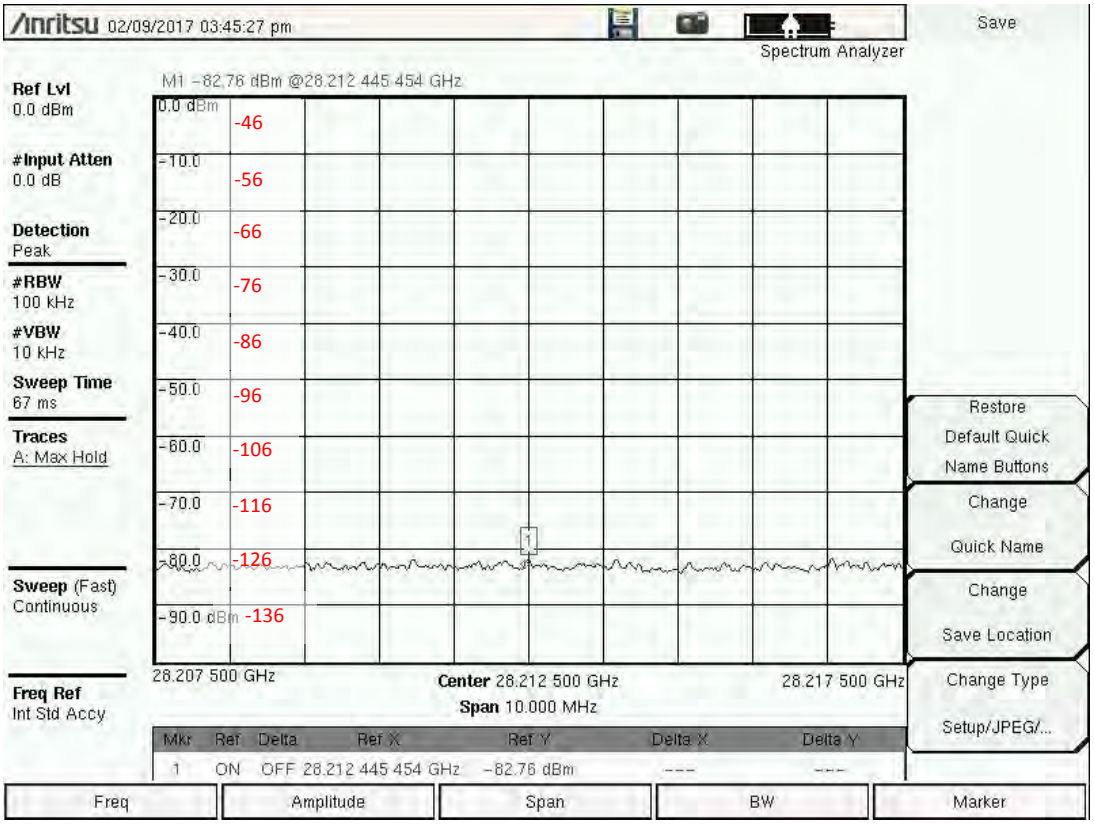

Figure 3.1-3 (V) Spectrum Photos 28 GHz - 100 kHz Res BW Site 11 at 2m AGL

Adjusted measurement values (dBm_I) shown in red

SECTION

FOUR

SECTION 4

SUMMARY OF RESULTS

The results of the measurements conducted at the ViaSat, Inc transmit site in Carlsbad, CA are presented in this section.

Ka-Band Measurements:

The tables on the next page contain the data collected during the RF Measurements on February 14, 2017.

Table 4.1
Data from RF Measurements at 10m Above Ground Level

Measurement Location	Latitude	Longitude	Azimuth From TX Antenna (°)	Azimuth to TX Antenna (°)	Test Antenna Height AGL (m)	Distance from TX Antenna (m)	Signal Value Recorded (dBm)	Signal Value Recorded (dBW)	Figure Number
Site 1	33.126722	-117.265194	170.29	350.29	10	66	-107.51	-137.51	3.1-3 (A)
Site 2	33.126778	-117.264917	147.79	327.79	10	69.5	-119.10	-149.10	3.1-3 (C)
Site 3	33.127194	-117.263972	95.76	275.76	10	126	-111.30	-141.30	3.1-3 (E)
Site 4	33.127583	-117.263194	81.23	261.23	10	200	-103.25	-133.25	3.1-3 (G)
Site 5	33.127222	-117.261917	91.72	271.73	10	317	-110.68	-140.68	3.1-3 (I)
Site 6	33.125778	-117.262028	118.97	298.97	10	350	-114.95	-144.95	3.1-3 (K)
Site 7	33.125611	-117.263000	131.08	311.08	10	286	-125.96 NF	-155.96 NF	3.1-3 (M)
Site 8	33.125444	-117.264028	149.86	329.86	10	239	-128.63 NF	-158.63 NF	3.1-3 (O)
Site 9	33.124667	-117.264583	166.9	346.9	10	301	-128.10 NF	-158.10 NF	3.1-3 (Q)
Site 10	33.124139	-117.264806	172.31	352.31	10	355	-128.60 NF	-158.60 NF	3.1-3 (S)
Site 11	33.127972	-117.265222	6.61	186.61	10	74.2	-127.48 NF	-157.48 NF	3.1-3 (U)

Table 4.2
Data from RF Measurements at 2m Above Ground Level

Measurement Location	Latitude	Longitude	Azimuth From TX Antenna (°)	Azimuth to TX Antenna (°)	Test Antenna Height AGL (m)	Distance from TX Antenna (m)	Signal Value Recorded (dBm)	Signal Value Recorded (dBW)	Figure Number
Site 1	33.126722	-117.265194	170.29	350.29	2	66	-128.19 NF	-158.19 NF	3.1-3 (B)
Site 2	33.126778	-117.264917	147.79	327.79	2	69.5	-125.56 NF	-155.56 NF	3.1-3 (D)
Site 3	33.127194	-117.263972	95.76	275.76	2	126	-129.65 NF	-159.65 NF	3.1-3 (F)
Site 4	33.127583	-117.263194	81.23	261.23	2	200	-130.00 NF	-160 NF	3.1-3 (H)
Site 5	33.127222	-117.261917	91.72	271.73	2	317	-117.78	-147.78	3.1-3 (J)
Site 6	33.125778	-117.262028	118.97	298.97	2	350	-124.82	-154.82	3.1-3 (L)
Site 7	33.125611	-117.263000	131.08	311.08	2	286	-128.19 NF	-158.19 NF	3.1-3 (N)
Site 8	33.125444	-117.264028	149.86	329.86	2	239	-128.63 NF	-158.63 NF	3.1-3 (P)
Site 9	33.124667	-117.264583	166.9	346.9	2	301	-129.44 NF	-159.44 NF	3.1-3 (R)
Site 10	33.124139	-117.264806	172.31	352.31	2	355	-128.77 NF	-158.77 NF	3.1-3 (T)
Site 11	33.127972	-117.265222	6.61	186.61	2	74.2	-128.78 NF	-158.78 NF	3.1-3 (V)

NF = Noise Floor of Test System

SECTION

FIVE

SECTION 5

CONCLUSIONS

5.1 Conclusions

Measureable signals above the measurement system's noise floor were observed at test sites 1 through 6 at 10 meters AGL. No measurable signals were observed above the measurement system's noise floor at sites 7 through 11 at 10 meters AGL.

Measureable signals above the measurement system's noise floor were observed at test sites 5 and 6 at 2 meters AGL. No measureable signals were observed above the measurement system's noise floor at all other sites at 2 meters AGL.

The highest observed signal was -103.25 dBm (-133.25 dBW) at site 4 at 10 meters AGL.

The values measured in this report are intended for use by ViaSat for incorporation into a larger analysis where ViaSat will perform the necessary calculations to convert the measured signals in dBm (dBW) to an equivalent power flux density in dBm/(m^2*MHz) and to determine, where possible, the effective signal attenuation over and above free space loss. As an element of a larger analysis, information in this report is not intended to be used on a standalone basis.

ATTACHMENT 3

555 Eleventh Street, N.W., Suite 1000
Washington, D.C. 20004-1304
Tel: +1.202.637.2200 Fax: +1.202.637.2201
www.lw.com

LATHAM & WATKINS LLP

FIRM / AFFILIATE OFFICES

Barcelona	Moscow
Beijing	Munich
Boston	New York
Brussels	Orange County
Century City	Paris
Chicago	Riyadh
Dubai	Rome
Düsseldorf	San Diego
Frankfurt	San Francisco
Hamburg	Seoul
Hong Kong	Shanghai
Houston	Silicon Valley
London	Singapore
Los Angeles	Tokyo
Madrid	Washington, D.C.
Milan	

September 25, 2017

VIA ELECTRONIC FILING

Ms. Marlene H. Dortch
Secretary
Federal Communications Commission
445 12th Street, SW
Washington, DC 20554

Re: ViaSat, Inc., Notice of *Ex Parte* Presentation, GN Docket No. 14-177; IB Docket Nos. 15-256 & 97-95; RM-11664; and WT Docket No. 10-112

Dear Ms. Dortch:

Chris Murphy and Daryl Hunter of ViaSat, Inc. ("ViaSat"), and the undersigned, met on September 21 and 22, 2017 with Commission staff listed below.

The purpose of the meetings was to discuss the report prepared by Roberson and Associates, LLC, enclosed as Attachment A, demonstrating the ability of small satellite earth station uplinks in the 47.2-48.2 GHz and 50.4-52.4 GHz band segments to coexist with terrestrial wireless operations. ViaSat also discussed the slides attached as Attachment B.

Please contact the undersigned if you have any questions regarding this submission.

Respectfully submitted,

/s/

John P. Janka
Elizabeth R. Park

Attachments

cc:
Office of Engineering and Technology (September 21)
Ronald Repasi
Bahman Badipour
Nicholas Oros

International Bureau (September 21)
Thomas Sullivan
Jim Schlichting
Jennifer Gilsenan
Kerry Murray
Jose Albuquerque
Chip Fleming

Wireless Telecommunications Bureau (September 22)
Joel Taubenblatt
Blaise Scinto
John Schauble
Matthew Pearl (by phone)

ATTACHMENT A

Roberson and Associates, LLC
Technology and Management Consultants ®

SPECTRUM FRONTIERS: Q/V BAND SATELLITE-5G COEXISTENCE

M. BIRCHLER, J. CHAPIN, P. ERICKSON, M. NEEDHAM & K. ZDUNEK

25 SEPTEMBER 2017

v1.0

This analysis was generated by Roberson and Associates, LLC for ViaSat.

Table of Contents:

1 EXECUTIVE SUMMARY

This analysis of a typical deployment scenario shows that small Fixed Service Satellite (FSS) Earth Stations (ES) with uplink transmissions between 47.2-50.2 and 50.4-52.4 GHz communicating with geostationary-orbit spacecraft can be located in the same urban areas as Fifth-Generation (5G) wireless Base Stations (BS) without the need for coordination.[1]

The analysis utilizes standard methodologies, parameters, metrics and models, extended and supplemented as necessary to support the specific scenario under study.

The primary coexistence metric utilized is the ratio of FSS ES received power density (I_{es}) to noise floor power density (η_{bs}) at the 5G BS demodulator input, or I_{es}/η_{bs}. This metric is used to determine 99%, 98% and 95% probability geographic contours for $I_{es}/\eta_{bs} \leq$ -6 dB.

The baseline confidence probability contour data has been evaluated with respect to absolute area, and also is described by way of example with respect to a specific urban region (i.e., Cook County, Illinois). The results indicate that any area where potential coexistence issues exist is very small, and the chances of such a circumstance actually arising in any given real-world deployment is extremely small.

The reported total 99% confidence probability contour area for $I_{es}/\eta_{bs} \leq$ -6 dB is less than 0.0036 km^2, and the 98% contour less than 0.00042 km^2, which constitute less than 0.00009% and 0.00001% of Cook County, respectively. Furthermore, the overall probability likelihood that an individual 5G BS will actually experience $I_{es}/\eta_{bs} >$ -6 dB is only 0.24% or approximately 1 chance in 416. Thus, the results of this analysis show that coexistence between FSS ESs and 5G BSs is feasible without the need for coordination.

Notably, these results are based on conservative assumptions, including path loss, use of peak side lobes (instead of actual lower values at different off-axis angles), considering only BS antennas with essentially omni-directional coverage, calculating much-higher confidence levels for received power density than commonly used, not accounting for attenuation from roof blockage, assuming all-outdoor 5G deployment, and never considering the operation of an ES at an elevation angle above a minimal value.

Moreover, the foregoing calculations do not take into account the mitigating effects of other factors, such as (i) inherent 5G BS antenna array techniques developed to allow 5G systems to cope with self-interference and interference between other 5G systems, or (ii) FSS ES physical isolation, both of which would virtually eliminate the chance of a real-world problem ever actually arising.

[1] Note: The results of this analysis depend on the characteristics of the satellite system at issue; the methodology readily could be applied to systems with other architectures or physical configurations.

2 SPECTRUM COEXISTENCE SCENARIO

2.1 Overview

This analysis provides a technical assessment for the case of a small Fixed Service Satellite (FSS) Earth Station (ES) transmitting to a spacecraft in geostationary orbit, and located near a Fifth-Generation wireless (5G) Base Station (BS). The assessment scenario under study is shown in the following figure.

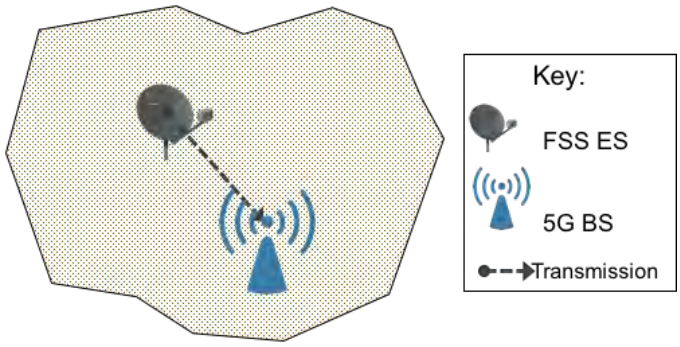

Figure 1. Spectrum Coexistence Scenario

The primary coexistence metric utilized is the ratio of FSS ES received power density (I_{es}) to noise floor power density (η_{bs}) at the 5G BS demodulator input, or I_{es}/η_{bs}. The specific spectrum of interest is the Q/V bands (i.e., 47.2-50.2 and 50.4-52.4 GHz).

This assessment utilizes standard methodologies, parameters, metrics and models to the greatest possible extent. Where necessary these resources were extended/supplemented to support the specific scenario under study. Primary sources for this work can be found in [1]-[11].

The following sections describe the key components of this analysis.

2.2 FSS ES System

The information in this section on FSS ES system deployment and parameters was provided by ViaSat.

2.2.1 General Description

The FSS ES system uses an offset fed parabolic reflector antenna of approximate 1.8-meter diameter. It can be installed using ground mounts or on existing structures such as building roofs. The antenna boresight is pointed at a nominal vertical elevation angle of between 35 and 55 degrees relative to the horizon as dictated by the orbital location of the target satellite.

The power amplified (PA) output in this study is typically 7.15 milliwatts per right and left hand circular polarization for each 1 MHz of modulated bandwidth.

2.2.2 ES Antenna Pattern

To determine the ES antenna parameters needed for this study, an antenna being developed for this application was modeled by ViaSat. The design is based on a commercially available reflector. When in operation the ES antenna is pointed substantially upward in elevation and must have clear view of the sky in the direction of the target satellite. In order to assess the interaction with terrestrial 5G systems, the ES antenna gain well off the main beam is of primary interest.

The ES antenna performance data indicate that for 10 to 90 degrees from the main beam, the side lobe peaks plotted in dB as a function of angle are a straight line. This follows the process of M.1851 Table 5 [2]. Other literature (i.e., ECC PT1 #54 [3]) shows several examples of a reflector antenna with similar side lobe response. Therefore, the following side lobe mask as a function of the angular distance from the main beam is appropriate.

$$GAIN_{es}(\alpha) = -5 - {}^{\alpha}/_{3} \quad (10^{o} \le \alpha \le 90^{o}) \qquad (1)$$

$$= -35 \quad (\alpha > 90^{o})$$

Where:

α = the arc distance to the main beam (not defined for $\alpha < 10^{o}$)

The following figure plots the mask of Equation (1).

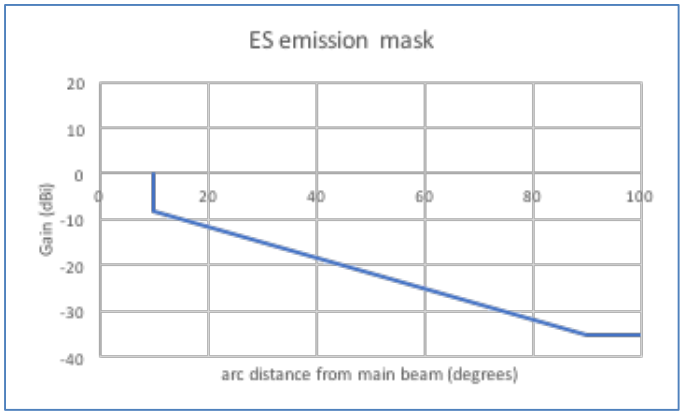

Figure 2. FSS ES Antenna Mask

The choice to use a mask matching the peaks (as opposed to the averages of the ripple) is conservative and ignores the possibility of lower sidelobes below this peak value in the final antenna design. However, this mask is more reflective of actual performance, compared with the 25.209 mask [4], which documents an upper bound regulatory limit.

2.3 5G BS System

2.3.1 General Description

The baseline deployment scenario used is described as the "Outdoor Urban hotspot" in Table 12 (Deployment-related parameters for bands between 45.5 GHz and 52.6 GHz) of [8]. These IMT-

2020 parameters were specified by the ITU [7] "to be used in sharing and compatibility studies for bands between 24.25 and 86 GHz."

- Antenna height (radiation center): 6 m (above ground level)
- Down-tilt: 10º
- Below rooftop base station antenna deployment
- Antenna polarization: Linear ±45º
- Horizontal/Vertical radiating element spacing: 0.5 of wavelength for both H/V
- 8x16 antenna array configuration

Continuing use of [8], we have selected the BS Noise Figure to be 12 dB as specified in the second table contained in Section 3 "System related parameters," column "37-52.6 GHz" (row 5.1).

2.3.2 BS Antenna Pattern

Since there are no commercial examples of 5G BS antennas in this band, a practical, conservative antenna performance model was needed. Using methods similar to M.2101 [5], the gain mask was determined from the theoretical linear array. An 8-element vertical by 16-element horizontal arrangement was assumed as it appears commonly in the literature.

The theoretical derivation of the normalized gain of a linear array is widely available. For example, [6] section 3, Equation 13.21 gives the normalized gain function with steering and uniform illumination. For this analysis, a broadside beam (i.e., no steering phase shift) with λ/2 element spacing is assumed. This results in the following equation.

$$AF_n = \frac{\sin(N\psi/2)}{N\sin(\psi/2)} \tag{2}$$

Where:

ψ = $\pi sin\phi$

ϕ = elevation angle above the main beam

Since there is a regular array of eight vertical elements, this results in the following elevation plot.

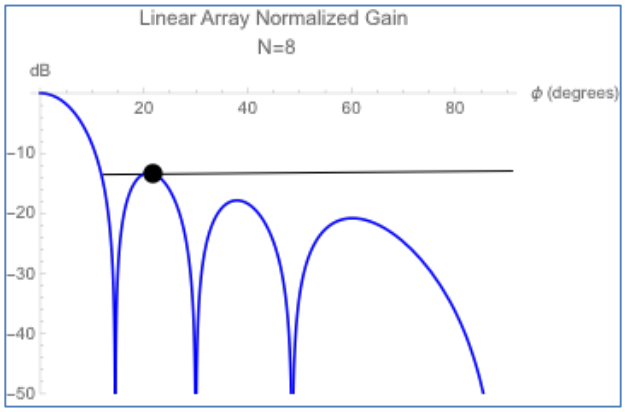

Figure 3. 5G BS Elevation Antenna Pattern

As the first side-lobe for this vertical configuration has a peak at approximately -13.3 dB, the mask was chosen to follow the theoretical value of the main lobe but limit the side-lobes to -13.3 dB. Because this analysis will be most sensitive to the sidelobe levels, the relatively small contribution of the element gain was not included. The peak gain is the product of the number of elements, so for the 8x16 array is $10\log_{10}(128)$ or 21 dB added to the normalized pattern.

In a similar manner, the horizontal gain of the 5G BS antenna is modeled based on a regular array of sixteen horizontal elements. This serves to narrow the main lobe of the pattern versus that of the vertical pattern. The relative gain in the horizontal pattern is shown in Figure 4 below for an assumed 120-degree sectored antenna. It is this pattern that will be used in determining the relative gain of the 5G BS as the antenna is rotated to different randomized orientations, per the methodology explained in Section 3.1.1. To simplify the analysis, a "block mask" of the pattern is employed, in which the relative gains of the main lobe (defined by the 3 dB beamwidth) and side lobes are constant as a function of angle. As with the elevation pattern, the relative gain in the side-lobes used in the analysis is also -13.3 dB. This approach is conservative, as it reflects the peak gains of the respective lobes, and does not factor in the lower actual gain of the side lobes and the associated nulls, as depicted in Figure 4.

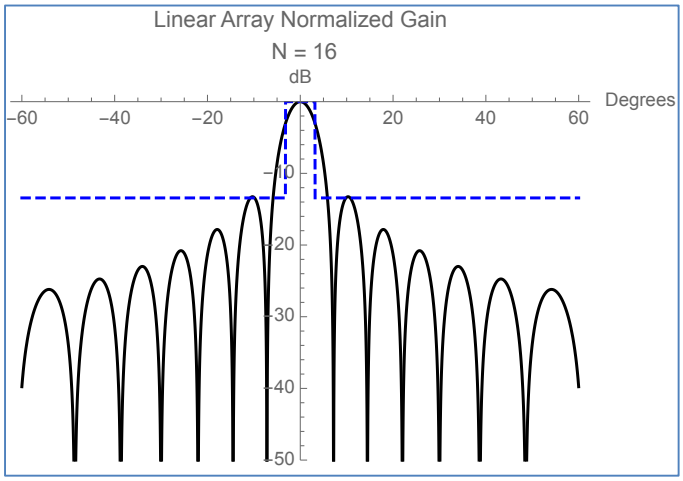

Figure 4. 5G BS Azimuthal Antenna Pattern with Block Mask

2.4 Coexistence Metric

The primary coexistence metric utilized is the ratio of FSS ES received power density (I_{es}) to noise floor power density (η_{bs}) at the 5G BS demodulator input, or I_{es}/η_{bs} (dB). The following two sections describe the metric threshold selection and define the coexistence metric components.

2.4.1 Threshold Selection

Received power from an FSS ES is assessed as acceptable if $I_{es}/\eta_{bs} \leq$ -6 dB.

The -6 dB I_{es}/η_{bs} threshold at the 5G BS demodulator input was selected to conform with an ITU Working Party 5D liaison to Task Group 5/1 for 5G system protection "*Irrespective of the number of cells and independent of the number of interferers*" [7]. This threshold is quite conservative. The 5G BS receivers are expected to be interference-limited because 5G is a multi-user system. Power received from other 5G co-channel transmissions will likely be much higher

than receiver noise power η_{bs}. Received FSS ES power at 6 dB below the noise floor will cause a negligible increase in total received undesired power given the presence of 5G co-channel transmissions. In other words, a more realistic assessment of 5G receiver performance would utilize I_{es}/I_{CO} (where I_{CO} is the co-channel, same-system interference power density), which would produce more favorable results with respect to coexistence of FSS ES and 5G BS in real-world scenarios.

2.4.2 Component Definitions

2.4.2.1 Noise Power Density

The 5G BS noise floor power density (η_{bs}) is defined as follows:

$$\eta_{bs} = -204 + NF_{bs} \quad (3)$$

Where:

η_{bs}	=	5G BS noise floor power density at the demodulator input (dBW/Hz)
–204	=	Absolute noise floor (kTB) power density (dBW/Hz)
NF_{bs}	=	Noise Figure of the 5G BS (dB)

2.4.2.2 Received Power Density

The FSS ES received power density (I_{es}) is defined as follows:

$$I_{es} = P_{T,es} + G_{es:\theta,\phi} + G_{bs:\theta,\phi} + G_{p:es,bs} - PL_{es\rightarrow bs}(d) \quad (4)$$

Where:

I_{es}	=	Received power density of the FSS ES at the 5G BS demodulator input (dBW/Hz)
$P_{T,es}$	=	Transmit power density of the FSS ES (dBW/Hz)
$G_{es:\theta,\phi}$	=	Antenna gain of the FSS ES in the azimuthal (θ) and elevation (ϕ) directions of the 5G BS (dBi)
$G_{bs:\theta,\phi}$	=	Antenna gain of the 5G BS in the azimuthal (θ) and elevation (ϕ) directions of the FSS ES (dBi)
$G_{p:es,bs}$	=	Polarization gain between the ES and BS antennas (dB)
$PL_{es->bs}$	=	Path loss between the FSS ES and 5G BS (incl. fading and deployment factors, dB)
d	=	Three-dimensional distance between the ES and BS antenna locations (m)

2.5 Propagation Model

We have implemented path loss models according to the methods described in the most recent versions of 3GPP TR 38.900 [10]. This document is largely equivalent to ETSI TR 138.900, "Study on channel model for frequency spectrum above 6 GHz" [11]. These documents describe propagation models to be used in evaluating 5G systems at frequencies from 6 to 100 GHz.

The relevant scenarios include "Urban Micro–Street Canyon" (UMi-SC) and "Urban Macro" (UMa), described in sections 6.2 and 7.2 of these documents. The UMi-SC model pertains to situations where 5G BSs are deployed below the rooftop levels of surrounding buildings, while UMa corresponds to BSs deployed above rooftop levels.

2.5.1 Median Path Loss

For the UMi-SC and UMa scenarios, the path losses are characterized in terms of sets of equations for the median path loss as functions of the 2D distance between BS and User Terminal (UT), the heights above ground of the BS and UT antennae, and the center frequency of transmission. For each of the two scenarios, there are equations for LOS and NLOS path losses (pertaining to cases where there is or is not a line-of-sight between the BS and UT antennae). Equations for the probability of being LOS are also provided for each scenario, which are a function of the 2D distance.

Values for an example set of input parameters are shown in Figure 5. Three curves are included, those being LOS, NLOS, and Combined median path loss. The Combined curve is the sum of the LOS and NLOS curves weighted by the respective probabilities of the path being LOS or NLOS.

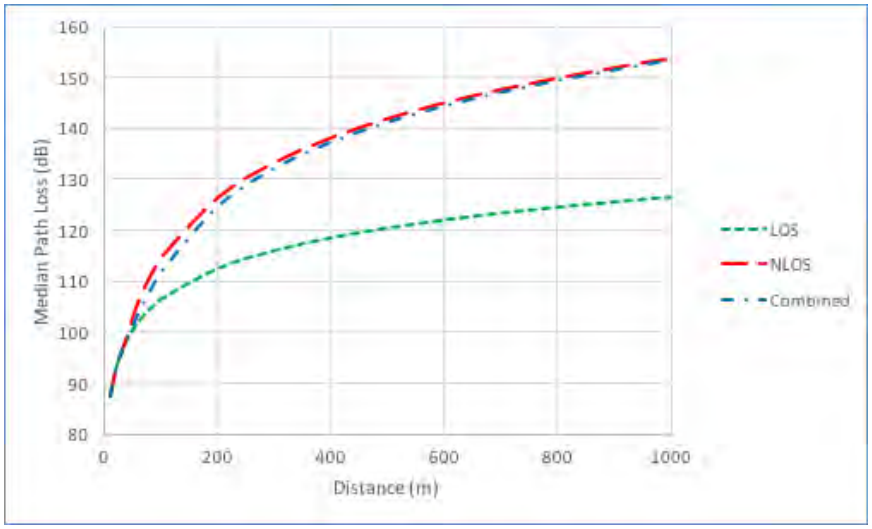

Figure 5. UMa Model Median Propagation Loss Curves

2.5.2 Log-Normal Shadowing

The models also include additive terms (in dB) to accommodate for statistical variation of the path loss to reflect location variability due to shadow fading, which is modeled according to a log-normal distribution (i.e. normal in dBs), with a specified standard deviation for each scenario and LOS/NLOS case.

Figure 6 shows example Probability Density Functions (PDFs) for a specific set of model input parameters. Three PDF curves are included, those being LOS, NLOS, and Combined path loss. The Combined curve is the sum of the LOS and NLOS curves weighted by the respective probabilities of the path being LOS or NLOS. Note that the LOS and NLOS curves have symmetric normally distributed PDFs while the Combined curve, being a weighted sum of the two constituent Normal curves, does not.

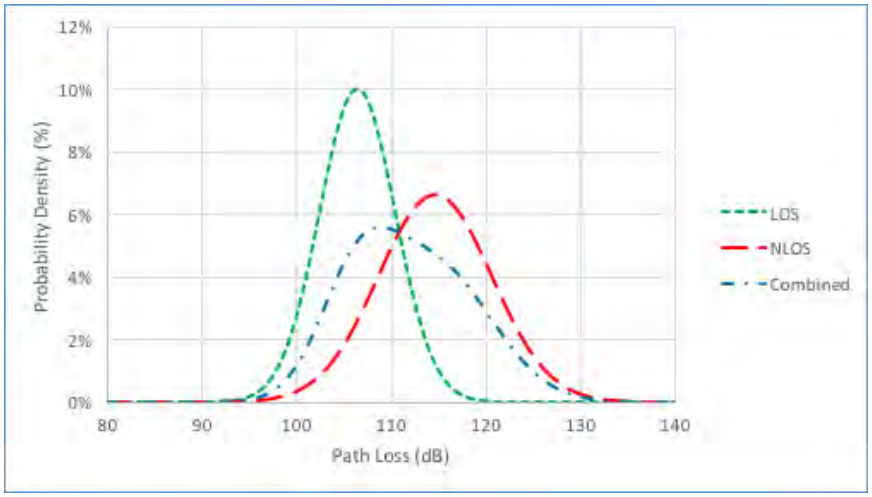

Figure 6. UMa Model Path Loss PDFs for a Given Distance

These PDFs will be used in the technical analysis to model probabilistic path loss, specifically to determine the probability that, at a given distance, the path loss will exceed the value necessary to achieve I_{es}/η_{bs}. = -6 dB.

Figure 7 shows the Cumulative Distribution Functions (CDFs) associated with the PDFs of Figure 6.

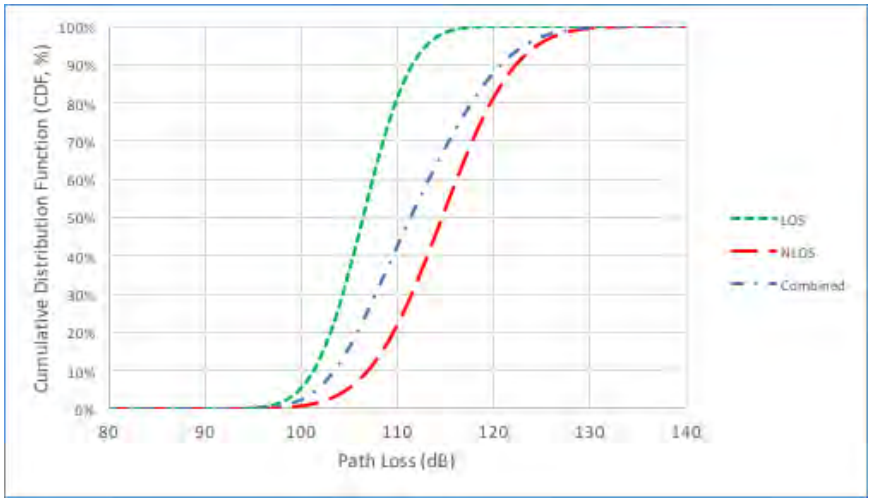

Figure 7. UMa Model Path Loss CDFs for a Given Distance

2.5.3 Path Loss Confidence Curves

The model can also be used to calculate path loss confidence curves. If a confidence value is specified, say X%, the path loss value for which there is a X% probability of being greater than or equal to as a function of distance can be determined. Figure 8 shows two path loss confidence curves (i.e., for 50% and 95% confidence values).

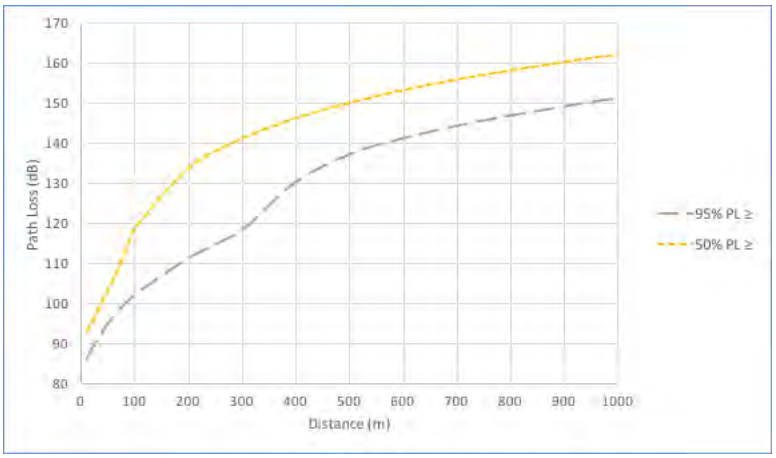

Figure 8. Example Path Loss Confidence Curves

Thus, at a distance of 500 m, there is a 50% likelihood that the path loss will be ≥ 150 dB and a 95% likelihood of being ≥ 137 dB. This path loss methodology will be used in the analysis to generate confidence curves for $I_{es}/\eta_{bs} \leq$ -6 dB.

2.6 System Description

A specific instance of the system under analysis is shown in Figure 9. Note that the environment is urban. The FSS ES antenna is located on the roof of a building (height 25 m, which is the recommended value for h_{BS} in the utilized UMa propagation model [11]) that is taller than most of the surrounding structures. The 5G BS antenna is located below the rooftops of the surrounding buildings (height 6 m). The 5G BS is placed "around the corner" relative to the FSS ES building to indicate that NLOS propagation is a possible case.

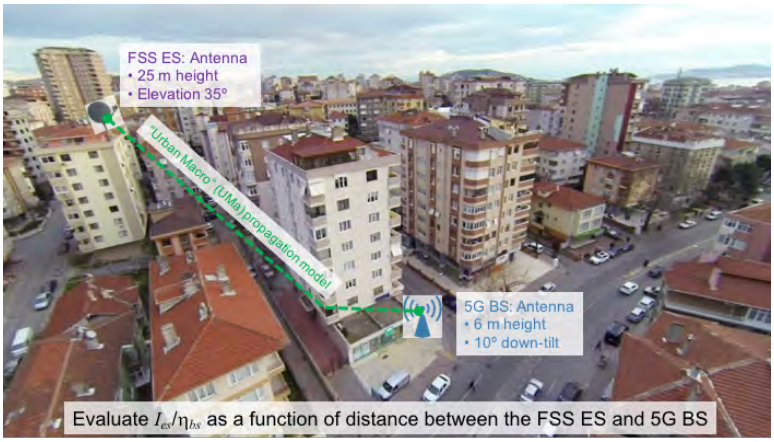

Figure 9. System Analysis Description

Additional details for the FSS ES and 5G BS characteristics/parameters can be found in sections 2.2 and 2.3, respectively.

Based on this system definition, we have selected the "Urban Macro" (UMa) propagation model [10]. The FSS ES plays the role of the "BS" and the 5G BS as the "UT" as defined in the UMa model. This is done because the UMa "BS" is defined as the device that is above surrounding rooftops while the UMa "UT" is defined to be below the rooftops.

In a LOS scenario, the highly unlikely "worst case" antenna configuration is that the boresights of both antennas are directly pointed at one another. We will allow the BS to be located along the full 360º around the fixed (in elevation and azimuth) ES. At each BS location, we will evaluate performance over the 360º range of random azimuthal BS antenna orientations.

3 TECHNICAL ANALYSIS

3.1 Methodology

3.1.1 General Overview

Figure 10 shows a simplified view of the analysis methodology. Recall that we have previously specified necessary system parameters such as antenna heights, elevation angles, etc., which are assumed to be in place.

We evaluate the possibility that the 5G BS may be placed at different locations around the FSS ES, while the ES is at a fixed location with a fixed antenna direction. The angle θ is used to denote the angle of the BS's location with respect to the ES; θ is defined to be 0º when the 5G BS is located in the azimuthal direction of the boresight of the FSS ES antenna.

Additionally, the azimuthal direction of the antenna of the BS is evaluated as being randomly oriented over a 360 degree range with respect to the ES. The BS antenna is assumed to comprise three sectored antennae, each with a beam capable of being scanned over 120 degrees, so that as the BS antenna is rotated in a random direction over 360 degrees the ES will always be within a sector's beamwidth.

This assumption is conservative, as a more likely case would have only a single sectored antenna, in which case the ES could be located in the BS antenna's back-lobe for many orientations. This more realistic assumption would result in two primary consequences, one, in most cases even if the BS antenna is looking toward the ES antenna it will not be located within the main beam of the ES antenna, and two, often the back lobe of the BS antenna will be oriented toward the ES antenna.

This often will be the case because the ES will be oriented in a southerly direction toward the geostationary orbital plane over the equator, and most BSs can be expected to be located outside the narrow main lobe of the ES antenna.

Conversely, the probability of the ES being in the BS antenna's main lobe, as opposed to a side lobe, is based on the relative beamwidth of the main lobe with respect to that of the side-lobe, as shown in Figure 4.

As the 5G BS is placed at different angles around the ES, the value of d for which $I_{es}/\eta_{bs} \leq$ -6 dB at a specified confidence level (X%) is calculated. The set of these points over 360º around the ES creates the probability contour. The red shaded region indicates where a 5G BS placement would result in $I_{es}/\eta_{bs} \leq$ -6 dB at less than, and the green region where $I_{es}/\eta_{bs} \leq$ -6 dB at greater than the specified confidence value (X%).

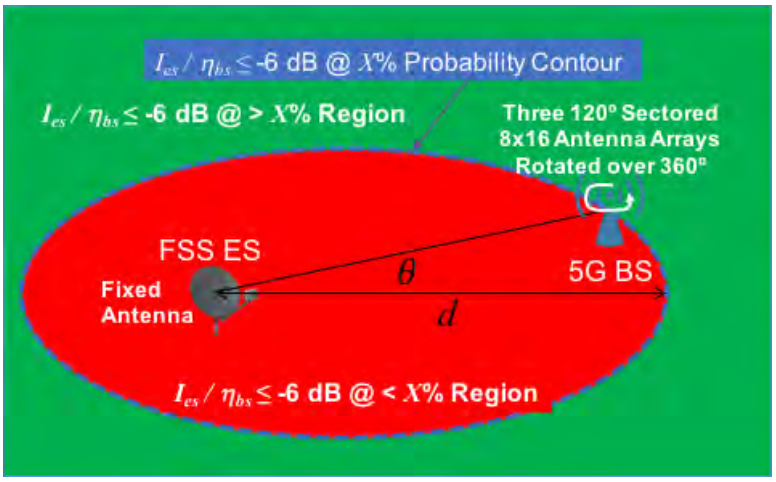

Figure 10. Analysis Methodology

Thus, the results of this analysis methodology enable insight into the sensitivity of 5G BS placement in the region of a FSS ES. The smaller the red region, the less sensitive the 5G BS is to placement.

We will calculate the probability contour using X = 99%, 98% and 95%, that is, the I_{es}/η_{bs} will not exceed the -6 dB threshold at that distance with these confidence levels. The confidence levels are based in turn on the statistical distribution of the received power density at the specified distance. The statistical variability from which this distribution arises is due to two variability factors: (1) the log-normal variation of the path loss around the calculated median path loss, as explained in Section 2.5.2, and (2) the probability of the ES being in the main lobe or side-lobe of the 5G BS as it is oriented in random directions, as explained above.

3.1.2 Assumption Discussion

Throughout the analysis, attempts have been made to use reasonably conservative assumptions whenever possible in constructing the coexistence model, particularly for cases where there might be uncertainty in actual deployments of FSS and 5G systems (especially for 5G, for which no actual deployments exist). Such conservative assumptions include:

- The location of the ES at a relatively high elevation, and the subsequent use of the Urban Macrocell path loss model (UMa), which provides lower path loss values than the Urban Microcell model (UMi – SC), for both LOS and NLOS cases;
- The modeling of the BS and ES antenna based on the peak values of the side-lobes, as opposed to, for example, average side-lobe gains;
- The assumption of 3-sectored BS antennas which provide essentially omni-directional coverage, as opposed to single-sectored antennae for which an ES might be located in the low-gain back-lobes; Notably this analysis does not consider the types of network

architectures that might be employed for other types of 5G deployments such as fixed-wireless applications that would not use an omni-directional antenna;

- The use of 99%, 98%, and 95% confidence levels for assessment of received power density levels, with the 99% and 98% being extremely conservative as compared to the already conservative 95% protection target used in [9];
- The assumption in the baseline analysis that there is no additional path loss attenuation due to shadowing from rooftop deployments, which would provide substantial additional attenuation of ES signals in the areas closer in to the ES location;
- The assumption that the 5G BS sites are located outdoors when, particularly at the high frequencies in question, indoor deployments might dominate; and
- The assumption that the ES elevation angle is at a minimal value of 35 degrees, while the elevation could extend up to 55 degrees.

3.1.3 Mathematical Formulation

If we substitute equations (3) and (4) for I_{es}/η_{bs} (in dB) the resulting composite expression is:

$$I_{es}/\eta_{bs} = P_{T,es} + G_{es:\theta,\phi(d)} + G_{bs:\theta,\phi(d)} + G_{p:es,bs} - PL_{es\rightarrow bs}(d) + 204 - NF_{bs} \quad (5)$$

Note that in this formulation we have explicitly accounted for the fact that the elevation angle (ϕ) at which we must evaluate the FSS ES and 5G BS antenna patterns are functions of the distance between these antennas (d). Thus, given a specified I_{es}/η_{bs} value (e.g., -6 dB), we can solve for the distance (d) at which the antenna gains and propagation loss sum to the required value. That is:

$$I_{es}/\eta_{bs} - P_{T,es} - 204 + NF_{bs} - G_{p:es,bs} = G_{es:\theta,\phi(d)} + G_{bs:\theta,\phi(d)} - PL_{es\rightarrow bs}(d) \quad (6)$$

Note that all of the values to the left of the equal sign in equation (6) are defined constants as shown in Table 1.

Parameter	Description	Value
I_{es}/η_{bs}	Ratio of FSS ES received power density (*Ies*) to 5G BS noise floor power density (η_{bs}) at the demodulator input (dB)	-6
$P_{T,es}$	Total transmit (i.e., both polarizations) power density of the FSS ES (dBW/Hz)	-78.46
NF_{bs}	Noise Figure of the 5G BS (dB)	12
$G_{p:es,bs}$	Polarization gain between the ES and BS antennas (dB) [looking for supporting reference]	-3

Table 1. Constant Parameter Definitions

Substitution of these constant values results in the following equation.

$$-116.54 = G_{es:\theta,\phi(d)} + G_{bs:\theta,\phi(d)} - PL_{es\rightarrow bs}(d) \quad (7)$$

The evaluation of equation (6) has been implemented in an Excel spreadsheet. The path loss solution uses the Combined (i.e., the weighted combination of the LOS and NLOS components)

PDF to determine the solution for a specified confidence level (e.g., the *PL* has a 95% probability of being greater than *x*), as was discussed in Section 2.5.2.

3.2 Results

The following results pertain to a set of system parameters and models that was chosen from key standards documents [7],[8].

3.2.1 Baseline

The analysis methodology described in Section 3.1 was applied to the system as described in Section 2. For convenience, the FSS ES parameters discussed in Section 2.2 are summarized in Table 2.

Parameter	Description	Value
Antenna Vertical Elevation	Boresight relative to the horizon (degrees)	35º
Antenna Height	Meters above the ground	25
Power Amplifier Output	Power density per right and left hand circular polarization (dBW/Hz)	-78.46

Table 2. FSS ES Parameter Summary

The 5G BS parameters discussed in Section 2.3 are summarized in Table 3.

Parameter	Description	Value
Antenna Height	Meters above the ground	6
Antenna Down-tilt	Degrees	10º
Antenna Location	Below local rooftops	N/A
Antenna Polarization	Linear	±45º
Antenna Array Size	Elements	8x16
Receiver Nose Figure	dB	12
BS Deployment Density	#/km^2	30

Table 3. 5G BS Parameter Summary

For the selected parameters of Table 1, Equation (7) shows the antenna port to antenna port coupling loss needed to keep I_{es}/η_{bs} from exceeding the -6 dB threshold is at least 116.54 dB. By combining the statistical variations of the path loss with those for the BS antenna gain variation due to random orientation of the BS azimuth, the following figure is the coupling loss at various confidence levels plotted as a function of separation distance.

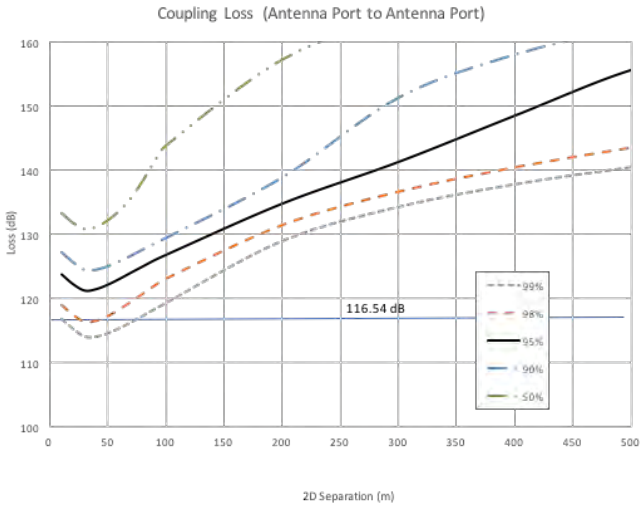

Figure 11. Antenna to Antenna Coupling Loss Confidence Curves

Note that at short separation distances, the elevation angles are large and antenna pattern losses dominate so for these parameters, the coupling loss has a minimum level at 35 m. Since only the 99 and 98 percentile confidence level curves have minima below the 116.54 dB threshold, only those two will provide non-trivial data for the subsequent analysis.

Figure 12 shows the results of the above described analysis. Only positive rotation angles are shown due to symmetry around 0º. The "Confidence Curve" shows the distance that the 5G BS would need to be placed from the FSS ES in order to achieve the specified $I_{es}/\eta_{bs} \leq$ -6 dB confidence level, absent consideration of any of the other factors discussed below. For example, for an angle θ (see Section 3.1.1) of 0º and a confidence level of 99%, the 5G BS would need to be placed at least 73 m from the FSS ES to achieve the specified result, absent the mitigating effects of other factors, such as inherent 5G BS antenna array techniques, and FSS ES physical isolation, as discussed in Sections 3.3.1 and 3.3.2. Note that the 95% plot is always 0 as explained above for Figure 11.

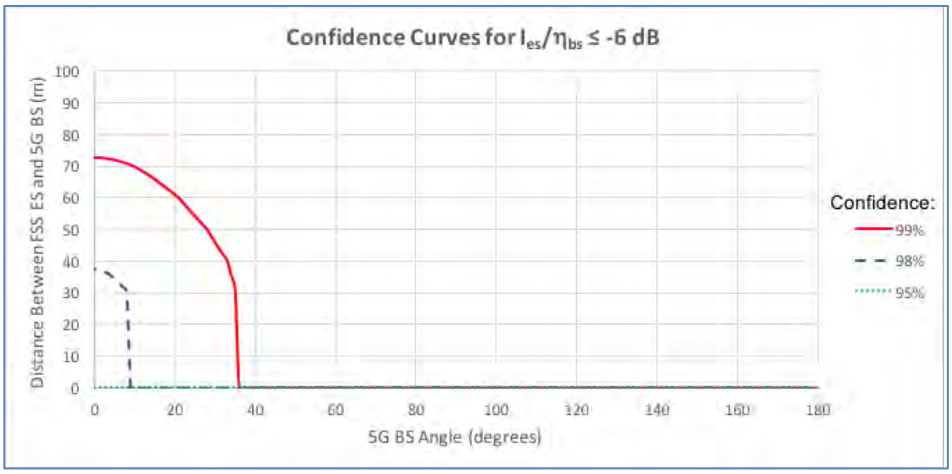

Figure 12. Baseline Analysis Results

Although Figure 12 is useful for obtaining distance information it does not provide a spatial context. This spatial contextual view is provided in Figure 13, which projects the distance data from Figure 12 onto a polar coordinate system.

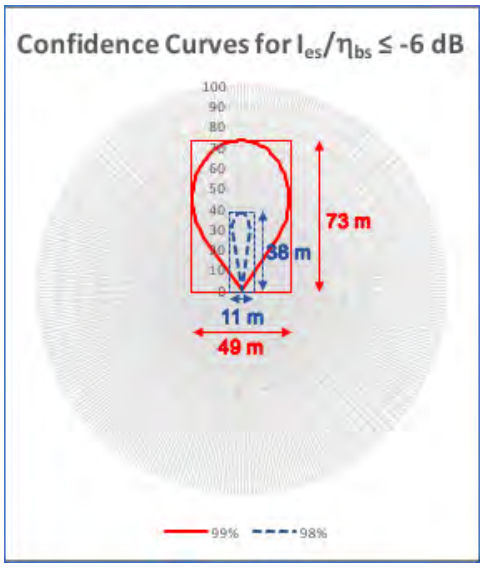

Figure 13. Baseline Analysis Results: Polar Projection

3.2.2 Coexistence Implications

Note that the area encompassed by the 99% contour is bounded by a rectangle of dimensions 73x49 m. Thus, the total area inside the 99% confidence curve is less than 0.0036 km^2.

The significance of a 0.0036 km^2 region can be assessed by comparison to a well-known urban county in which high capacity 5G mmWave BSs could likely be deployed, that being the Cook County, IL. Cook County is the second largest in the United States by population (2010 Census).

When "Cook County, IL" is entered into Google Maps, the returned region is shown by the light-red shaded area (see Figure 14). Note that the "Quick facts" section indicates that the population is 5.24 million and the area 4235 km^2.

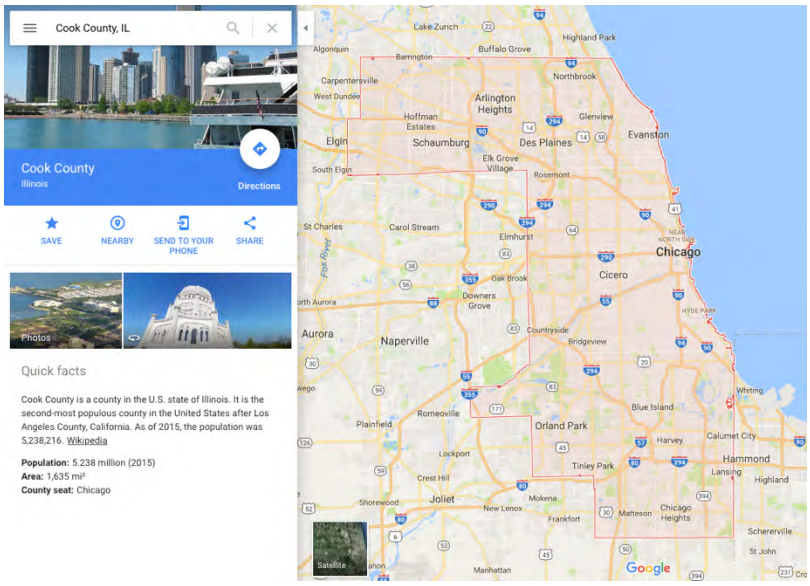

Figure 14. Google Maps: Cook County, IL

Therefore, a 0.0036 km^2 area constitutes only 0.00009% of the Cook County area. Were we to make the simplifying assumption of uniform population density, the number of Cook County residents living inside the 99% contour is approximately 4.4.

Note that if we use the still extremely conservative 98% contour the area is 0.00042 km^2, which is 0.00001% of the area with only 0.5 residents living inside.

Thus, given the availability of FSS ES deployment location flexibility, these extremely small footprints clearly support successful coexistence. Note that this is a worst-case result, as it neglects any improvements due to FSS ES antenna physical isolation and 5G antenna array techniques (see Sections 3.3.1 and 3.3.2).

3.3 Additional Mitigation Factors

The following two sections will discuss two likely mitigation techniques, those being FSS ES physical isolation and 5G BS antenna array techniques.

3.3.1 FSS ES Physical Isolation

Figure 15 shows the geometric implications for the case in which the FSS ES antenna is mounted on a modestly sized building. Note that the ES antenna is mounted 2 m above the roof of a 23 m tall building, resulting in a 25 m deployment height. The ES antenna is located at the roof center, which is a 16x16 m square.

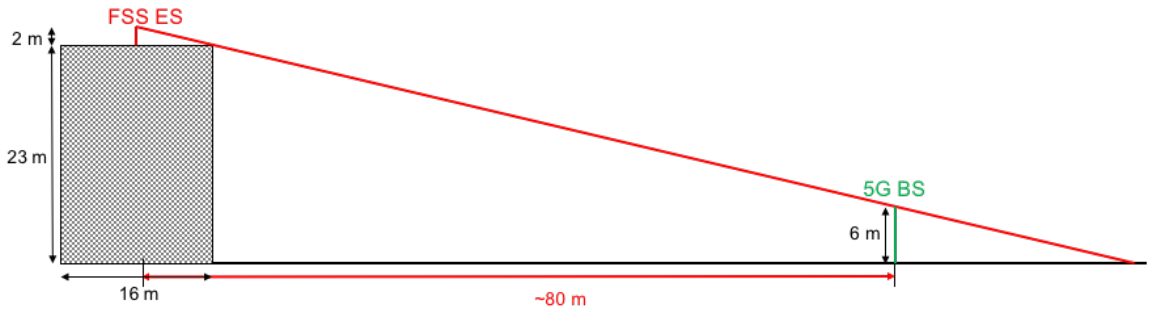

Figure 15. Geometry for Roof Blockage of FSS ES Signal

Drawing a line from the ES antenna that tangentially touches the building, we note that a 5G BS antenna that is 6 m above the ground will have "line of sight" to the ES antenna only at distances greater than approximately 80 m. If the BS is located closer than 80 meters then we would expect significant signal attenuation due to blockage by the roof itself. And, the closer the BS is to the building, the greater the R.F. attenuation due to roof blockage.

The FSS ES installation can be readily modified to provide additional R.F. isolation to a 5G BS. Figure 16 shows the case in which an R.F. barrier of height 0.5 m has been place on the roof edge in the boresight direction of the FSS ES antenna.

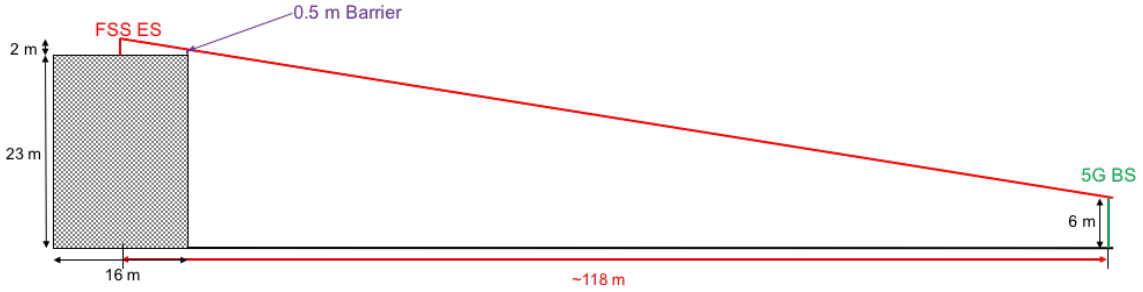

Figure 16. Geometry for Roof Plus Barrier Blockage of FSS ES Signal

Drawing a line from the ES antenna that tangentially touches the barrier top, we note that a 5G BS antenna that is 6 m above the ground will have "line of sight" to the ES antenna at a distance of approximately 118 m or greater.

In an open area, as the BS moves closer than 118 meters to the building blockage loss is primarily determined by diffraction loss. The height parameters used in Figure 16 were used to evaluate diffraction loss as a function of distance (2-D, from the ES antenna) at 50 GHz, with the resulting data shown in Figure 17 [12]. Note that at a distance of 100 m diffraction loss is greater than 7 dB, and at 90 m over 15 dB. Thus, significant additional diffraction loss can be expected.

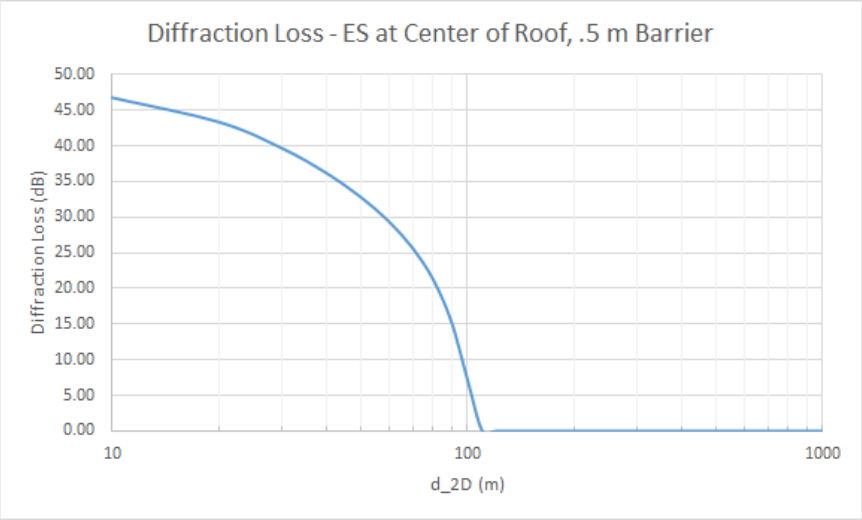

Figure 17. Diffraction Loss with a 0.5 m Barrier

Increasing the barrier height also increases to the "line of sight" distance and resulting diffraction loss at close-in distances. Given the directionality of the ES antenna, the barrier needs only be installed in the boresight antenna direction.

Certainly, scenarios can be envisioned that result in less favorable coexistence conditions. For example, the 5G BS antenna height could be increased to 10 or even 25 m, or the FSS ES antenna could be located off-center on the roof, or the building could be shorter and/or narrower. However, the above specific cases are intended to demonstrate that careful selection of ES deployment conditions can significantly enhance the ability of an FSS ES to coexist with a BS.

3.3.2 5G BS Antenna Array Techniques

Since it has direct and significant impact on system capacity and single user throughput, interference mitigation is a very active area in 5G research and standards. Many of the techniques developed for 5G systems to cope with self-interference and interference between co-existing 5G systems will provide an equal benefit against other co-existing systems, whether 5G or not. In order to provide some context in the area, examples of activity in each of the following classes are discussed.

3.3.2.1 Zero Forcing

Zero forcing is the 3D generalization of null steering in a cluttered local environment. Since there are multiple, indirect paths, this technique places a response null on any non-desired source. Thus, this technique is applicable in RF clutter environments using a Multiple Input – Multiple Output (MIMO) receiver. An example of work in this area can be found in "On the Performance of the MIMO Zero-Forcing Receiver in the Presence of Channel Estimation Error" [16], which discusses the performance of a MIMO Zero Forcing receiver with imperfect channel knowledge.

While MIMO techniques consider multiple paths through a cluttered environment, MultiUser MIMO (MU-MIMO) supports multiple users simultaneously. Thus MU-MIMO receivers are able to separate the signals from concurrent transmissions on the same frequency from different users. This is achieved by using the degrees of freedom provided by the multiple antenna and paths to separately isolate each individual signal. One relevant aspect of MIMO and especially MU-

MIMO is the suppression of other (non 5G) signals. Although, there is a paucity of literature of 5G MU-MIMO rejection of other wideband signals, there is a great deal on the ability to pick out a desired (or many desired) signals from a mix of other signals. An example of this capability is discussed in "LOS Throughput Measurements in Real-Time with a 128-Antenna Massive MIMO Testbed," [17], which provides performance results from a testbed designed to experiment with various aspects of Massive MIMO. Another paper, "AirSync: Enabling Distributed Multiuser MIMO With Full Spatial Multiplexing," [18] contains a study of a distributed Multi-User MIMO system using spatial multiplex and Zero Forcing that reports signal rejection of 25 dB.

3.3.2.2 Null Steering

Null steering is modifying the antenna pattern to produce a null in the direction of an interference source. As such, it implies a far field, plane wave model and is therefore commonly associated with phased arrays. When in an uncluttered RF environment, null steering works well. An example of work in this area can be found in "Optimization of Array Pattern for Efficient Control of Adaptive Nulling and Side Lobe Level," [14] which discusses an optimization technique applied to array synthesis with the constraint of reducing side lobe levels.

Null steering can achieve very deep rejections in many cases. "SoftNull: Many-Antenna Full-Duplex Wireless via Digital Beamforming," [15] analyses the performance of a transmit null steering algorithm to reduce self-interference for antenna structures supporting full-duplex operation, and reports reductions ranging from about 20 to 80 dB (see Figures 8-9 of [15]).

3.3.2.3 Antenna Side Lobe Control

The analysis provided in this paper assumes either standard reflectors for the ES and arrays with uniform amplitude taper for the BS antenna. These types of antennas, have a fairly high level of side lobes starting at -13.3 dB from the main beam. There exists a large number of techniques to further reduce the sidelobe level, each with its own characteristics; but industry standard antennas can readily achieve side lobe levels well below -20 dB. See "Side Lobe Level Reduction in Antenna Array Using Weighting Function," [13] which includes an analysis of various side lobe reduction techniques including a variety of commonly applied windows.

4 DISCUSSION OF RESULTS

The foregoing analysis of a typical deployment scenario shows that small Fixed Service Satellite (FSS) Earth Stations (ES) with uplink transmissions between 47.2-50.2 and 50.4-52.4 GHz, communicating with geostationary-orbit spacecraft, can be located in the same urban areas as Fifth-Generation (5G) wireless Base Stations (BS) without the need for coordination.[2]

The primary coexistence metric utilized is the ratio of FSS ES received power density (I_{es}) to noise floor power density (η_{bs}) at the 5G BS demodulator input, or I_{es}/η_{bs}. This metric is used to determine the 99%, 98% and 95% probability contours for $I_{es}/\eta_{bs} \leq$ -6 dB.

The baseline confidence probability contour data has been evaluated with respect to absolute area and also area relative to a specific county (i.e., Cook County, IL). The results indicate that for a

[2] Note: As noted earlier, the results of this analysis depend on the characteristics of the satellite system at issue; the methodology readily could be applied to systems with other architectures or physical configurations.

given ES, the area where a potential coexistence issue could exist is small, and the chances of such a circumstance actually arising in the real world is rare.

As reported in Section 3.2.2, the total 99% confidence probability contour area is less than 0.0036 km^2 and 98% contour less than 0.00042 km^2, which constitute less than 0.00009% and 0.00001% of Cook County, respectively. In order to assess how unlikely it is that a 5G BS will experience an I_{es}/η_{bs} greater than -6 dB, we will first utilize Figure 18, which is a magnified view of the region of interest from Figure 13.

We also have "turned around" the perspective to focus on confidence that the I_{es}/η_{bs} will be *greater than* (>) the -6 dB goal. So, if at a given distance the confidence of I_{es}/η_{bs} being ≤ -6 dB is X%, then the corresponding confidence that it will be > -6 dB is (100% - X%). Thus, the 99%, 98% and 95% regions become the 1%, 2% and 5% regions, respectively. Recall from Figure 11 that the 95 percentile curve never falls below the 116.54 dB threshold, so I_{es}/η_{bs} is less than -6 dB at all distances, and, we can therefore use the 5% percentile I_{es}/η_{bs} > -6 dB as a conservative ceiling value.

Therefore, the two regions of interest can be defined as follows:

- I_{es} / η_{bs} > -6 dB @ between 2% & 5% Region (Blue Shaded)
  - Area of the blue shaded rectangle
  - Size is ~420 m^2
- I_{es} / η_{bs} > -6 dB @ between 1% & 2% Region (Red Shaded)
  - Area of the red shaded rectangle minus area of the blue shaded rectangle
  - Size is ~3160 m^2

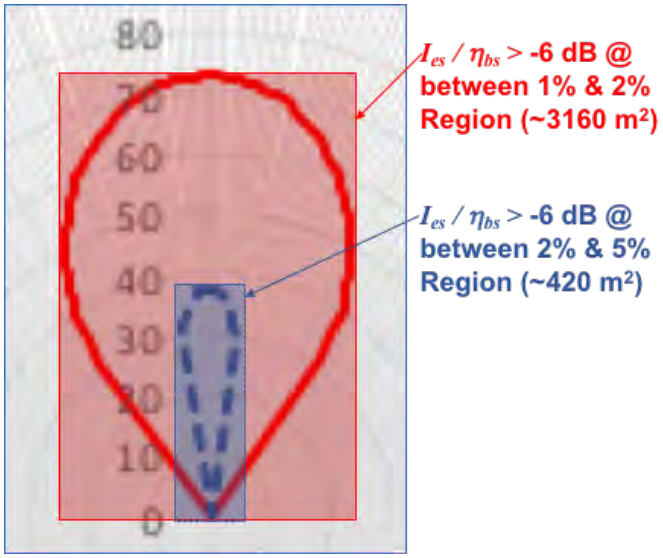

Figure 18. Approximate I_{es} / η_{bs} Greater Than -6 dB Confidence Regions

We can now make the conservative assumption that any 5G BS deployed in the red shaded region will have a probability of I_{es}/η_{bs} > -6 dB of 2% and in the blue shaded region of 5%. Thus, using the total region area (3160 m^2 + 420 m^2 = 3580 m^2) to weight these probabilities based on the

individual region areas, the resulting probability of I_{es}/η_{bs} > -6 dB assuming a uniform likelihood of 5G BS placement is approximately 0.024.

We can now make the (also conservative) assumption that the FSS ES is deployed in an area where 5G BSs are deployed at the standard density (specified in Table 12 of [7]) of 30 per km^2. Thus, the expected number of BSs falling within the confidence regions under discussion is approximately 0.1. That is, the chance of a BS being in the confidence regions under discussion is roughly 1 in 10.

This assumption is conservative because there will be large areas of, for example, Cook County in which no 5G BSs will be deployed. Moody's Investor Service recently published information claiming that 5G system deployment will likely cover only 50% of the United States population [19].

However, even if a 5G BS happens to be deployed in the discussed confidence regions (0.1 probability), the probability that the BS actually will experience an I_{es}/η_{bs} > -6 dB is 0.024. Therefore, the total probability that a 5G BS will actually experience I_{es}/η_{bs} > -6 dB under the terms of this analysis is only 0.0024, or approximately 1 chance in 416.

Notably, these results are based on conservative assumptions, including path loss, use of peak side lobes (instead of actual lower values at different off-axis angles), considering only BS antennas with essentially omni-directional coverage, calculating much-higher confidence levels for received power density levels than commonly used, not accounting for attenuation from blockage, assuming all-outdoor 5G deployment, and never considering the operation of an ES at an elevation angle above a minimal value.

Moreover, the foregoing calculations do not take into account the mitigating effects of other factors, such as FSS ES physical isolation and inherent 5G BS antenna array techniques, which virtually eliminate the chance of a real-world problem ever actually arising.

Thus, the results of this analysis show that coexistence between FSS ESs and 5G BSs (using the deployment scenario described in this paper) is feasible without the need for coordination.

5 REFERENCES

[1] "Sharing and Compatibility Studies of FSS and IMT Operating in the 37-50.2 GHz Frequency Range," Document No. USTG5.1_01, Task Group 5/1, 21 August 2017.

[2] Recommendation ITU-R M.1851, 06/2009 "Mathematical models for radiodetermination radar systems antenna patterns for use in interference analyses".

[3] ECC PT1 #54 Cascals, Portugal, 16-20 January 2017 issued 11 January "Sharing analysis on IMT-2020 and Inter-Satellite Service at 26 GHz.

[4] Antenna performance standards, FCC 47 CFR 25.209.

[5] Recommendation ITU-T M.2101-0. 6/2017 "Modelling and simulation of IMT networks and systems for use in sharing and compatibility studies."

[6] Nikolova 2016, Lecture 13: "Linear Array Theory – part 1."

[7] "Liaison Statement to Task Group 5/1: Spectrum Needs and Characteristics for the Terrestrial Component of IMT in the Frequency Range Between 24.25 GHz and 86 GHz," Document 5-1/36-E, Working Party 5D, 28 February 2017.

[8] "Attachment 2 on Spectrum Needs to a Liaison Statement to Task Group 5/1: Characteristics of Terrestrial IMT Systems for Frequency Sharing/Interference Analyses in the Frequency Range Between 24.25 GHz and 86 GHz," Working Party 5D, 28 February 2017.

[9] Kim, Seungmo, et al., "Coexistence of 5G With the Incumbents in the 28 and 70 GHz Bands," IEEE Journal on Selected Areas in Communications, Volume: 35, Issue: 6, June 2017.

[10] "Channel model for frequency spectrum above 6 GHz," 3GPP TR 38.900, Version 14.3.1, Release 14, July 2017.

[11] "Study on channel model for frequency spectrum above 6 GHz," ETSI TR 138 900, Version 14.2.0, Release 14, June 2017.

[12] Recommendation ITU-R P.526-13, Propagation by diffraction, P Series, Radiowave propagation, November 2013.

[13] Sarker, Roman, et. al., "Side Lobe Level Reduction in Antenna Array Using Weighting Function," International Conference on Electrical Engineering and Information & Communication Technology (ICEEICT) 2014.

[14] Sarker, Roman, et. al., "Optimization of Array Pattern for Efficient Control of Adaptive Nulling and Side Lobe Level," The 2015 IEEE International Conference on Communication, Networks and Satellite (COMNETSAT).

[15] Everett, Evan, et. al., "SoftNull: Many-Antenna Full-Duplex Wireless via Digital Beamforming," IEEE Transactions on Wireless Communications, Volume: 15, Issue: 12, December 2016.

[16] Wang, Cheng, et. al., "On the Performance of the MIMO Zero-Forcing Receiver in the Presence of Channel Estimation Error," IEEE TRANSACTIONS ON WIRELESS COMMUNICATIONS, VOL. 6, NO. 3, MARCH 2007.

[17] Harris, Paul, et. al., "LOS Throughput Measurements in Real-Time with a 128-Antenna Massive MIMO Testbed," Global Communications Conference (GLOBECOM), 2016 IEEE.

[18] Balan, Horia, et. al., "AirSync: Enabling Distributed Multiuser MIMO With Full Spatial Multiplexing," IEEE/ACM Transactions on Networking, Volume: 21, Issue: 6, December 2013.

[19] Moody's Investemnt Service, "Telcos will tailor their 5G strategies to match their individual strengths," https//www.moodys.com, September 2017.

ATTACHMENT B

V-Band: Current Plan and Proposals

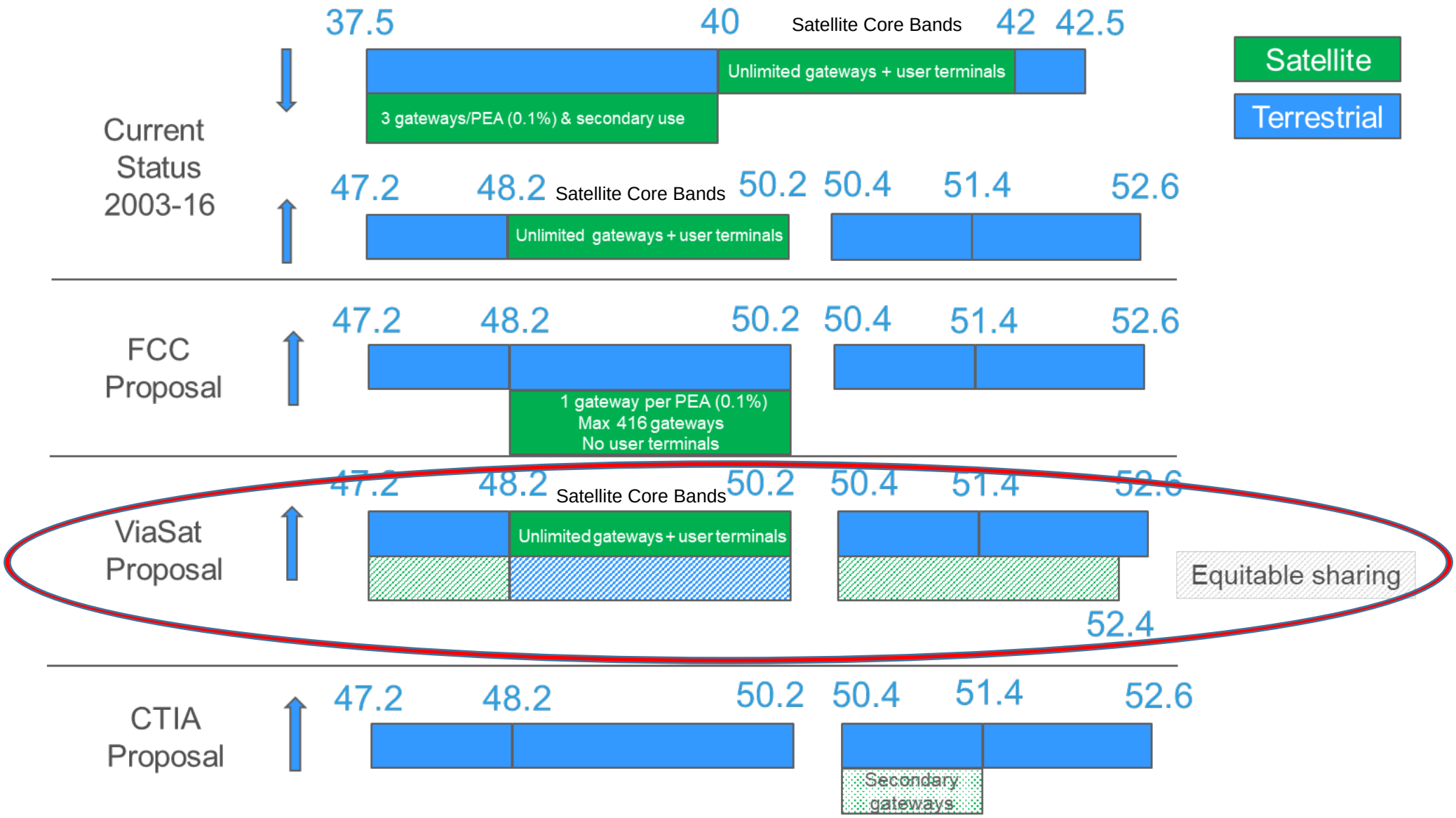

VS-2 Competitive Advantage

$$\text{Capacity} = W \times \log_2(1 + S/N)$$

Claude Shannon

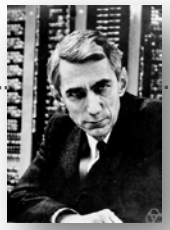

Spot beam satellite

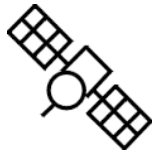

Fiber backhaul

W bandwidth

N gateways

Source: FCC filings and ViaSat estimates:
ViaSat-1: SAT-LOA-20110722-00132, dated July 22, 2011
Jupiter-1: SAT-LOI-20091110-00119 dated November 10, 2009
Jupiter-2: SAT-MOD-20141210-00127, dated December 10, 2014
ViaSat-2: SAT-MOD-20160527-00053, dated May 27, 2016
95W Filing: SAT-LOA-20170621-00092, dated June 21, 2017 (18 gateways @ 10 GHz each)

ViaSat

ATTACHMENT 4

555 Eleventh Street, N.W., Suite 1000
Washington, D.C. 20004-1304
Tel: +1.202.637.2200 Fax: +1.202.637.2201
www.lw.com

LATHAM & WATKINS LLP

FIRM / AFFILIATE OFFICES

Barcelona	Moscow
Beijing	Munich
Boston	New York
Brussels	Orange County
Century City	Paris
Chicago	Riyadh
Dubai	Rome
Düsseldorf	San Diego
Frankfurt	San Francisco
Hamburg	Seoul
Hong Kong	Shanghai
Houston	Silicon Valley
London	Singapore
Los Angeles	Tokyo
Madrid	Washington, D.C.
Milan	

October 2, 2017

VIA ELECTRONIC FILING

Ms. Marlene H. Dortch
Secretary
Federal Communications Commission
445 12th Street, SW
Washington, DC 20554

Re: ViaSat, Inc., *Ex Parte* Submission, GN Docket No. 14-177; IB Docket Nos. 15-256 & 97-95; RM-11664; and WT Docket No. 10-112

Dear Ms. Dortch:

Attached is an engineering report prepared by ViaSat, Inc. entitled, "Fixed-Satellite Service Earth Station Receiver and 5G Coexistence" illustrating that satellite earth station receivers in the 37.5-40.0 GHz band segment can coexist within close proximity to 5G operations.

Please contact the undersigned if you have any questions regarding this submission.

Respectfully submitted,

/s/

John P. Janka
Elizabeth R. Park

cc: Jose Albuquerque
Bahman Badipour
Simon Banyai
Paul Blais
Brian Butler
Stephen Duall
Chip Fleming
Diane Garfield
Michael Ha

Karl Kensinger
Kal Krautkramer
Kerry Murray
Charles Oliver
Nicholas Oros
Ronald Repasi
Alyssa Roberts
John Schauble
Catherine Schroeder
Blaise Scinto
Joel Taubenblatt
Jeff Tignor
Nancy Zaczek

FIXED-SATELLITE SERVICE EARTH STATION RECEIVER AND 5G COEXISTENCE

1 EXECUTIVE SUMMARY

This analysis of a typical deployment scenario considers the case of small Fixed-Satellite Service (FSS) earth stations (ES) operating with downlink (space-to-Earth) reception in the 37.5-40 GHz band from geostationary-orbit (GSO) spacecraft. It shows that those FSS ES can be located in the same urban areas as a Fifth-Generation (5G) wireless network without the need for coordination.

The analysis, similar to the Roberson Report [1], utilizes standard methodologies, parameters, and metrics, and also uses published characteristics of the 5G IMT system [2].

While the coexistence metric for FSS networks operating below 30 GHz has long been established as an increase in the thermal noise of the receiver of 6% commensurate with an I/N of -12.2 dB, the coexistence metric for FSS networks in the frequencies above 30 GHz is currently under consideration at the ITU. This analysis therefore considers a range of I/N values, namely -6, -10, and -12.2 dB.

The analysis considers a 1.8 meter earth station with the earth station antenna pointing in a fixed direction at a realistic elevation angle toward a GSO satellite, and uses a Monte Carlo simulation to place the earth station and the 5G cells (base station (BS) and associated user equipment (UE)) at random locations within a one kilometer square area. The simulation then develops statistics for earth station receiver I/N based on over one million random location samples that are then used to generate a cumulative distribution function (CDF) for the percent of locations where an I/N (-6, -10, or -12.2 dB) into the earth station receiver is exceeded.

The results demonstrate that in the case of a roof mounted 1.8 m antenna with 20 dB of additional attenuation from the roof line or parapet wall, the earth station can operate successfully inside a 5G deployment without the need for coordination because the earth station can operate in close proximity to the 5G network.

2 TECHNICAL ANALYSIS

Introduction

The study investigates the effect on an FSS receiver of a 5G system composed of several base stations and user equipment. In the simulation, which is performed using Visualyse Pro software from Transfinite, the FSS receiver is immersed inside the 5G distribution. The location of the ES is varied randomly within a one kilometer square area and then a number of 5G BS and associated UE stations are randomly placed within the area. The process is repeated for a million iterations with a snapshot taken at each iteration and a CDF of I/N versus location generated.

2.2 Characteristics of 5G (IMT-2020)

The 5G system parameters and deployment scenarios to be used in the sharing and compatibility studies are found in the ITU document that is being used internationally to analyze frequency sharing/interference between IMT systems (i.e., 5G) and FSS networks in frequency bands 24.25 GHz to 86 GHz [3].

The 5G systems setup is outlined in section 8 of Recommendation ITU-R M.2101. In this analysis, the following 5G parameters and configurations, and other salient methodologies, are used:

1. One million snapshots are used to generate the CDFs;
2. e.i.r.p. densities are -35.6 dBm/Hz for BS and -50.9 dBm/Hz for UE;
3. Micro urban hotspot below the roofline scenario with BS height at 6 m and UE at 1.5 m. All BS and UE are outdoor. One square kilometer area includes six BS and three active UE per BS. The BS and UE are placed inside that area;
4. The location of BS and UE vary for each snapshot. The UE are distributed in the area defined by the BS azimuth coverage of 120° degrees and up to 100 m from the BS. The BS azimuth coverage direction is random for every snapshot;
5. 20% network loading activity factor reduces the total number of active BS and UE by 80%;
6. There are 30 BS per km^2 and three UE that can be associated with each BS;
7. TDD factors reduces the simultaneous transmissions of BS by 20% and the UE by 80%;
8. At each snapshot, the following parameters are randomized:
    i. Locations of BS and the UE associated with that BS;
    ii. BS and UE antenna elevation and azimuth angles within a given sector depending on the link using beamforming antennas according to Recommendation ITU-R M.2101;
    iii. The BS and UE that are active (based on TDD factor);
    iv. The UE transmit power control level based on the UE proximity to the BS,
9. BS do not use power control in the downlink;
10. Reference emission bandwidth is 60 MHz for BS and UE;
11. The propagation model for the 5G system is from Doc. 5-1/36. Micro urban scenario is used with parameters from Recommendation ITU-R P.1411 "Propagation data and prediction methods for the planning of short-range outdoor radiocommunication systems and radio local area networks in the frequency range 300 MHz to 100 GHz". The parameters for the non-line of sight path loss with the coefficients (from P.1411 Table 4) where α=5.06, β=-4.68, γ=2.02 and σ=9.33.

The results are presented as CDFs for:

1. BS antenna gain toward the UE,
2. Downlink carrier-to-noise C/N ratio.

FIGURE 1

BS to UE antenna gain CDF

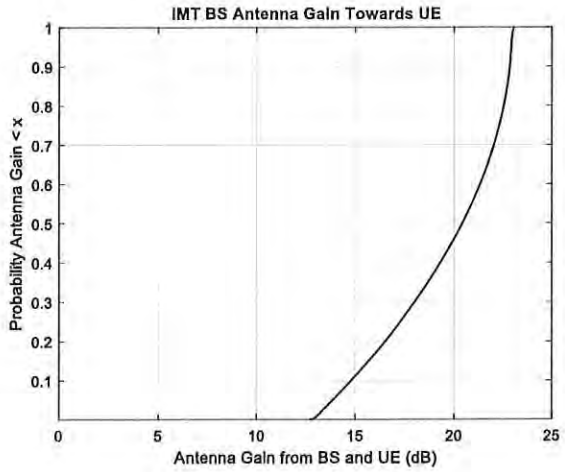

FIGURE 2

BS down link C/N

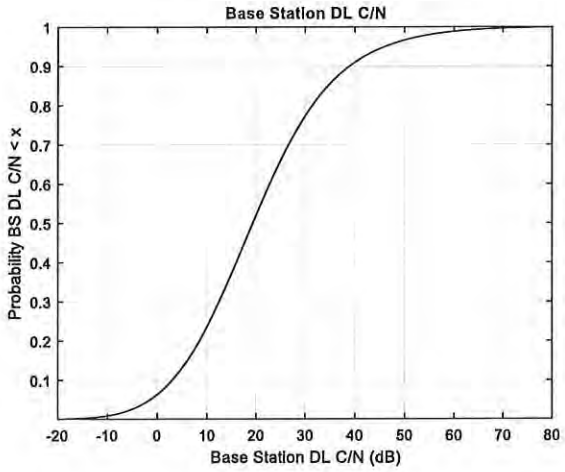

2.2 Characteristics of FSS systems

The FSS characteristics used in this analysis are shown in Table 1 below.

TABLE 1

FSS/BSS downlink parameters

Parameter	**Unit**	**1.8 m Diameter**
Frequency range	GHz	37.5-40
Noise bandwidth	MHz	50-500
Earth Station Antenna diameter	m	1.8
Peak receive antenna gain	dBi	55.4
Antenna receive gain pattern	–	Rec. ITU-R 465-6
System receive noise temperature	K	150
Minimum earth station elevation angle	°	35
Interference to Noise Ratio I/N	dB	-12.2, -10 and -6

2.3 Analysis scenarios and assumptions

The 5G setup is as described above. The 5G stations and the FSS earth station are randomly placed at each snapshot as shown around a center point in the analysis area, which is one km^2. The snapshot in Figure 3 is taken from one of one million iterations. Note in Figure 3 the earth station icon is immersed inside the 5G distribution and surrounded by the icons for the various BS and UE stations.

In each iteration of the simulation the orientation of the earth station and the 5G BS and UE stations will change. In some cases, the orientation of UE and BE stations will result in alignment with the main beam of the earth station and the BS antenna. In others, there will be an alignment with the UE beam, and so on. The Visualyse software's Monte Carlo process calculates and records the I/N into the ES receiver that results from that random placement of all the stations for that iteration.

FIGURE 3

Example snapshot of one million of the random placements of 5G BS and UE and the FSS station

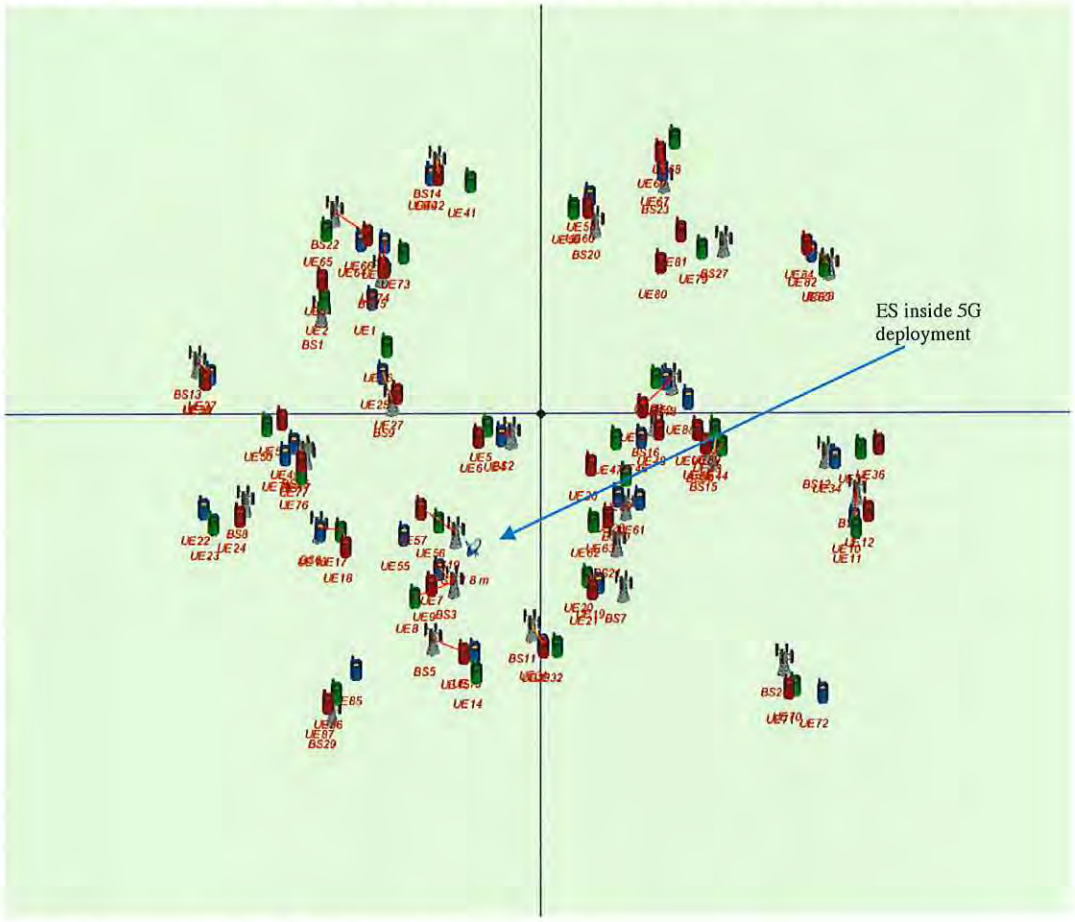

The following assumptions are also used:

1. The 5G network scenario is as described above;
2. Clutter models used for the transmit link from 5G towards the FSS receiver are from Document ITU-R TG 5-1/38. Two models are used. The first is Recommendation ITU-R P.2001 "A general purpose wide-range terrestrial propagation model in the frequency range 30 MHz to 50 GHz". The time percentages from 0 % to 100% are chosen randomly for each time sample. The other is Recommendation ITU-R P.2108 "Prediction of Clutter Loss" section 3.2. The clutter is applied at the 5G transmitter side

as well as the FSS receiver side according to Recommendation ITU-R P.2108. The percent of locations for clutter is random between 0% and 100% for every sample[1];

3. The FSS center frequency is 39 GHz;
4. FSS antenna height is 12 meters;
5. For each BS, three UE are employed at center frequencies of 38.933 GHz, 39.0 GHz and 39.067 GHz;
6. Frequency dependent rejection (FDR) is accounted for;
7. Polarization loss is set to 3 dB;
8. The FSS coexistence criteria is under discussion within the ITU-R working parties. For this analysis -12.2 dB, -10 dB and -6 dB are considered. The percent of time exceedance is needed to determine compatibility;
9. FSS bandwidths are 50 MHz and 500 MHz;
10. The 5G emission mask in dBc and 60 MHz measurement bandwidth are shown below;
11. The FSS receiver selectivity are shown below. The selectivity filters have -80 dB per decade slope from the -3 dB point to -70 dB floor. A faster filter roll-off can provide better rejection;
12. The 12-meter-high roof mount FSS ES installation is used, with a roofline, parapet wall or other shielding providing an additional R.F. isolation of 20 dB to the 5G BS and UE configuration.

FIGURE 4

Clutter loss

[1] Note these clutter models do not account for clutter closer than 250 m from the station.

FIGURE 5

5G emission masks

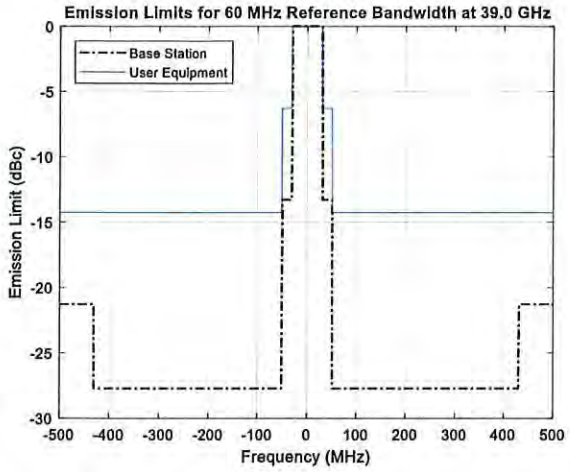

FIGURE 6

FSS receiver selectivity

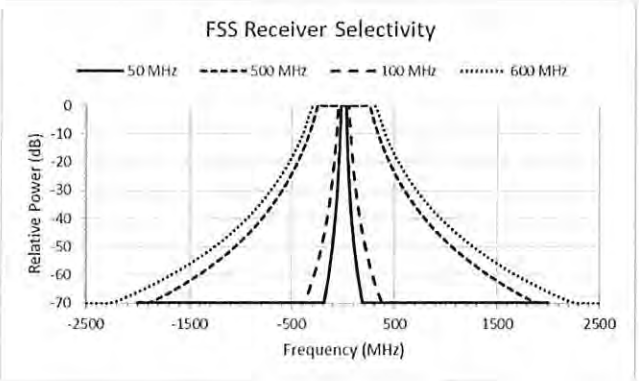

3 RESULTS

The results of the simulations for the three I/N values are shown below.

TABLE 2

5G and 1.8 m FSS summary of results

FSS Bandwidth (MHz)	50	500
Locations where -12.2 dB is not exceeded (%)	99.69	99.99
Locations where -10 dB is not exceeded (%)	99.87	99.99
Locations where -6 dB is not exceeded (%)	99.98	100

Table 2 indicates that with a greater than 99.69% confidence level (roughly 3 sigma) that an earth station of the type considered here, and with the additional 20 dB of attenuation reasonably expected of a roof top installation, could be deployed within a 5G network and not experience more than -12.2 dB I/N.

The CDF plot in Figure 7 below shows the percentage of simulation iterations where the I/N was greater than a given value. The plot shows that for the vast majority of random deployments of stations, the expected level of I/N was vanishingly small.

FIGURE 7

5G System and 1.8 m Diameter FSS ES at height of 12 m CDFs

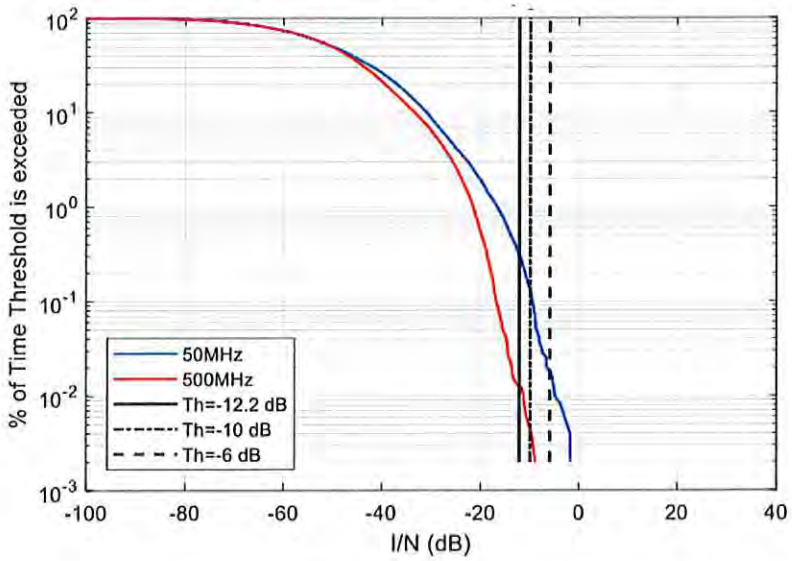

4 CONCLUSION

The analysis above shows that when a roof mounted 1.8 m diameter FSS is placed inside a 5G distribution in an urban clutter zone, and the roof line, a parapet wall, or other shielding provides an additional 20 dB of attenuation over normally expected clutter losses, the potential impact on the FSS receiver is negligible and coordination of stations is not required.

This result is consistent with measurements taken of a roof mount transmit earth station at 28 GHz which demonstrated the positive impact of locating the earth station in such a typical roof mount configuration [4], where in most cases the attenuation was greater than 20 dB, and more than 40 dB or beyond the measurement capability of the test equipment in many cases, and with the Roberson report which considered the uplink (Earth-to-space) scenario in an urban setting and that also concluded that coexistence is feasible without coordination because the transmit earth station can operate in close proximity to the 5G network.

5 REFERENCES

[1] Roberson Report, attached to ViaSat, Inc. Ex Parte Submission in GN Docket No. 14-177, September 25 2017

[2] ITU WP5D Liaison to TG 5/1

[3] Doc. ITU-R TG 5-1/36, Attachment 2

[4] Carlsbad Report, attached to ViaSat, Inc. Ex Parte Submission in GN Docket No. 14-177, April 20, 2017

Daryl T. Hunter, P.E.
Chief Technology Officer, Regulatory Affairs
ViaSat, Inc.
6155 El Camino Real
Carlsbad, CA 92009

October 2, 2017